

A COMPREHENSIVE SURVEY OF BUOYANCY AND SHEAR PARAMETERS  
FOR CALIFORNIA TORNADOES: 1951—2011

AS  
36  
2012  
GEOL  
.S78

A thesis submitted to the faculty of  
San Francisco State University  
In partial fulfillment of  
The Requirements for  
The Degree

Master of Science  
In  
Geosciences

By

Christopher J. Stumpf


San Francisco, California

May 2012

Copyright by  
Christopher J. Stumpf  
2012

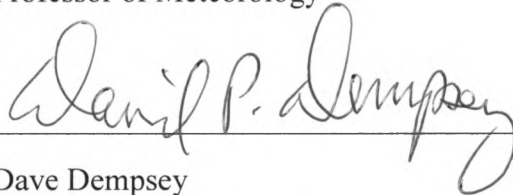
## CERTIFICATION OF APPROVAL

I certify that I have read A Comprehensive Survey of Buoyancy and Shear Parameters for California Tornadoes: 1951–2011 by Christopher Joseph Stumpf, and that in my opinion this work meets the criteria for approving a thesis submitted in partial fulfillment of the requirements for the degree: Master of Science in Geosciences at San Francisco State University.



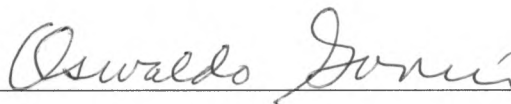
John Monteverdi

Professor of Meteorology



Dave Dempsey

Professor of Meteorology



Oswaldo Garcia

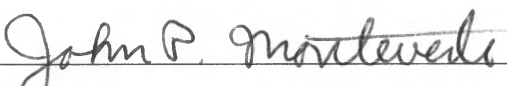
Professor of Meteorology

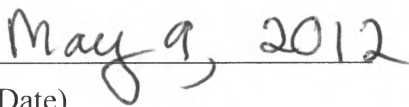
A COMPREHENSIVE SURVEY OF BUOYANCY AND SHEAR PARAMETERS  
FOR CALIFORNIA TORNADOES: 1951—2011

Christopher J. Stumpf  
San Francisco State University  
2012

The buoyancy and shear environments for 391 tornado events in California from 1951–2011 were evaluated on the basis of an analyses of proximity soundings and hodographs. The events were stratified into F0, F1, and F2/F3 categories or bins. The 0-1 km above ground level (AGL) Absolute Value Shear (ABVSHR), which is similar to positive shear [as defined in Lipari (2000)], was found to be a statistically significant discriminator between the bins, with increasing values of ABVSHR associated with the higher intensity tornadoes. Approximately 65% of the tornado events exhibited low level and deep layer shear values in the ranges consistent with mesocyclone formation in the parent thunderstorm. Shear values for F0 and F1 tornado events occurring before 1980 suggest that there was a systematic misrating of the tornadoes, with most probably assigned too high an F-rating. Case studies of two of the more damaging tornadic events (associated with the Sunnyvale F2 and Los Angeles F2) early in the California tornado record showed that both occurred in shear environments favoring tornadic supercells. Based upon an evaluation of documentary evidence, the author recommends that the Sunnyvale event should be re-rated to F3 and three additional tornadoes occurring on the same day should be added to the database. The Los Angeles tornado event was probably accurately rated.

I certify that the Abstract is a correct representation of the content of this thesis.

  
John Monteverdi  
(Chair, Thesis Committee)

  
(Date)



## ACKNOWLEDGMENTS

I would like to thank my colleagues at San Francisco State University. I am indebted to Dr. John P. Monteverdi for his encouragement; patience, knowledge, and invaluable assistance on this research project were remarkable. As a mentor and friend, his dedication to my understanding of meteorology and to the science of meteorology was indeed motivating. I would like to express a very special thanks to Dr. David Dempsey for his assistance in developing the shell script to automate the collection and processing of all the data. I would also like to thank Dr. Oswaldo Garcia and Karen Grove for their support and motivation. I would like to extend a special thanks to the Sunnyvale Historical Society for providing the newspaper clippings and photographs for the Sunnyvale Tornado. Thanks also to John Shewchuk of Environment Research Services for his help and support with the software package RAOB. Thanks as well to Gary Lipari for providing his radiosonde data he used in his study.

I would also like to express special thanks to the staff of the San Francisco NWS office in Monterey, California for their support and encouragement during this process. Finally, I need to thank my family and friends, especially my future wife Bridgett, for their tremendous support during my journey through graduate school.

## TABLE OF CONTENTS

List of Tables.....	ix
List of Figures.....	x
List of Appendices.....	xv
 1. Introduction .....	 1
1.1 Study Period and Scope of the Study .....	5
2. Deep Moist Convection – A Review.....	8
2.1 Buoyancy and Shear Characteristics.....	9
2.1.1 Instability.....	9
2.1.2 Vertical Wind Shear and Positive Wind Shear .....	10
2.1.3 The Role of Pressure Perturbations.....	13
2.2 Tornadoes and Tornadogenesis.....	15
2.2.1 Definitions of Tornadoes.....	15
2.2.2 Supercell Thunderstorms and Processes Leading to Tornadoes .....	18
2.2.3 Non-Supercellular Thunderstorms and Processes Leading to Tornadoes.....	23
3. Tornadoic Thunderstorms in California .....	28
3.1 Climatology of Tornado Events.....	28
3.2 Synoptic and Subsynoptic Features of Northern and Central California Tornadoic Storms .....	32
3.2.1 Leaside troughs .....	35
3.2.2 Topographically Generated Helicity .....	36
3.2.3 Barrier Jet-Induced Low Level Shear .....	37
3.2.4 Postfrontal troughs .....	38

3.3 Synoptic and Subsynoptic Features of Southern California Tornadoic Storms .....	38
3.3.1 Topographically Induced Low-Level Jet of the LA Basin.....	41
3.3.2 Convergence Zones and Topographically Generated Helicity .....	41
3.3.3 Thunderstorms in the Southeastern Deserts of California .....	44
4. Data and Methodology .....	46
4.1 Overview .....	46
4.2 Construction of Proximity Soundings and Hodographs .....	47
4.2.1 Proximity Sounding and Hodograph Estimation Procedure .....	48
4.2.2 Sources of Data .....	54
4.2.2.1 Hourly Surface Observations .....	54
4.2.2.2 Radiosonde Data .....	56
4.2.2.3 Tornado Locations and Data .....	57
4.2.2.4 Synoptically Analyzed Maps and Upper Air Charts.....	58
4.3 Selection and Computation Parameters .....	58
4.3.1 Overview .....	58
4.3.2 CAPE.....	59
4.3.3 0–3 km CAPE .....	61
4.3.4 Convective Inhibition.....	61
4.3.5 Wind Shear.....	62
4.3.6 Storm-relative helicity.....	63
4.3.7 Bulk Richardson Number.....	65
4.3.8 Energy Helicity Index .....	66
4.3.9 Vorticity Generation Parameter .....	66
4.4 Statistical Procedures .....	67
5. Results of the Study .....	69
5.1 Buoyancy and Shear Parameters for California tornadoes 1951–2011 ...	70
5.1.1 Analysis of Buoyancy .....	70
5.1.2 Analysis of Absolute Value Shear and Bulk Shear.....	72

5.1.3 Analysis of Environmental Storm-Relative Helicity .....	82
5.1.4 Analysis of Rotational Parameters (BRN, EHI, and VGP).....	85
5.2 Composite Soundings .....	87
5.3 Buoyancy and Shear Parameters Before 1980 and After 1980.....	91
6. Case Studies of the 1951 Sunnyvale F2 and the 1983 LA Convention Center	
Tornadoes .....	99
6.1 The 1951 Sunnyvale F2 tornado .....	100
6.1.1 Synoptic and Mesoscale Environment .....	101
6.1.2 Buoyancy and Shear Environment.....	105
6.1.3 Damage Assessment.....	107
6.1.4 Findings.....	115
6.2 The Los Angeles Convention Center F2 Tornado .....	117
6.2.1 Synoptic and Mesoscale environment.....	118
6.2.2 Buoyancy and Shear Parameters .....	122
6.2.3 Damage Assessment.....	124
6.2.4. Findings.....	130
7. Discussions and Conclusions .....	131
7.1 Synopsis .....	131
7.2 Limitations of Methodology .....	135
7.3 Future Work .....	136
References .....	138
Appendix .....	138

## LIST OF TABLES

Table	Page
2.1 Fujita Tornado Damage Scale and Enhanced Fujita Scale implemented in 2008 (from SPC's EF-scale FAQ).....	17
3.1 Mean path length and width of California and Great Plains tornadoes. (Data for Great Plains tornadoes from Smith and Mirabella (1972) and data for California tornadoes was taken from this study).....	17
3.2 The number of tornado assigned a particular F-rating during the period 1951–2011 is shown here .....	17
4.1 List of parameters calculated for each tornado proximity sounding. ....	17
5.1 Shows 0-1 and 0-6 km ABVSHR values for (F0, F1, and F2/F3) tornado events before and after 1980.....	17

## LIST OF FIGURES

Figure	Page
1.1 Map displaying the location of all tornado reports in California from 1951–2011. The tornado events are indicated by a yellow circle and cities with large populations are indicated by a red circle. ....	17
2.1 Conceptual model of a “Classic” supercell at the surface developed by Lemon and Doswell (1979) through radar studies, surface analysis and visual observations. The green shading encompasses the radar echo; the thunderstorm gust front structure is depicted by the thick blue line. The surface positions of the updraft location (UD) is stippled red, the rear flank downdraft (RFD) and the forward flank downdraft (FFD) are in blue. Streamlines depicting ground-relative flow are shown as lines terminating with arrowheads. The tornado location (if present) is shown by the red triangle. (Figure 2 from Doswell, 2012). ....	17
2.2 Schematic showing the tilting of vortex tubes or vortex lines toward the surface coincident with the formation of a downdraft (Figure 10.3 from Markowski and Richardson, 2010). ....	21
2.3 A schematic representation of convergence zones or topographically generated vorticity, which is stretched vertically by the formation of an updraft. During this stretching additional horizontal vorticity (not shown) may be ingested into the updraft and a stronger vortex at the lower levels can form (Figure 10.3 from Markowski and Richardson, 2010). ....	24
3.1a Monthly distributions of California tornadoes (indicated by total column height and numerical value at top of column) for the period 1951–2011. ....	30
3.1b Hourly distribution of California tornadoes for the period 1951–2011. ....	30

3.2	Schematic chart showing the location of major synoptic and subsynoptic features associated with tornado events in California's Central Valley. Isotachs are labeled in meters per second. The location of the subsiding flow west of the leeside trough and surface southeasterlies in central and eastern Central Valley are shown by light gray arrows. The circled "A" indicates the major focus for supercell thunderstorm formation. (From Braun and Monteverdi, 1991; Monteverdi and Quadros, 1994).....	33
3.3	Schematic showing the mean position of the jet stream (arrow) and cold front at the time of tornado occurrences. The hatched area indicated the typical location of the low centers at the surface, 850, 700, and 500 mb levels (Hales, 1985) .....	40
3.4	Map of Southern California showing the convergence zones developing during westerly flow regimes (Figure 6. from Small et al., 2000) .....	43
4.1	Map displaying the location of all available hourly surface observing sites. The surface observing sites are indicated by a small yellow circle and cities with large populations are indicated by red circles .....	55
4.2	Map displaying the location of all available radiosonde launch sites. The radiosonde sites are indicated by a yellow triangle and cities with large populations are indicated by a red circle .....	56
5.1	Box and Whisker plot of Total CAPE for each F-scale rating (F0, F1, with F2's and F3's binned together). The red box represents the 50% quartile with the mean value represented by the top of the red box. The green box represents the 75% quartile. The bottom whisker represents the lowest value of CAPE and the top whisker represents the highest value of CAPE .....	71
5.2	Maximum, 75 <sup>th</sup> percentile (green box), 25 <sup>th</sup> percentile (red box), and minimum values of Absolute Value Shear observed for F0, F1, and F2/F3 bins .....	75

5.3	Maximum, 75 <sup>th</sup> percentile (green box), 25 <sup>th</sup> percentile (red box), and minimum values of Bulk Shear observed for F0, F1, and F2/F3 bins.....	76
5.4	Absolute value shears for 391 cases included in this study (diamonds = F0, filled squares = F1, triangles = F2, and black plus = F3. Black lines represent upper and lower bounds of shear values.....	81
5.5	Maximum, 75 <sup>th</sup> percentile (green box), 25 <sup>th</sup> percentile (red box), and minimum values of Absolute Storm-Relative Helicity observed for F0, F1, and F2/F3 bins .....	85
5.6	Composite F0 profile of T, T <sub>d</sub> , wind, and the composite hodograph derived from 232 tornado proximity soundings. The area denoted by red on the sounding profile shows CAPE present. ....	88
5.7	Composite F1 profile of T, T <sub>d</sub> , wind, and the composite hodograph derived from 95 tornado proximity soundings. The area denoted by red on the sounding profile shows CAPE present .....	89
5.8	Composite F2/F3 profile of T, T <sub>d</sub> , wind, and the composite hodograph derived from 25 tornado proximity soundings. The area denoted by red on the sounding profile shows CAPE present .....	90
5.9	ABVSHR quartiles for 0-1 km and 0-6 km shear for each F-rating before and after 1980. ....	95
5.10	ABVSHR shear space 0-1 km ABVSHR on the Y-axis and 0-6 km ABVSHR on the X-axis. The dark blue diamonds represent the F0 events before 1980 and the light blue diamonds represent the F0 events after 1980. ....	96
5.11	Scatter plot of 0-1 km ABVSHR on the Y-axis and 0-6 km ABVSHR on the X-axis. The dark squares represent the Pre 1980 F1 tornadoes and the lighter squares represent the Post 1980 F1 tornado events. ....	98



6.1	The 500 mb Geopotential Height field at 1800 UTC on January 11, 1951. Shortwave trough axis is centered over northern California with the longwave trough axis centered over the Great Basin region .....	102
6.2	The 300 mb vector wind speeds show a jet streak approaching the California coast. The Bay Area region was located in the left exit region of this jet streak .....	103
6.3	Mesoscale analysis over central California, in the hour before the Sunnyvale tornado. Synoptic scale low and postfrontal trough located over the Bay Area.....	104
6.4	Proximity sounding and hodograph generated for Sunnyvale at 15 UTC on January 11, 1951.....	106
6.5	Estimated damage path through Sunnyvale California on January 11, 1951.....	108
6.6	Broken telephone pole in the foreground and large section of roof removed from the train station in Sunnyvale, CA on January 11, 1951 .....	109
6.7	Corrugated iron and frame garage in Sunnyvale, CA knocked down on January 11, 1951.....	110
6.8	A Metal Building System as described by the Damage Assessment guide. Damage to this building resembles the damage to the metal garage in Figure 6.7.....	111
6.9	Second story exterior wall removed from home located near Delmas Ave. in San Jose on January 11, 1951.....	112
6.10	Estimated path of the San Jose tornado on January 11, 1951 .....	113
6.11	Locations and suggested F-rating for tornadoes occurring on January 11, 1951.....	115

6.12	Upper air and jet stream diagram for 1200 UTC on March 1, 1983. 250 mb Geopotential height solid black lines, 250 mb isotachs color fill, and wind barbs for 250 mb wind.....	119
6.13	Mesoscale analysis over southern California at 1500 UTC, the hour before the tornado. Cold front located off the coast with a mesoscale trough out ahead of the cold front.....	120
6.14	Tornado proximity sounding for the LA Convention Center tornado. The red area indicates CAPE present in the sounding and the blue area indicated CIN present in the sounding. Modest buoyancy is present but the 0-6 km hodograph in the upper right corner shows strong curvature in the lower levels of the atmosphere .....	123
6.15	Telephone pole snapped about half way up the pole.....	125
6.16	Damage to storefront windows. Collapse of masonry parapet and part of roof .....	126
6.17	Section of roof removed from house located near the Convention Center .....	127
6.18	Collapse of entire roofing structure, house located near the Convention Center.....	127
6.19	Damage to the Los Angeles Convention Center shortly after tornado moved through.....	129
6.20	Removal of side panels along exterior walls from the Los Angeles Convention Center.....	129

## LIST OF APPENDICES

Appendix	Page
1      Compilation of Buoyancy and Shear Parameters for 391 Tornado events from 1951–2011 .....	151
Table A1    Compilation of results from 22 tornado proximity soundings for the 1950s .....	151
Table A2    Compilation of results from 26 tornado proximity soundings for the 1960s .....	152
Table A3    Compilation of results from 42 tornado proximity soundings for the 1970s .....	153
Table A4    Compilation of results from 63 tornado proximity soundings for the 1980s .....	155
Table A5    Compilation of results from 137 tornado proximity soundings for the 1990s .....	158
Table A6    Compilation of results from 102 tornado proximity soundings for the 2000s .....	164

## 1. Introduction

The systematic documentation of the environments of California tornadic thunderstorms has been a relatively recent phenomenon. Until the late 1980s and early 1990s, California tornadoes were poorly understood, probably under documented and often miscategorized as “freak” wind events [*Monteverdi and Quadros*, 1994]. The reasons for this are intertwined with the evolution of tornado forecasting in the United States [*Monteverdi et al.*, 2003].

From the mid-20th century through the 1970s, tornado forecasting was centered on a pattern-recognition approach that was thought to be the key in the early successes forecasters had in anticipating tornadoes [*Moller et al.*, 1994]. This approach was based upon a conceptual model that directed forecasters’ attention to the warm sector of wave cyclones progressing across the Great Plains.

The explosion of knowledge on the critical factors associated with tornadic thunderstorm environments that occurred from the 1970s through the late 20th century was based upon observational studies and numerical modeling of tornadic thunderstorms in the Great Plains [*Lemon and Doswell*, 1979; *Moller et al.*, 1994]. This led to the development of the so-called “ingredients-based” approach that centered on the meteorological factors that contribute to the development of tornadic thunderstorms, rather than on the synoptic pattern that typically occurs in one geographic area when tornadic thunderstorms occur there. As a result, the Great Plains “warm sector” model

was largely abandoned by the research community as a general pattern recognition forecast tool since many other patterns can provide the ingredients favorable for the development of tornadic thunderstorms. This model was also abandoned by operational meteorologists who were directly connected to those research efforts. Unfortunately, the integration of the ingredients based approach into the forecasting environments of areas in the country outside of the Great Plains did not occur for several decades. This was particularly true in California [*Monteverdi et al.*, 2003].

The imposition of the Great Plains warm sector model for forecasting tornadic thunderstorm development continued as a pattern recognition technique for California meteorologists and constrained their understanding of tornado events occurring before 1980. This was because the synoptic pattern of many tornado events in California did not resemble the Great Plains model in advance (meaning in the forecasts), thus meteorologists in California were not anticipating tornadoes. Since they were not anticipating tornadoes, when any tornadoes did occur they were either not recognized as tornadoes or misidentified as wind damage, because the forecasters thought that the pattern could not support the development of tornadic thunderstorms [*Braun and Monteverdi*, 1991; *Monteverdi et al.*, 2003].

During the mid-1980's and 1990's studies of severe convection in California showed that the majority of the tornadic storms occurred during the cool season (November to March) [*Hales*, 1985; *Braun and Monteverdi*, 1991; *Blier and Batten*,

1993(b), 1994]. It was Hales (1985) who developed the first prototype synoptic pattern associated with tornadic events in southern California that showed tornadoes occurred in the cold sector of wave cyclones. However, many meteorologists in California remained skeptical of the occurrence of tornadic thunderstorms in California.

Braun and Monteverdi (1991) were the first to publish a complete analysis of the occurrence of a tornadic supercell in California on the basis of an ingredients-based approach. The buoyancy and shear values associated with an F2 tornado (as classified by the F-scale system of Fujita (1971, 1981); see section 2.2.1) were consistent with the values of tornadic thunderstorms as documented elsewhere in the country. It was hypothesized that topographic forcing in the Central Valley for certain synoptic patterns can locally produce shear profiles favorable for these tornadic thunderstorms. A prototype synoptic pattern was developed for northern and central California [*Braun and Monteverdi*, 1991] and has been observed in other occurrences of tornadic thunderstorms occurring in the Central Valley [*Monteverdi and Quadros*, 1994; *Monteverdi and Johnson*, 1996]. Additional studies have made considerable strides in the documentation of these tornadic events but have only focused on one or two events.

The first attempt to characterize the buoyancy and shear environments for a larger set of tornado events in California appeared in Monteverdi et al. (2003). Their study provided an analysis of the buoyancy and shear environments for 30 tornadic and

30 non-tornadic thunderstorms that occurred in the period 1990-1994 in northern and central California.

Their findings were consistent with those in similar studies of tornadic thunderstorm environments in the Great Plains, namely, that shear is the distinguishing characteristic between environments that support tornadic thunderstorms and those that do not. In particular, the shear values they found for the stronger tornado events in the data set (i.e., thunderstorms producing F1 and F2 tornadoes) were consistent with those observed with tornadic events in the Great Plains associated with a class of thunderstorms called “supercells”. Buoyancy values were not found to be a distinguishing characteristic, thus underscoring the fact that causes for California tornadoes are no different than those for their more frequent Great Plains’ counterparts. Although this finding does not seem earthshaking now, it did represent a “paradigm shift” for forecasters in California, who up until the late 20<sup>th</sup> century were wedded to buoyancy as the main causative factor in the development of tornadic thunderstorms.

Some key questions could not be answered on the basis of the results in Monteverdi et al. (2003). Since their data set included only 30 tornadoes, would their findings be representative of a similar study of all tornado events in the California record? If so, in that record, were there any remarkable events that appeared to be associated with buoyancy and shear environments that were not consistent with what is known about such environments now? In essence, Monteverdi et al. (2003) can be

considered to be a pilot study. The present study is meant to extend the analysis over the entire tornado data set that now exists for California (back through 1951) both to answer the questions above and, perhaps, to pose some new questions that might be answered in future research efforts.

### **1.1 Study Period and Scope of the Study**

The primary purpose of this study is to document the buoyancy and shear characteristics associated with all California tornado events tallied in the Storm Prediction Center (SPC) database. This record extends back to 1951 and contains 391 tornadoes [SPC SVRGIS, 2012]. The distribution of these tornadoes (see Figure 1.1) is consistent with the climatologies developed in Braun and Monteverdi (1991) and Blier and Batten (1994) in which California's "tornado alley" (i.e., the Central Valley) and Los Angeles Basin/coastal (LA Basin) waters maxima were first identified.

A second important purpose for the study is to determine whether the shear and buoyancy parameters for all California tornado events in the record stratify in the same way as those summarized in Monteverdi et al. (2003). There are some key issues here regarding the role of low level (i.e., 0-1 km shear) in encouraging tornado formation that Monteverdi et al. (2003) found were especially marked for the California cases they studied. The overarching point-of-view the author feels would be important to illustrate is that the shear environment in California, strongly influenced at low levels by



topographic forcing, should be as evident a control on tornadic thunderstorms for the larger data set as it was for the 30 cases studied in Monteverdi et al. (2003).

As an illustration of the role of shear in contributing to the development of the tornadic thunderstorms throughout the California record, the author has chosen to complete case study analyses of two important historical tornadic events, that of January 11, 1951 in Sunnyvale and of March 1, 1983 in Los Angeles. Clearly, the buoyancy and shear environments for these two tornadic thunderstorm events generally should be consistent with the intensity (and, perhaps, number) of tornadoes observed.

A subsidiary issue, discussed at length below, is that a study such as the present one must, by definition, use the F-scale ratings for these tornadoes assigned by the National Weather Service. However, it is well known that there are important questions, discussed below, about the accuracy of these ratings before the late 1980s. Thus, a final major purpose of the study is to analyze these two damaging tornado events on the basis of photographic and other documentary evidence perhaps to establish whether what is known about the relationship of damage to F-scale rating is consistent with the rating given.

The study is organized into sections and subsections. A background on tornadic thunderstorms is provided in Chapter 2. A review of the climatology and controls on tornadic thunderstorms in California is provided in Chapter 3. A detailed overview of the methodology and sources of data used in this study is provided in Chapter 4. An

analysis of the buoyancy and shear environments for all of the California events shown in Figure 1.1 is provided in Chapter 5. The case studies of two damaging tornado events occurring in California are provided in Chapter 6 and 7. Finally, a discussion of the results and conclusion is provided in Chapter 8.

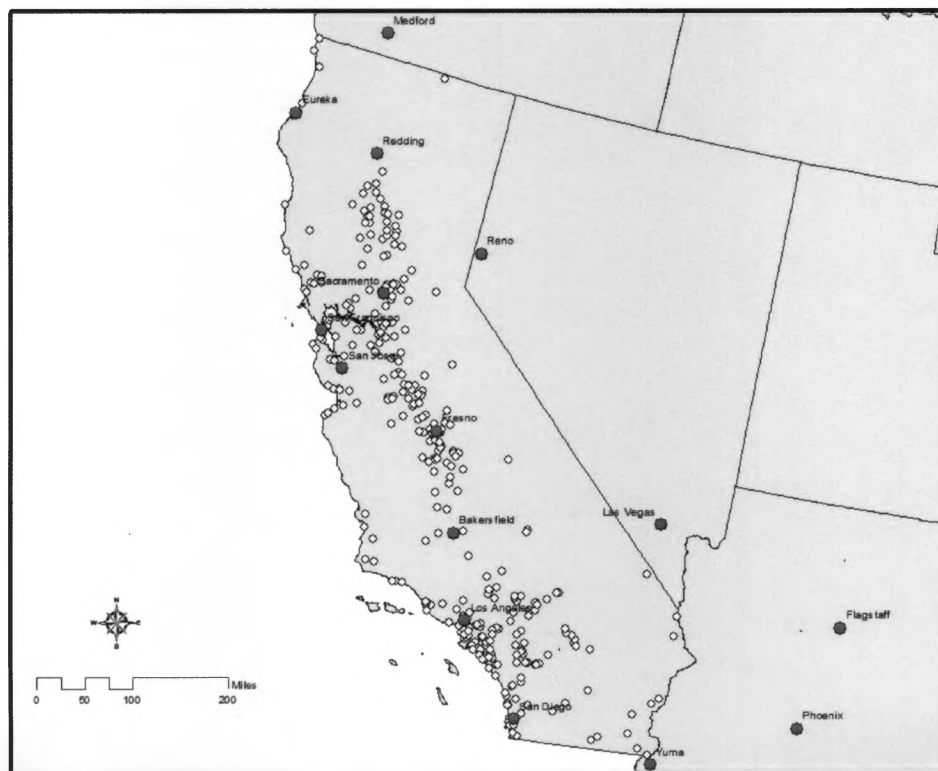


**Figure 1.1** Map displaying the location of all tornado reports in California from 1951–2011. The tornado events are indicated by a yellow circle and cities with large populations are indicated by a red circle.

## 2. Deep Moist Convection – A Review

Thunderstorms are the product of a set of processes that result in deep moist convection (DMC). DMC has the following primary ingredients: moisture, instability, and lift [*Johns and Doswell, 1992*]. Instability in association with sufficient moisture needs to be present in the environment for any convection to initiate. Next, a lifting mechanism is required to tap into the instability and initiate DMC. The thunderstorms that are a manifestation of DMC are classified as severe, according to the National Weather Service (NWS), if one or more of the following are observed: 1. Wind gusts of 50 knots or greater; 2. Hail measuring one inch in diameter or larger; and, 3. Any report of a tornado [*NWS Glossary, 2012*].

The morphology and evolution of severe thunderstorms are governed by the buoyancy and vertical wind shear characteristics of the environment [*Weisman and Klemp, 1984; Johns et al., 1990; Johns and Doswell, 1992*]. There are two types of severe thunderstorms in which tornadoes are produced: supercell thunderstorms and non-supercell thunderstorms.

A supercell thunderstorm is defined as a thunderstorm with a single, quasi-steady, rotating updraft, which lasts longer than the time it takes for one air parcel to flow completely through it [*Houze, 1993; Bluestein, 1993*]. The quasi-steady rotating updraft is known as a mesocyclone, and is considered a small scale, cyclonic vortex with large values of vertical vorticity. These rotating updrafts range in size from 4 to 8

km in diameter [Burgess, 1976] and have lifetimes on the order of tens of minutes to several hours. On the other hand, thunderstorms that lack a rotating updraft are known as non-supercell thunderstorms, which tend to be disorganized and typically short lived [Moller *et al.*, 1994].

There are many influences on the type of tornadic thunderstorms relating to buoyancy and shear profiles. To provide context, a review of these is presented here. The following sections present an overview of buoyancy and shear, pressure perturbations, tornadoes and tornadogenesis, supercell thunderstorms and processes leading to tornadoes and non-supercell thunderstorms and processes leading to tornado development.

## **2.1 Buoyancy and Shear Characteristics**

### **2.1.1 Instability**

Of the various measures of stability used in the operational forecasting of thunderstorm potential, the most widely used is Convective Available Potential Energy (CAPE). It is defined as the vertically integrated positive buoyancy of a rising air parcel from the level of free convection (LFC) to the equilibrium level (EL) [Blanchard, 1998]. The LFC is defined as the level above which a saturated air parcel becomes warmer than its environment and rises freely. The EL is defined as the level at which an

air parcel becomes colder than its environment and is no longer able to rise freely. By ignoring the pressure perturbation force and the entrainment of cooler/drier air into the updraft, a value for the maximum velocity an air parcel will have upon reaching the EL can be obtained from the following (Equation 3.16, from *Markowski and Richardson*, 2010):

$$w_{max} = \sqrt{2 \times CAPE}. \quad (1)$$

Using this equation for updraft strength larger values of CAPE (1500 to 3000 J kg<sup>-1</sup>) can be associated with stronger convection; however, Johns et al. (1990) found that severe thunderstorms can form in low values of CAPE (< 1500 J kg<sup>-1</sup>) when also collocated with highly sheared environments. In their review of tornado forecasting Doswell et al. (1993) stated that CAPE alone is not a good discriminator between non-supercellular and supercellular thunderstorms and rather the vertical wind shear is an important factor to consider. The results presented by Monteverdi et al. (2003) suggest that using CAPE as a forecasting discriminator between weak tornadoes (F0) to strong tornadoes (F1 and F2) in California is not possible.

### 2.1.2 Vertical Wind Shear and Positive Wind Shear

The vertical wind shear environments associated with supercell development have been studied and modeled [*Davies-Jones et al.*, 1990] and thunderstorms containing mesocyclones are found in environments with large wind shear [*Rasmussen and Blanchard*, 1998; *Weisman and Klemp*, 1982]. The wind profile in the low levels

(the storms inflow layer) and the strength of the wind shear through the mid-levels are crucial to mesocyclone induced tornadoes. Through various studies it is now apparent that supercells are associated with particular wind shear patterns.

The production of horizontal vorticity is another important aspect of wind shear, which can be tilted vertically to produce a rotating updraft. The term vorticity is defined as a vector measure of local rotation in a fluid flow [Glickman, 2000]. While there are both horizontal and vertical components to vorticity, the development of vertical vorticity is more important. Horizontal wind shear can produce horizontal vorticity and when tilted vertically can become the source of updraft rotation and vertical vorticity.

The vertical component of vorticity can be explained by the following equation [Holton, 2004]:

$$\begin{aligned} \frac{D}{Dt}(\zeta + f) = & -(\zeta + f) \left( \frac{\partial u}{\partial x} + \frac{\partial v}{\partial y} \right) - \left( \frac{\partial w}{\partial x} \frac{\partial v}{\partial z} - \frac{\partial w}{\partial y} \frac{\partial u}{\partial z} \right) \\ & + \frac{1}{p^2} \left( \frac{\partial \rho}{\partial x} \frac{\partial p}{\partial y} - \frac{\partial \rho}{\partial y} \frac{\partial p}{\partial x} \right). \quad (2) \end{aligned}$$

The first term on the right hand side of the equation is the stretching or convergence term. This represents the weakening or strengthening of local vorticity by horizontal divergence and horizontal convergence, respectively. The second term on the right hand side of the equation is the tilting term. This represents the tilting of horizontal vorticity

vertically, which is the source for vertical vorticity. The last term to the right of the equation represents vorticity generation by solenoids of pressure-density.

The development of a rotating updraft is contingent on the orientation of the horizontal shear vorticity vector to the storm-relative wind vector. When the horizontal vorticity vector is oriented perpendicular to the storm-relative wind vector the vorticity is known as “crosswise” and the development of updraft rotation is minimal. On the other hand, when the horizontal vorticity vector is oriented parallel to the storm relative wind vector, the vorticity is known as “streamwise” and the development of updraft rotation is maximized.

Strong and organized wind shear serves many purposes in supercell development. First, horizontal vorticity created by the wind shear itself may be tilted into the vertical enhancing updraft rotation [*Rotunno and Klemp, 1985*]. Second, wind shear can induce dynamic pressure perturbations within the storm due to its interactions with the updraft. As a result of these pressure perturbations the updraft may strengthen or the storm itself may change its motion [*Rotunno and Klemp, 1982*]. This change in motion of the updraft will enhance storm relative flow and assist in removing precipitation from the updraft. Lastly, the strength of wind shear in the mid-levels affects the storm motion and indirectly affects the strength of the inflow into the storm [*Brooks et al., 1993*].

The currently accepted way to diagnose the character of the vertical wind shear is by a careful analysis of the wind profile as it is depicted on the hodograph [Doswell, 1991]. One parameter used to assess the veer of the wind with height is mean shear, which is the hodograph length divided by the depth of the layer of interest [Rasmussen and Wilhelmson, 1983; Davies, 1989]. Setting the mean shear vector to a magnitude of zero for the hodograph segments in which the ground-relative winds back significantly with height, returns positive mean shear or positive shear. Thus, positive shear is evaluated by dividing the cumulative length of all hodograph segments showing neutral or clockwise curvature by the depth of the layer [Davies, 1989; Johns *et al.*, 1990]. In addition to positive shear there is a parameter called negative shear, which is evaluated in a similar fashion as positive shear, but only for hodograph segments that show neutral to counter-clockwise curvature. Both of these parameters measure the mean-inflow layer shear, which contributes to the updraft rotation and is useful in determining the structure of the vertical wind shear environment. Both of these parameters have been used extensively in supercell thunderstorm studies [Johns *et al.*, 1993; Korotky *et al.*, 1993].

### 2.1.3 The Role of Pressure Perturbations

The tilting of horizontal vorticity into updrafts of thunderstorms can create rotation in the midlevels and induce dynamic pressure perturbations. Rotunno and Klemp (1982, 1985) took these dynamic pressure perturbations and split them into a



linear and non-linear term. They found that thunderstorms that develop in a wind environment characterized by a clockwise (counterclockwise) turn of the hodograph will propagate to the right (left) of the hodograph because of effects associated with the linear pressure term. In the case of a clockwise turning hodograph the pressure perturbations that develop will move to different flanks of the updraft. This development of differential pressure perturbations on either side of the updraft produces non-hydrostatic upward directed pressure gradient accelerations located on the right flank of the storm and downward directed pressure gradient accelerations on the left flank of the storm for clockwise hodographs. Numerical simulations of these storms have shown the development of a mesolow in the inflow region of supercells created from the interaction of the updraft with these vertical pressure perturbations. The development of this mesolow acts to strengthen the inflow into the storm [Brooks *et al.*, 1993].

The non-linear term can explain storm splitting or storm movement off a straight hodograph, and storm propagation induced from rotation. For straight (unidirectional) hodographs Klemp and Wilhelmson (1978) demonstrated that storms will split into two mirror storms, one that moves to the left of the mean wind and another that moves to the right of the mean wind. The sense of rotation will be opposite for the two storms, due to the sense of the horizontal vorticity being tilted into the vertical by the updrafts. The left moving storm will rotate anticyclonically, and the right moving storm will maintain a

cyclonic rotation. The location of maximum vertical pressure perturbations on the right flank causes the storms to propagate to the right [Rotunno and Klemp, 1982].

In environments characterized by low buoyancy and high positive or negative shear, these linear pressure perturbations play a crucial role in the development of severe storms and supercells [Monteverdi and Quadros, 1994; Wicker and Cantrell, 1996]. These upward directed pressure gradient accelerations created by turning of the wind with height can augment the vertically-directed buoyancy acceleration (associated with the CAPE) by a factor of two or more [McCaul, 1993]. McCaul (1990, 1991) demonstrated that the low buoyancy and high shear environments of hurricanes can spawn tornadic supercells which develop from the non-hydrostatic vertical pressure gradients. The low buoyancy and high shear environments found in hurricanes is comparable to the observed buoyancy and shear environments of California tornadic supercell events [Monteverdi and Quadros, 1994].

## **2.2 Tornadoes and Tornadogenesis**

### **2.2.1 Definitions of Tornadoes**

The AMS Glossary defines a tornado as a “violently rotating column of air, in contact with the surface, pendant from a cumuliform cloud, and often (but not always) visible as a funnel cloud.” On average there are around one thousand tornadoes in the

United States and cause on average about 60 fatalities every year [Edwards, 2008]. Blier and Batten (1994) noted that California averages around six tornadoes every year and the average number per year is up to seven as of 2011. Through the entire period of study there have been no fatalities from tornadoes occurring in California. While any thunderstorm can produce a tornado, those associated with supercell thunderstorms account for a disproportionately large amount of the tornado related deaths, injuries, and damage [Johns and Doswell, 1992]. Tornadoes that form as a result of a series of processes that occur sequentially in a supercell thunderstorm are known as “mesocyclone induced” and those that form from non-supercellular processes are termed “non-supercell tornadoes” or “mesocyclones. Before the Doppler radar era it was believed that half of the supercells thunderstorms were tornadic. However, recent research using Doppler radars have shown that about 25% of supercells actually progress to produce a tornado [Trapp *et al.*, 2005].

Tornado intensity is determined by a survey of the damage done to structures. The rating scale, known as the Enhanced Fujita Scale (EF-scale), has criteria based upon the stringent evaluation of the engineering and structural design of the structures damaged and/or destroyed. The EF-scale is an update to the original Fujita scale, which was developed by Ted Fujita in 1971 [SPC *EF-Scale FAQ*]. The wind speed estimates determined from the damage and the subsequent rating given to each can be found in Table 2.1.

F-Scale	Wind Estimate in MPH	Typical Damage	EF-Scale	Wind Estimate in MPH
F0	45 – 78	Light Damage: Some damage to chimneys; branches broken off trees; shallow-rooted trees pushed over, sign boards damaged	EF0	65 – 85
F1	79 – 117	Moderate Damage: Peels surface off roofs; mobile homes pushed off foundations or overturned; moving autos blown off roads	EF1	86 – 110
F2	118 – 161	Considerable Damage: Roofs torn off frame houses; mobile homes demolished; boxcars overturned; large trees snapped or uprooted; light-object missiles generated; cars lifted off ground	EF2	111 – 135
F3	162 – 209	Severe Damage: Roofs and some walls torn off well-constructed houses; trains overturned; most trees in forest uprooted; heavy cars lifted off the ground and thrown	EF3	136 – 165
F4	210 – 261	Devastating Damage: Well-constructed houses leveled; structures with weak foundations blown away some distance; car thrown and large missiles generated	EF4	166 – 200
F5	262 – 317	Incredible Damage: Strong frame houses leveled off foundations and swept away; automobile-sized missiles fly through the air in excess of 100 meters (109 yards); trees debarked	EF5	Over 200

**Table 2.1** Fujita Tornado Damage Scale and Enhanced Fujita Scale implemented in 2008 (from SPC's EF-scale FAQ).

### 2.2.2 Supercell Thunderstorms and Processes Leading to Tornadoes

Supercell thunderstorms develop in environments characterized by buoyancy and moderate to strong environmental wind shear. Recent research has indicated that low level wind shear (e.g. 0-1 km AGL) may be fundamental in distinguishing between tornadic and non tornadic supercells [Markowski *et al.*, 1998a, and 1998b]. While much of the research on supercells has been conducted in the Great Plains, Lipari and Monteverdi (2000) found that wind shear in the lower levels of the atmosphere is a good discriminator between strong and weak tornadoes in California. They also suggest that wind shear estimates in the mid-levels (e.g. 0–3 km or 0–6 km) are capable of distinguishing between non-supercell and supercell type thunderstorms. Rasmussen (2003) suggests that storm relative winds in the middle troposphere are better at distinguishing between supercell environments and ordinary thunderstorm environments and that lower level winds are more important in the development of supercells and tornadoes by enhancing the strength of low level mesocyclones.

As a result of deep-layer shear and storm-relative winds, precipitation produced by the storm is moved to the forward flank. A forward-flank downdraft (FFD) develops as a result of evaporation of precipitation, which leads to negative buoyancy and cool descending air. On the upshear side of the updraft, a rear-flank downdraft (RFD) is created by the entrainment of dry air, melting and evaporation of precipitation, and non-hydrostatic pressure perturbations within the storm [Markowski and Richardson, 2010].

As the mesocyclone strengthens, precipitation is wrapped around to the west and south side of the storm and leads to the development of a “hook echo” on radar. A visualization of these supercell features can be found in Figure 2.1. The development of hook echoes and the association between them, the RFD, and tornado development has been recognized but still remains poorly understood [Markowski, 2002].

As the air in the downdrafts strike the ground, a gust front develops on either side of updraft. Along the edges of the FFD and RFD gust fronts, baroclinic generation of horizontal vorticity occurs and can enhance the environmental horizontal vorticity already present [Rotunno and Klemp, 1985; Markowski and Richardson, 2010]. This interaction between storm generated horizontal vorticity and environmental vorticity can be ingested back into the updraft and vertical accelerations associated with the updraft can further enhance rotation by vorticity stretching [Davies-Jones, 1986]. Recent field studies of supercells have revealed that only weak baroclinically generated horizontal vorticity exists along these gust fronts and in cases of very large environmental horizontal vorticity the baroclinically generated vorticity is not important [Markowski and Richardson, 2008]. There is evidence that strong cold pools from downdrafts are damaging to supercells and tornadogenesis as they limit the amount of vorticity stretching near the updraft by undercutting the updraft [Markowski et al., 2002, 2003; Shabbott and Markowski, 2006; Grzych et al., 2007]. However, it could be that

some amount of baroclinity is needed for tornadogenesis to occur, but too much can be damaging to the storm.

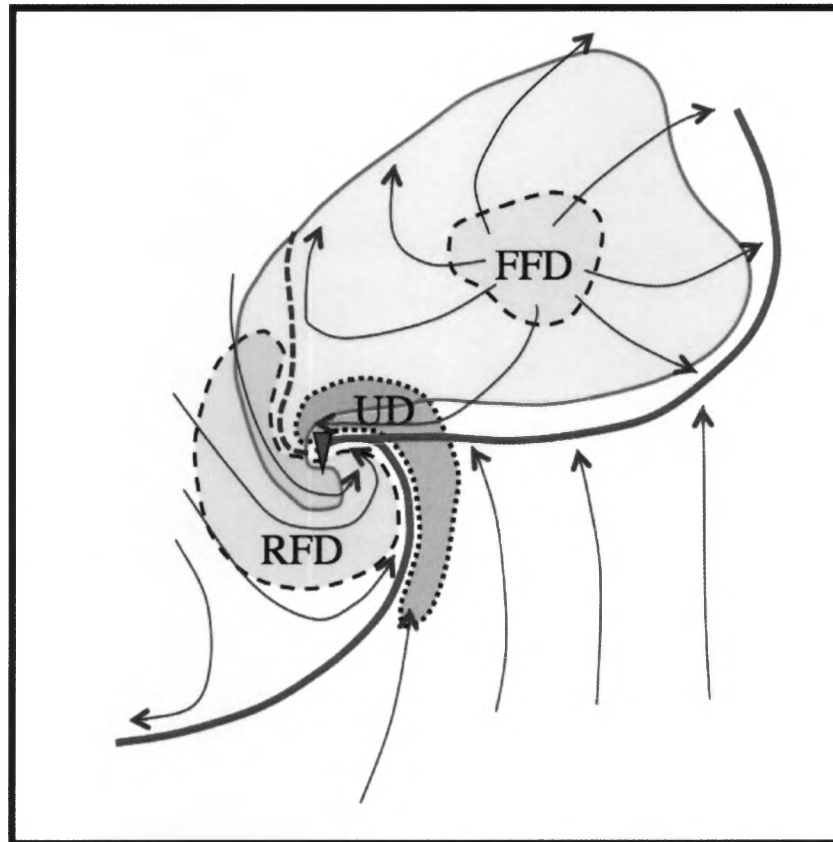


**Figure 2.1** Conceptual model of a “Classic” supercell at the surface developed by Lemon and Doswell (1979) through radar studies, surface analysis and visual observations. The green shading encompasses the radar echo; the thunderstorm gust front structure is depicted by the thick blue line. The surface positions of the updraft location (UD) is stippled red, the rear flank downdraft (RFD) and the forward flank downdraft (FFD) are in blue. Streamlines depicting ground-relative flow are shown as lines terminating with arrowheads. The tornado location (if present) is shown by the red triangle. (Figure 2 from Doswell, 2012).

It is true that supercell thunderstorms already have significant vertical vorticity and helicity present in the lower and midlevels of the troposphere. However, the tilting of horizontal vorticity vertically into the updraft by itself is not enough to produce strong vertical vorticity at the surface because air is rising away from the surface [Markowski and Richardson, 2008]. In supercells, the formation of downdrafts and their interaction with the surface can create enhanced vertical vorticity through stretching of the vertical vorticity, which can lead to tornadogenesis as seen in Figure 2.2 [Davies-Jones and Brooks, 1993; Davies-Jones et al., 2001; Markowski and Richardson, 2008].

(a) vertical vorticity is initially negligible at the surface

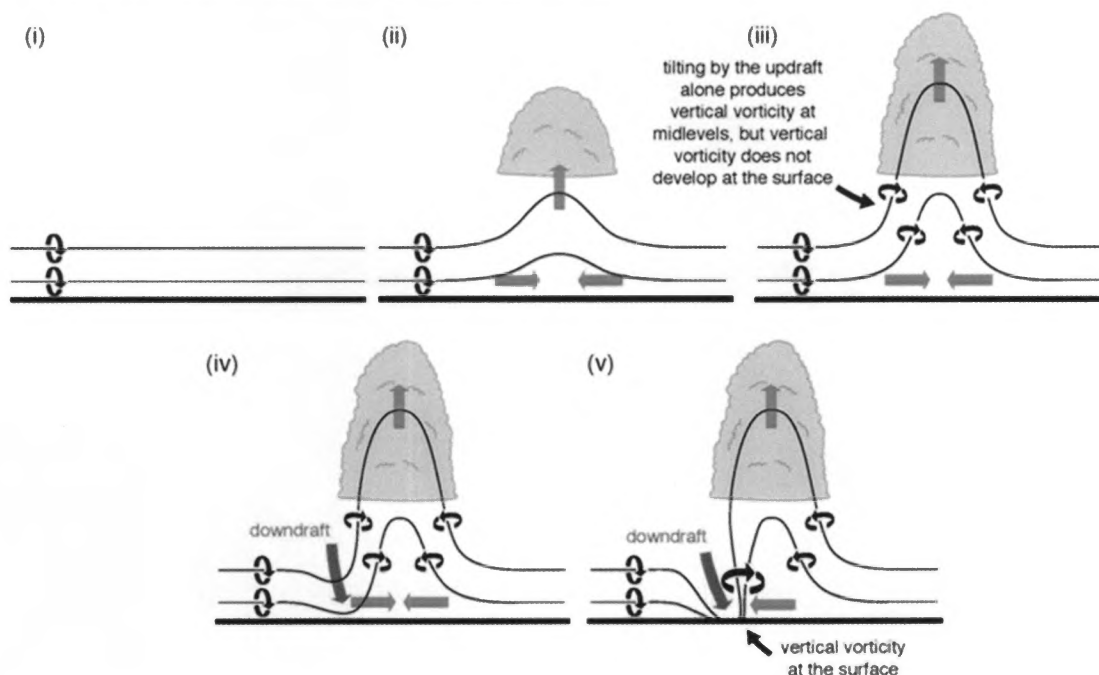


**Figure 2.2** Schematic showing the tilting of vortex tubes or vortex lines toward the surface coincident with the formation of a downdraft (Figure 10.3 from Markowski and Richardson, 2010)



Numerical simulations of supercell thunderstorms have shown that tornadoes occur as soon as an RFD develops. However, the RFD has to have temperature characteristics similar to that of the inflow air into the storm; otherwise a tornado will not develop [Brandes, 1978; Rotunno and Klemp, 1985; Walko, 1993; Grasso and Cotton, 1995; Wicker and Wilhelmson, 1995; Alderman *et al.*, 1999].

An additional supercellular process linked to tornadogenesis is the dynamic-pipe effect (DPE) [Trapp and Davies-Jones, 1997]. This can be viewed as a vortex in cyclostrophic balance where there is little to no inflow radially into the core, due solely to the balance between the pressure gradient force and the centrifugal force. This allows for upward (downward) accelerations from below (above) the core of the vortex due to vertical pressure gradient force induced from the rotation of the vortex [Trapp and Davies-Jones, 1997]. This effect can be thought of like a “pipe” drawing air towards the lower end of the vortex [Smith and Leslie, 1979]. As a result of air being drawn into the bottom of the vortex, a concentration of ambient vertical vorticity develops and a new level of cyclostrophic balance develops at both ends of the pipe. This process continues to propagate downwards until a vortex reaches the surface. The interaction of the vortex with the surface produces friction, slows the rotation, and allows for additional convergence and vorticity stretching immediately near the ground [Rotunno, 1986; Rasmussen *et al.*, 1994] and eventually a tornado is produced at the surface.

### 2.2.3 Non-Supercellular Thunderstorms and Processes Leading to Tornadoes

When thunderstorms develop in a weak shear environment they tend to be weak and disorganized, with a few exceptions [Moller *et al.*, 1994]. Non-supercell thunderstorms can be briefly strong and be associated with large hail and misocyclone tornadoes. A misocyclone tornado is defined as: “a horizontal vortex with a width of between 40 m and 4 km” [AMS Glossary, 2012]. These types of storms go through their life cycles rather quickly. Any severe weather associated with these storms will occur immediately prior to the storms dissipating. The development of severe weather is related to the interaction of the outflow from the storms with each other as well as interactions with any additional boundaries already present in the area. An increase in the amount of buoyancy or shear can lead to more organized convection [Moller *et al.*, 1994]. An example of more organized convection is an organized multicell storm in the form of a squall line. Any severe weather that does develop with these organized storms may last for a longer period of time than with an unorganized storm.

Tornadogenesis in non-supercell thunderstorms can originate in the lower levels as small vortices created from shearing instability along convergence lines [Wilson, 1986]. The interaction of subsynoptic boundaries or convergence zones with these thunderstorms may produce misocyclone tornadoes, also known as landspout tornadoes or high based cold core funnel clouds [Cooley, 1978; Bluestein, 1979; Burgess and

Donaldson, 1979; Monteverdi *et al.*, 1988]. An example of this interaction is depicted in Figure 2.3.

(b) **preexisting vertical vorticity at the surface**

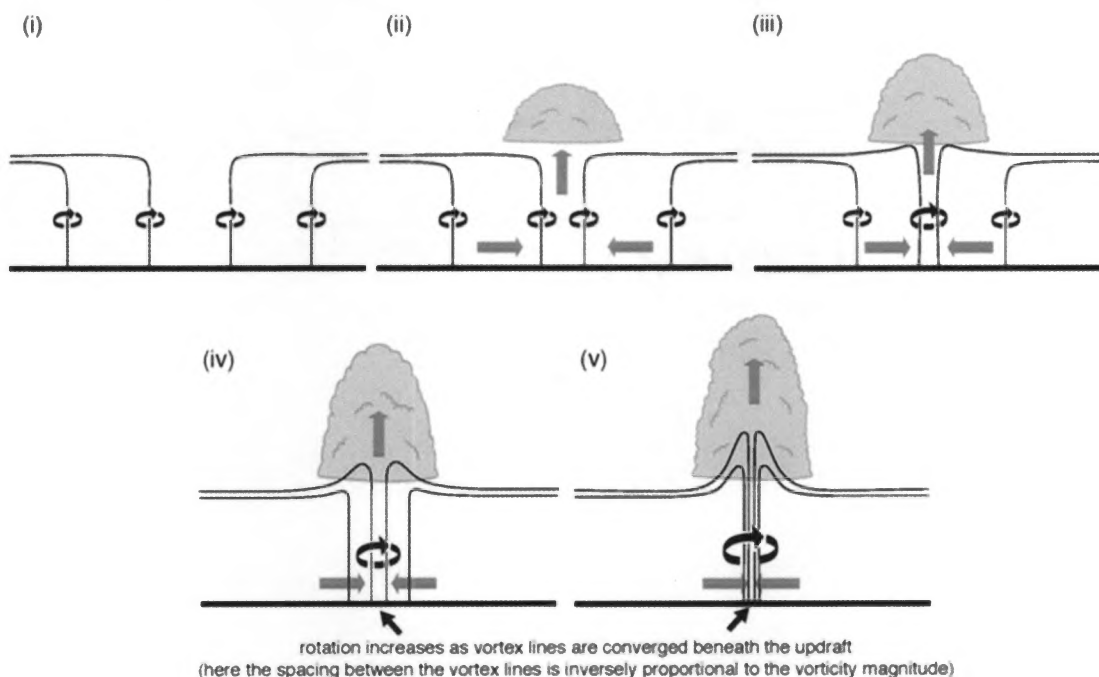


**Figure 2.3** A schematic representation of convergence zones or topographically generated vorticity, which is stretched vertically by the formation of an updraft. During this stretching additional horizontal vorticity (not shown) may be ingested into the updraft and a stronger vortex at the lower levels can form (Figure 10.3 from Markowski and Richardson, 2010)

Bluestein (1985) introduced the term “landspout” to describe a boundary-layer forced tornado developing under a line of rapidly growing cumulus towers. This insight stemmed from observations of vortex development in Oklahoma during benign synoptic conditions. Landspouts typically occur in weak shear environments, along an almost

stationary, pre-existing front-like boundary. Waterspouts, as observed by Golden (1971), are believed to form in a similar manner, in which the development of a vortex or tornado is directly related to the local stretching of vorticity by the intersection of outflows and the updraft. The processes leading to the development of these lower level vortices show similarities to the processes leading to the development of a mesocyclone-induced tornado [Davies-Jones and Brooks, 1993; Doswell and Burgess, 1993]. The interaction of baroclinically generated vorticity that develops from downdrafts in supercell tornadoes is also found during the development of non-supercellular tornadoes. In the processes leading to non-supercellular tornadoes neighboring rain showers provide some of the baroclinically generated vorticity, which is tilted vertically on the cool-air side of these low-level vortices.

The tornadic vortices found in cold-core funnels or cold pool vortices are similar to those found in waterspouts [Cooley, 1978; Bluestein, 1979; Burgess and Donaldson, 1979; Monteverdi *et al.*, 1988]. The processes involved in the formation of these cold pool vortices can explain the funnel clouds observed in California during postfrontal synoptic events [Monteverdi *et al.*, 1988]. One of the first references to cold pool vortices in California was that of Cooley (1978), who described forming funnel clouds as being associated with cold pools aloft. Sources for these types of tornadic events can be from postfrontal troughs and squall line convective lines.

Carbone (1982, 1983) noted updrafts associated with linear convection in the Central Valley that were being forced along a frontal zone, where locally enhanced circulation centers developed along the frontal boundary. One of the thunderstorms that formed along the convective line eventually became a supercell, and a tornado developed below an area of deep cyclonic rotation. It was determined that the tornado developed as a result of the intersection of outflow from the bowed segments of the squall line. The lower level environmental conditions leading to the development of the low level rotation were similar to those observed for non-supercellular tornadoes elsewhere. However, the development of a supercell suggests that the environment possessed satisfactory deep layer shear but the sequential steps leading to the development of a mesocyclone induced tornado did not appear to apply in this case.

The number of research projects focusing on non-supercell tornadoes has grown recently. These studies have found that the strength of these tornadoes is not limited to the low end of the Fujita scale [*Wakimoto*, 1983; *Wakimoto and Wilson*, 1989; *Johns and Doswell*, 1992] and damage from these events can reach as high as F4 [*Wakimoto*, 1983]. It has been suggested that non-supercell tornadoes might account for a significant percent of the F0 and F1 rated tornadoes [*Brady and Szoke*, 1988]. Many of the non-supercell tornadoes occurring in the Los Angeles Basin were documented as waterspouts that moved onshore [*Golden*, 1973]. Non-supercellular tornadogenesis has been presumed to account for a large portion of the tornadoes occurring in California

[*Blier and Batten*, 1994]. However, Lipari and Monteverdi (2000) found that the non-supercellular processes might explain or account for only 40% of all the tornado occurrences in their study.

### 3. Tornadic Thunderstorms in California

#### 3.1 Climatology of Tornado Events

The notion that tornadoes exist and are a part of the climatology of California has been recognized in the literature [e.g. *Hales*, 1985; *Blier and Batten*, 1994; *Monteverdi and Quadros*, 1994; *Monteverdi et al.*, 2003]. During their climatological analysis of tornado occurrences in California, Blier and Batten (1994) identified the Central Valley (containing the Sacramento and San Joaquin Valley's) as well as the Los Angeles Basin as regions with high tornado frequencies compared to other areas of the state. The climatology of California tornado occurrences is both similar and different than those observed in the Great Plains and Midwest. As shown in Figure 3.1a tornadoes occurring in California are generally limited to cool season (November to March). This is in contrast to the seasonal peak of tornadoes in the Great Plains (April to June or late spring to early summer). However, both regions have a peak occurrence of tornadoes during the afternoon hours as shown in Figure 3.1b. This coincides with an increase in CAPE through diurnal heating that is often associated with the initiation and evolution of tornadic thunderstorms in both parts of the country [*Blier and Batten*, 1994; *Johns and Doswell*, 1992].

One interesting feature of note about the monthly distribution of tornadoes is the peak in tornado frequency during the month of March (as shown in Figure 3.1a). As suggested by Blier and Batten (1994) this could be due to the combination of a strong

jet stream still present over California and increased low-level diurnal heating due to higher sun angles. This increase in diurnal heating during the late winter and early spring months in combination with a moisture rich low level environment allows more buoyancy to be present over California.

There are stark differences between the tornadoes observed in the Great Plains and in California. The average duration of tornado events in California is much shorter than those found in the Great Plains, and both the path length and the path width are markedly smaller on average than those found elsewhere in the United States (shown in Table 3.1). The amount of damage produced by California tornadoes on average is generally less than the tornado events in the Great Plains. This can explain why the

Location	Mean Path Length	Mean Path Width
F0 California Tornadoes	~1.0 km (0.6 miles)	27.4 m (29.9 yards)
F1 California Tornadoes	2.5 km (1.6 miles)	51.1 m (55.9 yards)
F2 California Tornadoes	5.43 km (3.4 miles)	95.4 m (104.3 yards)
Great Plains Tornadoes	>6.4 km (>4.0 miles)	>155.4 m (>170 yards)

**Table 3.1** Mean path length and width of California and Great Plains tornadoes. (Data for Great Plains tornadoes from Smith and Mirabella (1972) and data for California tornadoes was taken from this study)



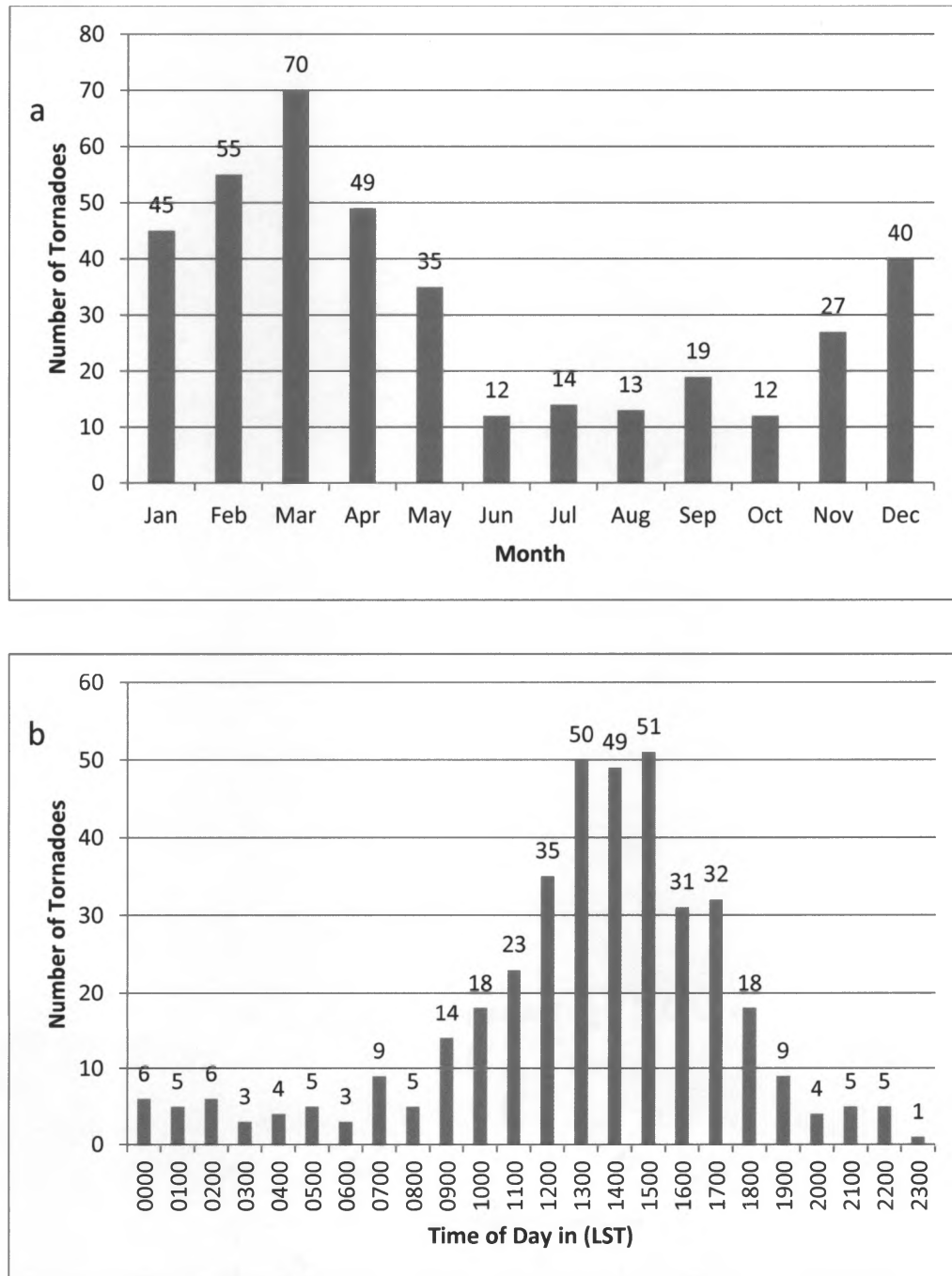


**Figure 3.1** (a) Monthly distributions of California tornadoes (indicated by total column height and numerical value at top of column) for the period 1951–2011. (b) Hourly distribution of California tornadoes for the period 1951–2011.

majority of California tornadoes are rated F0 or F1 for damage; F2 cases are uncommon, and only two F3 events have been recorded. No events rated higher than F3 have been reported in California.

Since 1951 there have been no reported fatalities with any tornado occurring in California. The strength of tornadoes during this time period ranges from F0 to F3 and the number of tornadoes assigned a particular F-rating can be found in Table 3.2. There were 39 tornadoes where an F-rating was not assigned. According to SPC California has on average more tornadoes than any other West Coast state and the average number of tornadoes occurring over the study period is 6.5 [SPC SVRGIS, 2012].

F-rating	Number of Tornadoes for each F-rating
F Unknown	39
F0	234
F1	93
F2	23
F3	2

**Table 3.2** The number of tornado assigned a particular F-rating during the period 1951–2011 is shown here.

As is the case elsewhere in the United States, severe thunderstorms, in particular supercells, are associated with significant damage in California. One such example is of a supercell moving through Fresno, California on March 5, 1994 where an estimated \$12 million dollars of damage was produced from large hail [*Monteverdi and Johnson, 1996*]. In addition some residential damage and one injury was associated with a pair of anticyclonically rotating tornadoes on May 4, 1998, in the cities of Sunnyvale (F2 rating) and Los Altos (F1 rating), California [*Monteverdi et al., 2001*].

### **3.2 Synoptic and Subsynoptic Features of Northern and Central California**

#### **Tornadic Storms**

The synoptic conditions present for northern and central California severe weather events have been identified in numerous studies. The typical pattern and locations of synoptic and subsynoptic features for these events is shown schematically in (Figure 3.2) [*Braun and Monteverdi, 1991; Monteverdi and Quadros, 1994*]. A short-wave trough in the middle and upper troposphere progresses through the main long wave trough located off the coast of California. Associated with this short-wave trough is a surface cold front and a jet streak embedded in the jet stream pattern. As the cold front passes through northern and central California, differential cold air advection (CAA) is observed. [*Monteverdi and Quadros, 1994*]. The CAA acts to destabilize the

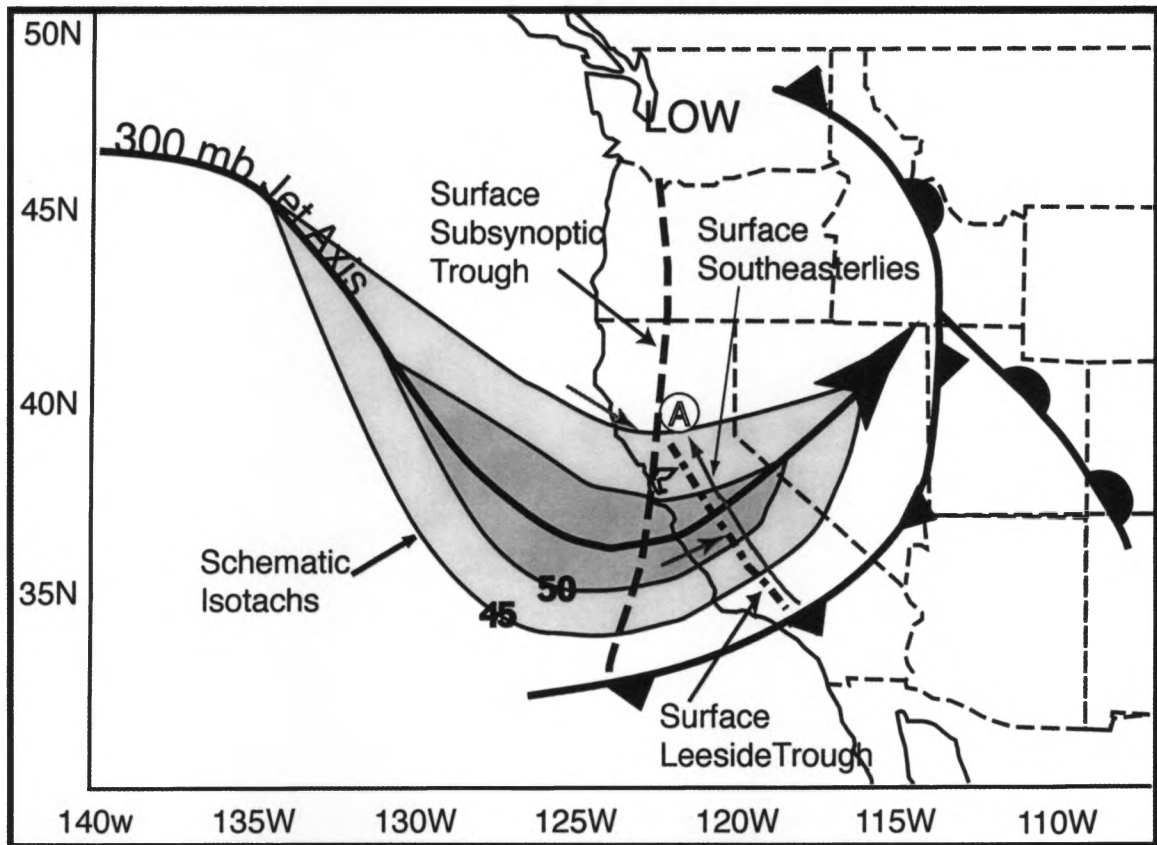


**Figure 3.2.** Schematic chart showing the location of major synoptic and subsynoptic features associated with tornado events in California's Central Valley. Isotachs are labeled in meters per second. The location of the subsiding flow west of the leaside trough and surface southeasterlies in central and eastern Central Valley are shown by light gray arrows. The circled "A" indicates the major focus for supercell thunderstorm formation. (From Braun and Monteverdi, 1991; Monteverdi and Quadros, 1994).

middle tropospheric layers, which in turn decreases static stabilities and enhances the ability for vertical motions to develop through quasigeostrophic forces.

As the short-wave trough progresses through California the jet streaks left exit region (depicted in Figure 3.2 as a circled "A") begins to move over California. This

region of the jet streak, in addition to the right entrance region, has been identified to be associated with divergence in the upper troposphere. Convergence at the surface works in concert with upper tropospheric divergence, and as a result vertical motions develop in the middle troposphere [McNulty, 1978; Bluestein and Thomas, 1984; Kocin *et al.*, 1986; Meier, 1993]. While this synoptic forcing may be weak, combining this with stronger mesoscale forcing can lead to strong upward motions.

Differential cyclonic vorticity advection (CVA) out ahead of the progressing short-wave provides forcing for upward vertical velocities in the middle troposphere [Reed and Blier, 1986; Monteverdi *et al.*, 1988; Braun and Monteverdi, 1991; Monteverdi and Quadros, 1994; Monteverdi and Johnson, 1996]. These upward motions in the middle troposphere layer-lift air vertically, destabilize the environment, and increase the amount of CAPE present in the atmosphere. This lowers the level of free convection (LFC) making it easier for turbulent motions to bring a surface air parcel to the LFC.

A synoptic scale surface and mid-tropospheric trough moving through California is often linked to the development of cold sector convection. Upward motions and decreased atmospheric stability associated with the trough are evidenced by an area of enhanced open-cell cumulus approaching the coast of California [Reed and Blier, 1986; Monteverdi *et al.*, 1988]. While the synoptic-scale features create a favorable thermodynamic and shear environment for convection to develop, an

additional mechanism must act to initiate convection. Subsynoptic scale features that are created by the interaction of the synoptic scale atmospheric flow with the unique topography of northern and central California can further enhance the buoyancy and shear environments. The next few sections will outline these subsynoptic or mesoscale features.

### 3.2.1 Leaside troughs

During periods of significant cross-mountain flow over the Coast Range and Sierra Nevada (as shown in Figure 3.2 above) a leaside trough (also known as mesoscale low pressure area) develops in the middle and lower third of the troposphere of the Central Valley [*Braun and Monteverdi*, 1991; *Monteverdi and Quadros*, 1994]. As a result of the development of this leaside trough, winds in the Central Valley turn southerly/southwesterly on the east side of the trough axis and west or northwesterly on the west side of the trough axis. These southerly/southeasterly winds often advect moisture pooled in the southern portions of the Central Valley northward, raise dewpoints at the surface, and provide an area of moisture convergence [*Monteverdi and Quadros*, 1994]. Enhanced moisture convergence at the surface can lead to a destabilization of the boundary layer and an increase in the buoyancy of an air parcel.

As a result of the change in wind directions due to this leaside trough, the wind shear environment over the Central Valley can become more favorable for severe weather. These southeast surface winds are related to stronger low-level wind shear (0-1

km and 0-2 km) on the eastern side of the trough axis [*Monteverdi and Quadros, 1994*]. An example of the leeside trough enhancing the wind shear can be found in Lipari (2000). In their study of thirty tornadoes in California they found the sample average mean 0-1 km and 0-2 km positive shear values for F1 and F2 tornadoes to be  $18.9 \times 10^{-3} \text{ s}^{-1}$  and  $10.1 \times 10^{-3} \text{ s}^{-1}$  respectively. These values fall into the range of positive shear values associated with strong and violent supercell tornadoes found elsewhere in the country by Johns et al. (1993).

### 3.2.2 Topographically Generated Helicity

The unique orientation of the Coast Range and Sierra Nevada in northern and central California sets the stage for low-level wind channeling, which can enhance the helicity environment in the Central Valley. The Bay Area is also susceptible to this type of low-level channeled flow that can augment or enhance the shear and/or helicity environment. Sea breeze and Bay breeze boundaries can develop and generate low-level vorticity as well. An example of this low-level helicity enhancement is from Monteverdi et al. (2001), where a boundary generated from a sea breeze interacted with a developing thunderstorm and two tornadoes were spawned (the Los Gatos F1 and Sunnyvale F2) both of which were rotating anticyclonically.

Another example where channeled flow had a role in the development of a supercell was in the September 1986 F2 tornado in the northern Sacramento Valley [*Braun and Monteverdi, 1991*]. The Sutter Buttes, a topographic feature found in the

Sacramento Valley enhanced the shear profile through channeling of the wind around this feature. This produced a strongly veered wind profile, which when combined with ongoing convection led to the development of the tornado [*Braun and Monteverdi, 1991*].

### 3.2.3 Barrier Jet-Induced Low Level Shear

Low-level jets induced by terrain in the eastern half of the Central Valley have been documented by Parish (1982) to form in the synoptic patterns described earlier. During the passage of middle and upper tropospheric troughs, cross-mountain wind flow develops and is topographically dammed by the Sierra Nevada. Initially stable air is then forced to rise and as a result a low pressure field develops along the mountains. This leads to the development of a jet found in the 600-1500 m AGL layer flowing parallel to the mountains [*Parish, 1982*]. The jet has an average width of 100 km and southeasterly wind speeds can exceed 50 knots at the top of this jet, about 1500 m AGL [*Lipari, 2000*].

The development of this jet contributes to local warm air advection (WAA) in the region behind the synoptic-scale cold front and leads to further destabilization of the environment. The combination of southerly surface winds resulting from the leeside trough and the low-level jet strengthen the wind shear profile of the environment. As a result, a strongly veered hodograph in the lower to mid-troposphere can develop, which is favorable for the development of supercells [*Monteverdi and Quadros, 1994*].



#### 3.2.4 Postfrontal troughs

The subsynoptic surface trough or postfrontal trough as depicted in (Figure 3.2) can be subtle and difficult to resolve on the basis of an analysis of wind data obtained from the sparse observation network alone. However, this feature can be seen in the Central Valley as a moisture or wind shift line resulting from collisions of southerly flow in the southern half of the valley with cooler/drier northwest flow from the northwestern portion. In some cases these troughs resemble squall lines on radar or can be seen by visible satellite imagery. They generally move across the state towards the southeast and when combined with a leeside trough can locally enhance the development of severe thunderstorms.

### 3.3 Synoptic and Subsynoptic Features of Southern California Tornadoic Storms

The unique terrain of the Los Angeles Basin and southern California has been found to be a key player in the development of severe weather along the coast. In this area, the topographic influences on severe convection appear to have a greater effect than anywhere else in the state [*LaDochy and Brown, 2001*]. However, the synoptic patterns in which the severe thunderstorms of southern California develop differ very little from the synoptic conditions found in the Central Valley tornado cases. Hales (1985) concluded that the southern California thunderstorms are postfrontal, with the main synoptic low pressure area located off the coast of Central California (Figure 3.3).

Cold air advection behind the front acts to destabilize the environment in the middle and lower troposphere. Low-level moisture and surface temperatures increase as a result of the long over water trajectory of the air [Hales, 1985]. Weak to moderate CAPE develops in response to these factors providing an environment favorable for convective initiation. An area of CVA is present over the area and through quasigeostrophic forcing for upward motion, the air is layer lifted and the amount of CAPE present over the area is increased. When these factors are in place over the region, the interaction of the convectively favorable environment with the unique topography can initiate convection.

Recent research conducted by Small et al. (2009) has suggested an additional synoptic environment favorable for severe thunderstorm development in southern California, which differs slightly from the model suggested by Hales (1985). They describe a synoptic low pressure centered to the east of the Sierra Nevada Mountain range with a cold front located further east than the location depicted by Hales (1985). Embedded in the broad 500 mb trough in this pattern is what can be described as a “tropospheric vortex river”, which Small et al. (2009) define as a long ribbon of vortex maxima with values larger than  $24 \times 10^{-5} \text{ s}^{-1}$  that stretch for 750 –1000 miles or more. Downstream from each of these slow moving vorticity centers is an area of CVA. When this area of CVA is present for an extended period of time, quasigeostrophically-forced upward motions develop. This area of enhanced lift creates an environment favorable for the development of thunderstorms. These storms then interact with the complex



**Figure 3.3** Schematic showing the mean position of the jet stream (arrow) and cold front at the time of tornado occurrences. The hatched area indicated the typical location of the low centers at the surface, 850, 700, and 500 mb levels (Hales, 1985)

terrain and can form supercells [Small *et al.*, 2009]. In some cases, additional synoptic environments lacking a strong jet stream and a progressive shortwave can lead to

conditions favorable for the development of severe thunderstorms. These conditions will be addressed in section 3.2.4.

### **3.3.1 Topographically Induced Low-Level Jet of the LA Basin**

The topography of southern California, especially that of the LA Basin is such that mountains border the area to the north and east. These ranges rise vertically up to 1600 m to the north and 1200 m to the east. As surface low pressure systems approach the coast, southerly to southwesterly wind flow develops off the coast. These winds then interact with the topography to create stronger southerly flow immediately south of the LA Basin, southeasterly flow in the LA Basin, and easterly flow along the Santa Barbara coast [*Blier and Batten, 1994*]. This wind pattern along the coast can extend vertically up to 850 mb (the height of the mountains immediately surrounding the coast). This topographically enhanced wind flow along the coast coupled with southwesterly to westerly flow above 850 mb can create a veering wind shear profile with height, which is favorable for the development of strong thunderstorms and supercells.

### **3.3.2 Convergence Zones and Topographically Generated Helicity**

As has been seen, the interaction of the synoptic environment with the topography of northern and central California can create a favorable environment for convective development in local mesoscale foci in the Central Valley. The topography of southern California plays an even larger role in the development of a convectively

favorable environment and provides more mesoscale opportunities for convective initiation. As wind moves off the Pacific Ocean and interacts with the terrain of southern California, frictional convergence develops at the immediate coast. This convergence can locally enhance upward vertical motions needed for convection to initiate. Additional topographical features can provide centers for convective initiation, produce locally favorable shear profiles, and generate areas of focused horizontal and vertical vorticity known as convergence zones.

The islands located off the coast of southern California can create convergence zones on the downwind side of the islands. Another zone of convergence is found in the LA Basin on the downwind side of the Palos Verde Peninsula (which has a peak elevation of 452 m). Low-level wind channeling by the coastal mountains can also create localized areas of convergence (as shown in Figure 3.4). One such area is the Elsinore Convergence Zone (ECZ), bordered to the north and east by the 3500 m Transverse Mountain range and the 1740 m Santa Ana Mountains to the west [Aldrich, 1970]. During the late morning and afternoon, sea breezes develop and are able to move inland around the northern and southern ends of the Santa Ana Mountains and collide, forming the ECZ [Small *et al.*, 2009]. The May 22, 2008 events over this area produced several tornadoes, which were created by the interaction of the ECZ with thunderstorm outflow boundaries. These interactions created local areas of enhanced horizontal and

vertical vorticity, which was able to be tilted vertically and stretched by thunderstorm updrafts.

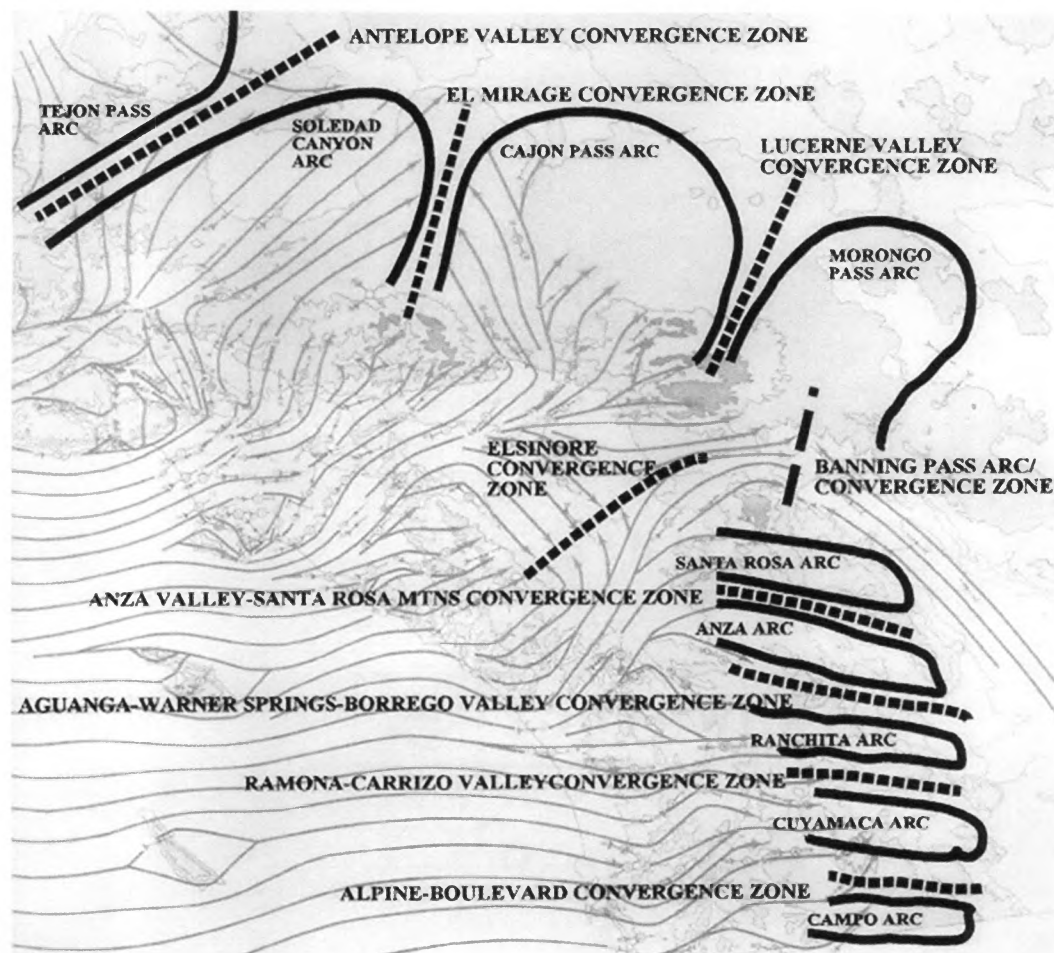


**Figure 3.4** Map of Southern California showing the convergence zones developing during westerly flow regimes (Figure 6. from Small et al. 2000).

### 3.3.3 Thunderstorms in the Southeastern Deserts of California

The rainy season for most of California is at a peak during the months of November through March, and little to no rain is observed during the months of May through September. However, during the summer months the southwestern deserts of the United States receive a considerable amount of the yearly rainfall. This is due to the development of what is known as the North American Monsoon (NA monsoon). While the term monsoon is often linked to the monsoons over the Indian subcontinent, monsoon circulations are present over other areas of the globe.

In the transition from winter to summer, the jet stream retreats northward and in this process the subtropical high pressure system also shifts northward. Intense surface heating over the Mojave Desert during the summer months creates an area of rising air and a surface low pressure system known as a thermal low. The northward drift of the subtropical high and the development of the thermal low act in concert to create southerly to southeasterly flow over the desert southwest. This southerly flow pulls moisture northward out of three main sources: the Gulf of Mexico, the Gulf of California, and the Pacific Ocean [*Hales, 1972*].

Air with higher dewpoints from these source areas advected into the hot deserts, can produce very large CAPE values ( $\text{CAPE} > 4000 \text{ J kg}^{-1}$ ). When this air interacts with the topography of high deserts, intense thunderstorms can form. This storm environment is often characterized by very large CAPE but weak deep layer wind shear.

However, outflow from these thunderstorms can interact with the mountainous terrain and local convergence zones can develop. When these thunderstorms pass over an area of enhanced convergence, any vorticity present may be stretched vertically, and a non-supercellular tornado may develop. In cases where strong outflow from thunderstorms is present, the lower levels of the atmosphere will have large values of low-level wind shear. When these areas of large low-level shear are collocated with weak to moderate deep-layer wind shear, short-lived supercells can develop and produce a brief mesocyclone induced tornado.



## 4. Data and Methodology

### 4.1 Overview

Estimating the thermodynamic and wind shear characteristics in the proximity of developing thunderstorms has been a subject of some debate in the literature [*Brooks et al.*, 1994]. Since the late 1990's or so the use of model-estimated soundings and hodographs has become an accepted procedure, although there are contentions that the temperature/moisture and wind profiles obtained that way do not meaningfully estimate actual proximity environments any better than subjective techniques [*Doswell and Evans*, 2003].

Although it is now possible to create soundings for past events using the National Center for Atmospheric Research's North American Regional Reanalysis (NARR) data set, [*Mesinger et al.*, 2006] the soundings and hodographs obtained do not have great vertical resolution. Also, the NARR data do not extend past 1979. Brooks et al. (1994) suggest that a consistent approach be used when establishing a data base of proximity soundings and hodographs.

Since the NARR data do not extend across the period of record for which California tornadoes have been observed, the methodology used for this study is a combination of subjective and objective criteria in modification of existing radiosonde data. The general procedure was outlined in Monteverdi et al. (2003) and used in many previous studies of tornadic thunderstorms (see, e.g., *Braun and Monteverdi*, 1991).

This procedure was adapted specifically for this study and will be summarized in detail in the next sections.

#### **4.2 Construction of Proximity Soundings and Hodographs**

The ultimate goal in using proximity soundings is to estimate or sample the near storm environment. Ensuring that these soundings are actually representative of the storm environment can be problematic [Brooks *et al.*, 1994a]. The problems with using proximity soundings as a means of sampling the storm environment are that storms and ultimately tornadoes do not form in homogeneous environments [Doswell, 1982]. Thus, the manner in which a proximity sounding is selected, takes into account that the environment is likely characterized by some changes and therefore only requires a sounding to be close in space and time to the storm event. Darkow (1969) used the following criteria to define a proximity sounding: 1. the radiosonde release must be within 105 minutes prior to the tornado event; 2. the radiosonde release point must be within 50 statute miles of the tornado; and 3. the sounding must not be contaminated by convection.

More recent studies using proximity soundings, such as Rasmussen and Wilhelmson (1983), Davies and Johns (1993), Brooks *et al.* (1994a), Rasmussen and Blanchard (1998), Craven (2001), Brooks and Craven (2002), and Brooks *et al.* (2003), have used a different set of criteria for selecting proximity soundings. They suggest that

a sounding must be within 46 statute miles of the tornado event and be within one and half hours of the event. Many of these studies had thresholds of CAPE values no less than  $150 \text{ J kg}^{-1}$  or CAPE values which are less than the value of the CIN, in which case the soundings were eliminated. These thresholds, however, are not useful for California events because many of the events are characterized by low CAPE.

Recent proximity soundings have also been conducted using point soundings generated by the Rapid Update Cycle computer model. The model data to perform this type of sounding analysis goes back to 2002 and could be used for all California events since 2002. But in an effort to be consistent through the entire dataset this was not used. However, this is may be used in future research.

#### **4.2.1 Proximity Sounding and Hodograph Estimation Procedure**

In order to efficiently process the large number of proximity soundings and hodographs needed for this study, the author devised a set of procedures that were coded as shell scripts to automate the process. Each tornado event had an identification number assigned to it and the following data was obtained from a spreadsheet for all California events: month, day, year, hour, latitude, and longitude. One of the shell scripts searched for the nearest three sounding sites for any sounding data that existed 24 hours prior and 12 hours after each tornado event. Every sounding that fell within this range was collected and put into a file based on the tornado identification number. This collection method was able to locate upwards of 15–20 individual soundings for

each tornado event, depending on the frequency of radiosonde launches and time of the tornado event.

The next shell script collected searched for the nearest ten observing sites to each particular tornado event. Hourly surface observations were collected for the four hours before and two hours after a tornado event for each of the ten sites. This comprised of a collection of seven hourly surface observations of (temperature, dewpoint, wind direction, and wind speed) for each site. The elevation of each observation site was collected in addition to the hourly surface observations. This was then grouped together and listed from nearest to furthest from the tornado event. The data was then organized and put into a file ordered by the decade the tornado event fell. Finally, the hourly surface observations for the nearest surface site that occurred the hour before a tornado event were then checked to ensure there was data available the hour before the tornado. If no data existed for the hour before a tornado, the shell script would then check the second closest observing site for data available the hour before the tornado event. Once the script found a valid set of surface observations for the nearest surface site the temperature, dewpoint, wind direction and wind speed from the surface observation site were then inserted into and replaced the data at the base of all soundings gathered for each tornado event [*Hales and Doswell, 1982; Monteverdi, 1993*].

The initial data collection process closely followed to the procedure devised by Darkow (1969). However, the author found that due to the lack of available sounding data a different procedure would need to be devised. Thus, a more in depth and thorough analysis was needed to ensure that each proximity sounding accurately represented the near storm environment. The author used the data from the initial collection process but this data was modified using the following set of procedures described below.

Soundings in this study were selected on the basis of the following criteria: (a) when a tornado occurred between 1800 Coordinated Universal Time (UTC) and 0600 UTC the 0000 UTC sounding was selected; (b) otherwise a 1200 UTC sounding was selected to construct the proximity sounding. However, since it was not possible to use this selection method for every tornado event the author analyzed each event individually in order to select the sounding which best represented the near storm environment.

The selection criteria for soundings were modified using the following methods:

1. The Medford, OR sounding (KMFR) was selected for tornadoes occurring along the Northern California coast such as Eureka, Crescent City, and others. The KMFR sounding has a ground elevation of 405 m and was lowered to sea level to represent the actual storm environment of the coastal tornado events. In one instance a sounding was generated between KMFR

and KOAK using the interpolation feature found on the software program called Rawinsonde Observation (RAOB) cross section tool.

2. In some cases the 0000 UTC radiosonde had the best near storm environment wind profile but the temperature and dewpoint profile were not accurate. Therefore the 1200 UTC temperature and dewpoint profile were selected in combination with the 0000 UTC wind profile. In a few cases the 1200 UTC sounding had the best wind profile and the 0000 UTC sounding had the most representative temperature profile. In this case the 0000 UTC temperature profile was used but with the 1200 UTC wind profile. These combinations were all performed using the “Merge” soundings tool in RAOB.
3. For tornado events occurring in southeastern California or in very elevated terrain, the sounding selected had the temperature, dewpoint, and wind profile removed from the surface or base of the sounding up to the elevation of the tornado event.
4. For a few tornado events occurring in the southeastern deserts soundings from neighboring states were selected, such as: KVEF/KDRA (Las Vegas, NV/Desert Rock, NV), KTUS (Tucson, AZ), and KFLG (Flagstaff, AZ). These were mainly selected for events occurring during the summer months, when the North American Monsoon is present.

5. For tornadoes that occurred between synoptic radiosonde launches (1200 UTC and 0000 UTC) and neither sounding accurately represented the near storm environment; the merge tool in RAOB was used to combine or average the soundings together.
6. For tornado events that occurred in slightly elevated terrain the nearest sounding was selected and then a feature in RAOB called “Lift sounding” was used to lift the entire sounding as if it were being forced upwards by terrain. Each sounding was lifted to the height of the tornado event to best represent the near storm environment.

For those cases in which the tornado location differed so much from the closest observing site that the data at that site would not be representative of the proximity conditions, observations from a time up to four hours before a tornado event were used. This was done because the surface observation the hour before the tornado event may not have been representative due to convective outflow, bad data, no data observed, and other factors. Observing sites at elevations not representative of the elevation of the tornado were removed and another site was selected, which was then subject to the same checks to ensure the observations were representative of the near storm environment.

After a sounding was selected using the above selection criteria, the selected surface observations (temperature, dewpoint, wind speed, and wind direction) using the

criteria above was inserted into and replaced the data at the base of the sounding. Upon completion of the above steps it was necessary to smooth the new atmospheric profile to eliminate superadiabatic temperature lapse rates and/or artificial dewpoint lapse rates created from replacing the hourly observations with the data at the base of the sounding. In modifying the wind profile, the smoothing method suggested by Monteverdi (1993) and Monteverdi and Quadros (1994) was used. The profiles of soundings in coastal valleys and those in the Central Valley are smoothly adjusted in both direction and speed from the surface observation to about 500–1500 m above MSL; i.e. depending on the height of the Coast Range and nearby mountains at the latitude of interest. The wind profiles for coastal southern California and the southeastern desert tornadic events were also smoothly adjusted vertically from 200–2000 m above MSL depending on the height of the mountains and nearby topographic features surrounding the tornadic event.

Then, RAOB was used to generate the buoyancy and shear parameters for each tornado event using the completed sounding and hodograph. Additional parameters were generated using RAOB and are listed in Table 4.1. Lastly, a composite sounding of temperature and dewpoint and a composite hodograph was constructed for each of the separate F-ratings. The Merge tool found in RAOB was able to generate each of these composite soundings and composite hodographs.



## **4.2.2 Sources of Data**

### **4.2.2.1 Hourly Surface Observations**

The hourly surface observation data were obtained from the National Climatic Data Centers (NCDC) online archive of global surface observations dating back to 1901. These sites were then paired down using a geographic information system software program called ArcGIS (ESRI, 2012) to select sites in California including the buoys adjacent to the coast as shown in (Figure 4.1). Each individual observing contains an entire year of surface observations. In addition to the date and time of the surface observations an inventory of the location and elevation of each site is maintained by NCDC. There are hourly observations of wind speed, wind direction, temperature, and

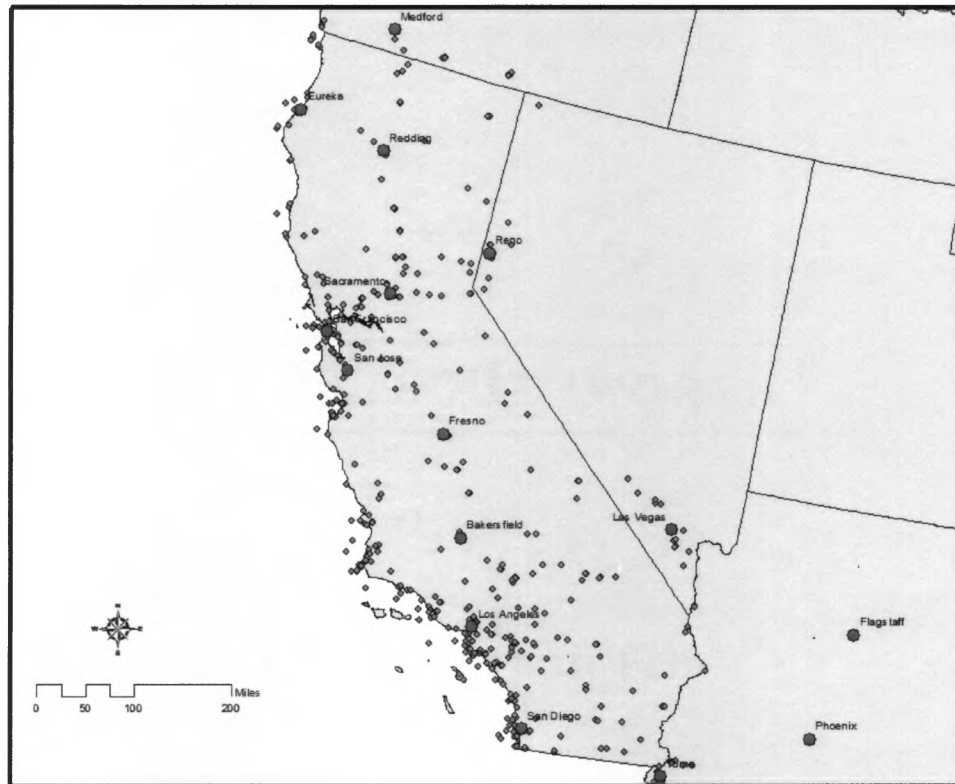


**Figure 4.1** Map displaying the location of all available hourly surface observing sites. The surface observing sites are indicated by a small yellow circle and cities with large populations are indicated by red circles.

dewpoint, which are listed by the year, month, day, hour, and minute (in UTC time) they were taken.

#### 4.2.2.2 Radiosonde Data

The radiosonde data was obtained from a CD and DVD-ROM set entitled Rawinsonde Data of North America 1946-1996. Sounding data from 1997-2011 was obtained from an online source maintained by the Forecast Systems Laboratory (FSL)

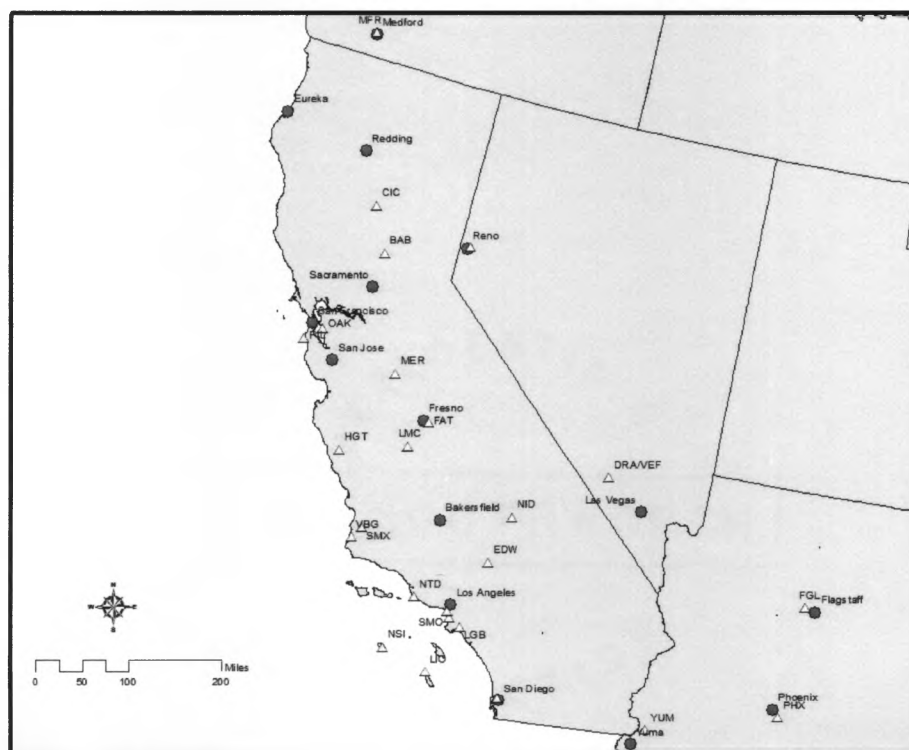


**Figure 4.2** Map displaying the location of all available radiosonde launch sites. The radiosonde sites are indicated by a yellow triangle and cities with large populations are indicated by a red circle.

at <http://raob.fsl.noaa.gov>. The data contained in each of these two sources consisted of every radiosonde launch in North America for the particular time period available on

the CD and DVD set. A map of the location of each of the sounding sites used in this study can be found in Figure 4.2. Very few of the sites found in California have data available for every tornado event, which became a complication in the selection of certain sounding sites for a particular event. A few radiosonde sites had consistent launches in the 1950's, 1960's, and 1970's but no launches after that or some sites had sporadic launches throughout the time period, which made the selection process difficult.

#### 4.2.2.3 Tornado Locations and Data

The tornado location data was obtained from SPC's Severe Geographical Information System (SVRGIS) webpage. The author compared the SPC tornado reports against the reports found in the *Storm Data* publication for any errors present in either database and only four errors were found between the databases. These events have the following identifiers (tornado id #'s 26, 75, 85, and 391). The first event (#26) was located in the wrong county, the second (#75) had the incorrect longitude, the third (#85) also had the wrong longitude, and the fourth (#391) was in the *Storm Data* database but not listed in the SPC GIS database. The author notes that in some instances two different tornado reports in close proximity may in fact be one tornado event, but all events listed in the SVRGIS database were used.

The tornado attributes consisted of: the tornado number in that year, latitude and longitude of touchdown, path length, path width, time of occurrence, estimate of

damage, number of injuries, number of fatalities, and an estimate if possible of the magnitude or strength of the tornado event and given an F-scale rating. The exact locations for all tornadic events are provided in Figure 1.1 found in Chapter 1. An F-scale rating is missing for 39 tornadoes, all of which occurred before 1981. The exact time of a tornado occurring was provided in Central Standard Time (CST), which was converted to (UTC) for use in the shell script. The tornado times were also converted into Pacific Standard Time (PST) or Local Standard Time (LST) for additional analysis.

#### **4.2.2.4 Synoptically Analyzed Maps and Upper Air Charts**

The daily upper air charts and subjectively analyzed surface charts used by the author are archived by NOAA Central Library's U.S. Daily Weather Maps Project. These maps are made available through an online source (<http://www.hpc.ncep.noaa.gov/dwm/dwm.shtml>) and are organized into a seven day collection of maps. However, any maps before 1967 are not organized by week but rather limited to a specific day.

### **4.3 Selection and Computation Parameters**

#### **4.3.1 Overview**

Because supercells account for a disproportionately large amount of the severe weather observed in the United States, it is important for forecasters to be able to

quickly identify the environments that are favorable for the development of supercell thunderstorms. Meteorologists and researchers have developed measurements or indices that are helpful to forecasters in determining the types of synoptic environments that are more favorable for the development of supercells and tornadoes. In Table 4.1 is a list of commonly used indices that will be analyzed in this study.

#### 4.3.2 CAPE

Previous studies of CAPE related to the development of severe thunderstorms found that CAPE values greater than  $1500 \text{ J kg}^{-1}$  are related to supercells [*Weisman and Klemp*, 1986]. It was Johns et al. (1990), however, that found supercell thunderstorms can form in environments characterized by low CAPE but high wind shear. Many of the tornadic thunderstorms found in California can be characterized by this low CAPE and high wind shear environment.

There are three different methods of calculating CAPE which are: 1. the surface based method (SBCAPE), 2. the parcel layer method, and 3. the most unstable method (MUCAPE). The SBCAPE method uses the temperature and dewpoint of the surface parcel to calculate the buoyancy available. The parcel layer method averages values of temperature and mixing ratio in a defined layer (usually the lowest 100 mb) to estimate a chosen parcels temperature and dewpoint. The temperature and dewpoint of the most unstable parcel found in the lowest 300 mb of the troposphere are used in the MUCAPE method [*Doswell and Rasmussen*, 1994]. The use of the MUCAPE method generally

provides the maximum amount of buoyancy found in the environment and was the method used to calculate CAPE for all tornado cases in this study.

Parameters	Units	Range Favorable for Supercells
CAPE	$\text{J kg}^{-1}$	Any Positive Value
CAPE 0 to 3 km AGL	$\text{J kg}^{-1}$	Any Positive Value
Convective Inhibition	$\text{J kg}^{-1}$	$< 150$
0 to 1 km Wind shear	$\text{s}^{-1} (\text{ms}^{-1}/\Delta z)$	$> 8.0 \times 10^{-3}$
0 to 6 km Wind shear	$\text{s}^{-1} (\text{ms}^{-1}/\Delta z)$	$> 3.0 \times 10^{-3}$
0 to 1 km storm relative helicity	$\text{m}^2\text{s}^{-2}$	$> 100$
0 to 3 km storm relative helicity	$\text{m}^2\text{s}^{-2}$	$> 250$
Energy Helicity Index (EHI)	Dimensionless	$> 1-2$
Bulk Richardson Number	Dimensionless	10 to 45
Vorticity Generation Parameter	$\text{ms}^{-2}$	$> 0.2$

**Table 4.1** List of parameters calculated for each tornado proximity sounding

#### 4.3.3 0–3 km CAPE

A study conducted by McCaul (1991) found that a larger distribution of CAPE in the lowest 3 km of the atmosphere can provide low-level accelerations needed for development of low-level rotation. It has been found that 0–3 km CAPE is able to distinguish between tornadic supercells and non-tornadic supercells, but lacks the ability to discriminate between non-supercell thunderstorms and supercells [Rasmussen, 2003]. This suggests that some 0–3 km CAPE is necessary for tornadogenesis and that the interaction of this positive buoyancy with low level wind shear can increase the low level updraft strength [Rasmussen, 2003]. Values of 0–3 km CAPE of  $60 \text{ J kg}^{-1}$  or greater have been linked to environments favorable for tornadic storms [Davies, 2001; Rasmussen, 2003].

#### 4.3.4 Convective Inhibition

Convective Inhibition (CIN) is a measure of the strength of the “capping,” or amount of energy needed to lift an air parcel vertically from a level to its LFC [AMS Glossary, 2012]. Bluestein (1993) stated that an air parcel forced upward in an area of CIN will exhibit decelerations proportional to the magnitude of the CIN. Research conducted by Rasmussen and Blanchard (1998) and Davies (2004) found that large values of CIN do not provide an environment favorable for the development of tornadoes.



#### 4.3.5 Wind Shear

The values of wind shear are calculated as the vector difference between wind velocities at two different levels in the atmosphere. They are generally measured from the surface to a specified height (e.g. 1 km, 3 km, and 6 km) AGL. Another name for wind shear between two levels is Bulk Shear [*Rasmussen and Blanchard*, 1998]. In this study bulk shear was calculated between the surface and two different levels: 1 km and 6 km AGL, which can be referred to as low level and deep shear, respectively. Recent studies involving proximity soundings have found that bulk shear in the lower levels of the atmosphere (0–1 km AGL) to be a clear distinguisher between tornadic soundings and normal thunderstorm soundings [*Craven et al.*, 2002; *Markowski et al.*, 2002].

Positive shear is defined as the portion of the hodograph for which the winds either veer from one layer to the next, or stay the same. This is calculated from the surface to a specified layer (e.g. 1 km, 3 km, and 6 km) AGL. The magnitude or strength of the positive shear has been found to a good discriminator between stronger F2 or greater tornado events [*Davies and Johns*, 1993] and Monteverdi et al. (2003) found them to be better at discriminating between F1/F2 tornado events and the F0 tornado events here in California.

While most supercells have cyclonically turning hodograph, those that are anticyclonic would be characterized by hodographs with a backing wind shear vector with height. Shear parameters with similar absolute values, but with a negative sign

(e.g. *Monteverdi et al.*, 2003). This would appear as counterclockwise turning of the hodograph with height and can be referred to as negative shear and is calculated for the same levels as positive shear. Due to the complex terrain of California and the presence of both positive and negative shear in certain storm environments an attempt was made in the study to treat cases of negative shear as positive shear by taking the absolute value of the negative shear. These absolute value shears are calculated from the surface to a specified layer (e.g. 1 km and 6 km) AGL. The magnitude or strength of positive shear has been found to be a good discriminator between stronger F2 or greater tornado events [*Davies and Johns*, 1993] and Monteverdi et al. (2003) found positive shear to be better at discriminating between F1/F2 tornado events and the F0 tornado events here in California. Thus the magnitudes of the absolute value shears will be compared against the positive shear values found in the literature. The wind shear itself plays an important role in supercell development but additional factors such as storm motion can influence the strength of the rotation.

#### 4.3.6 Storm-relative helicity

The combination of vertical wind shear and the storm's motion have been found to be associated with an updraft that is able to tilt horizontal vorticity vertically, producing what is known as a "helical" updraft [*Browning and Landry*, 1963; *Johns and Doswell*, 1992]. A measure of the helical nature of the updraft is storm-relative helicity (SRH), which has been found to be a useful parameter in forecasting the rotational

characteristics of thunderstorms [*Davies-Jones et al*, 1990]. Markowski et al. (1998a) define SRH as the amount streamwise vorticity generated from vertical wind shear available in the inflow environment of a thunderstorm and is integrated over a certain depth (e.g. 0-1 km or 0-3 km). In a study of tornado proximity soundings conducted by Kerr and Darkow (1996) they found that the magnitude of 0-3 km SRH values increase systematically with the F-scale rating of tornadoes. Rasmussen (2003) concluded that SRH values from 0-1 km are a better discriminator between tornadic and non-tornadic supercells. However, in the study by Markowski et al. (1998a) they suggest that helicity values vary rapidly both temporally and spatially making the 0-1 km SRH nearly impossible to measure.

While, much of these studies have been conducted in the Great Plains, Monteverdi and Quadros (1994) found that the values of 0-3 km SRH associated with California tornadic storms are comparable to those found in the Great Plains. Additionally, 0-1 km SRH values for F1 and F2 rated California tornadoes are significantly higher than the 0-1 km SRH values for F0 rated tornadoes [*Monteverdi et al.*, 2003]. The values of 0-1 km and 0-3 km SRH that have been identified as useful distinguishers between tornadic and non-tornadic supercells can be found in (Table 4.1).

An important aspect in determining the potential for rotating updrafts is the exact motion storms will follow. Knowing the storm motion will produce a better estimate of the SRH values. However, due to the large dataset and inability to determine

the exact storm motion for all cases the method of predicting the storm motion as described by Bunkers et al. (2000) was used. This method has been shown to be superior to other methods of determining the forecasted storm motion and is able to account for non-typical hodographs such as the counterclockwise turning hodographs [Bunkers et al., 2000].

#### 4.3.7 Bulk Richardson Number

The combined effects of buoyancy and shear on storm structure were examined first by Weisman and Klemp (1982, 1984) and they defined a parameter known as the bulk Richardson number (BRN). They found this index useful to discriminate between thunderstorm types (e.g. single-cell, multicell, and supercell). In environments with CAPE values between 1500 and 3500 J kg<sup>-1</sup> and moderate to strong wind shear BRN values range from (15 – 40) and have correlated well with the development of supercells [Weisman and Klemp, 1986]. However, for large values of CAPE (e.g. > 4000 J kg<sup>-1</sup>) the BRN number is large (>40) and is unable to discriminate between thunderstorm types [Stensrud et al., 1997]. In environments characterized by low values of CAPE (e.g. < 1500 J kg<sup>-1</sup>) and moderate to strong wind shear have BRN values of (2–14), which are similar to those found by Monteverdi et al. (2003). Using BRN values that fall into this range are not useful, from a forecasting standpoint in discriminating between supercells and non-supercell [Johns et al., 1993].

#### 4.3.8 Energy Helicity Index

In proximity sounding analyses conducted by Rasmussen and Blanchard (1998) a parameter known as the Energy Helicity Index (EHI) was developed. The EHI combines CAPE and storm-relative helicity over a given layer and is able to provide an estimate of the strength of rotation in storms. They found that for 0-3 km EHI values larger than 1.0 there is potential for supercells to develop and for values larger than 2.0 there is an enhanced probability of tornadic supercells. The 0-3 km EHI is useful in distinguishing between tornadic supercells and general thunderstorms rather than between strong and weak tornadoes [Rasmussen, 2003]. In the study conducted by Edwards and Thompson (2000) they found a mean value of 0-1 km EHI of 2.4 for strong tornadoes and a value of 1.1 for weak tornadoes. Rasmussen (2003) also suggests that instead of using 0-3 km EHI use 0-1 km EHI as a more precise means of discriminating between strong and weak tornadoes.

#### 4.3.9 Vorticity Generation Parameter

The idea of tilting and stretching horizontal vorticity vertically into a thunderstorm lead Rasmussen and Blanchard (1998) to develop a parameter known as Vorticity Generation Parameter (VGP). They concluded that the VGP parameter was a useful discriminator between storm types. The VGP was also able to distinguish between strong and weak tornadoes in a similar fashion to the EHI parameter but to a

lesser extent. Hamill and Church (2000) tested the VGP again with a different dataset but determined that the results were similar to that of Rasmussen and Blanchard (1998).

#### 4.4 Statistical Procedures

The wind shear values for all tornado events were collected. The exact nature of the wind shear either positive or negative is important in determining rotation of storms but the magnitude or strength of the wind shear is of greater concern. Thus, the author used the absolute value of the negative shears and compared these values to the positive shear values. The total CAPE values used represent the larger of either the MUCAPE or the SBCAPE. While this does provide a possible over estimation of the total CAPE present for each tornado event, this was necessary procedure due to problems discovered in the calculation of CAPE by RAOB. The mean values of all variables used in the study were calculated and then compared.

The Levene's test for equal variances was used to ensure each parameter was from the same population. Then, an independent two-sample *t*-test for CAPE, absolute shear, SRH, and all other parameters was performed. This independent sample *t*-test was performed assuming equal and unequal variances (depending on the results of Levene's test) and was calculated at the  $p < 0.05$  or (5% confidence level). These tests can reveal statistically significant relationships between each of these parameters, which

will allow for a potential determination of the independent or dependent nature of each parameter as it pertains to tornado intensity.

## 5. Results of the Study

The procedures outlined in section 4.2.1 were utilized to determine the environmental buoyancy and shear for each tornado event shown in Figure 1.1. A proximity sounding and hodograph was constructed for each tornadic thunderstorm, and the calculations summarized in section 4.3 were performed for each event.

The results are presented in several ways to aid in the discussion and in the statistical analyses summarized below. The entire set of convective, rotational and the thermodynamic parameters calculated as discussed in section 4.3 are presented in Appendix 1 Tables A1-A6. The table represents the compilation of all the base results grouped by the decade the tornado occurred (e.g. 1950s, 1960s, 1970s, 1980s, 1990s, and 2000s). The data taken from 2011 is grouped with the values for the 2000s decade.

The buoyancy and shear calculations were used to develop buoyancy and shear “space” for the tornado events stratified by F-scale rating, as is the procedure followed in many studies of Great Plains tornado events, and also that utilized in Monteverdi et al. (2003). Tables of convective and rotational parameters were obtained for each set of tornado events, grouped by F-scale rating. One exception to this procedure involved the combination of the F2 and F3 events, since there were only two F3 events in the record. Thus, three groupings were defined, and termed the F0, F1, and F2/F3 “bins”.

The buoyancy and shear values for each bin then made subgroupings. The means for each of these subgroupings then could be evaluated on the basis of statistical



techniques summarized in section 4.4. To compare the distribution of buoyancy and shear parameters for each bin box and whisker plots were generated for each bin. Box and whisker plots represent a powerful tool to visualize the distribution of data. Each box represents the range of values for the middle 50% of the distributions. The bottom of each box denotes the 1<sup>st</sup> quartile (25<sup>th</sup> percentile), the top line of the box denotes the 3<sup>rd</sup> quartile (75<sup>th</sup> percentile), the line inside the box denotes the 50<sup>th</sup> percentile or median value. The bottom whisker denotes the 10<sup>th</sup> percentile while the top whisker denotes the 90<sup>th</sup> percentile.

## **5.1 Buoyancy and Shear Parameters for California tornadoes 1951–2011**

### **5.1.1 Analysis of Buoyancy**

The first step in analyzing the tornado proximity soundings was to determine if buoyancy alone could discriminate between weak and strong tornadoes. The CAPE values for the California tornado ranged from less than 100 J kg<sup>-1</sup> to 5600 J kg<sup>-1</sup> (see Tables A1-A6 in Appendix 1) Most of the values shown in Figure 5.1 are not greater than 1000 J kg<sup>-1</sup>. The average CAPE value for all the events was 588 J kg<sup>-1</sup>. This value is indicative of the relatively weak buoyancy environments associated with tornadic thunderstorms in the state and compares favorably with the average value of CAPE (465 J kg<sup>-1</sup>) Lipari (2000) found for a much smaller data set.

CAPE values were stratified on the basis of value observed for each event and grouped into the F0, F1, and F2/F3 bins (Figure 5.1). As shown in Figure 5.1 the median value at the center of each box are less than  $250 \text{ J kg}^{-1}$  for each of these bins. The mean values were compared using the independent t-test as described in section 4.4. This test failed to show any statistically significant differences in the median values between any of the bins. In fact, the greatest median and maximum CAPE values were associated with the F0 bin. Thus, there is no statistical justification for organizing the cases on the basis of CAPE alone.

While CAPE is clearly important in determining the strength of the thunderstorm updrafts, the magnitude of CAPE found in the layer just above the LFC, in the 0-3 km layer has been shown to be associated with tornado formation elsewhere in the county. Thus, the next logical step is to examine to what degree this is valid for California tornado events. The mean values of 0-3 km CAPE were tested for statistically significant differences using the independent t-test as described in section 4.4. The independent t-test test failed to find any statistically significant difference in the average magnitude of this measure of lower tropospheric buoyancy.

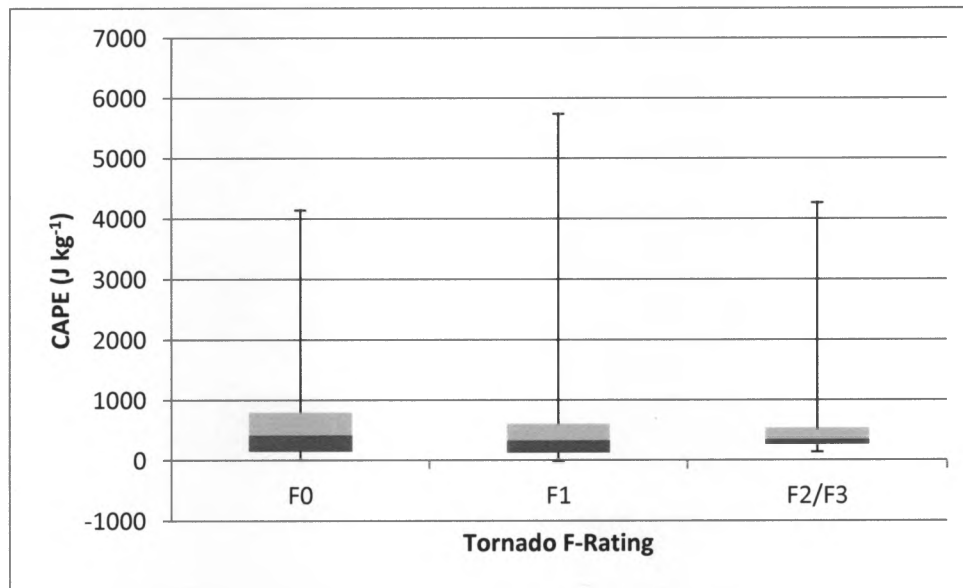


**Figure 5.1** Box and Whisker plot of Total CAPE for each F-scale rating (F0, F1, with F2's and F3's binned together). The red box represents the 50% quartile with the mean value represented by the top of the red box. The green box represents the 75% quartile. The bottom whisker represents the lowest value of CAPE and the top whisker represents the highest value of CAPE.

The results show that CAPE values alone, whether in the layer from the Level of Free Convection to the Equilibrium Level, or smaller layers in the lower troposphere, were unrelated to the intensity of California tornadoes during the study period. The overall result is consistent with that found by Monteverdi et al. (2003) for their smaller California data set and is also consistent with what is known of the buoyancy associated with Great Plains tornadic thunderstorms.

The results of this study with respect to the relation of the magnitude of 0-3 km CAPE to tornado intensity are not consistent with what is known about the relation of

tornado strength to the vertical distribution of CAPE in Great Plains tornadic thunderstorms. Thus, it appears that no parameter associated with buoyancy can be used to distinguish between the intensity of tornadoes in California, at least for the tornadic events considered in this study.

#### **5.1.2 Analysis of Absolute Value Shear and Bulk Shear**

One of the primary goals of the study was to determine the environmental shear magnitudes for all California tornado events and to determine if these values were consistent with those found by Monteverdi et al. (2003) for a smaller sample of tornado events in California. Another important issue was whether or not the shear magnitudes coincided with those reported in the literature for supercell tornado events in the Great Plains.

Monteverdi et al. (2003) compared the shear parameters observed to be critical thresholds for tornadic supercells in the Great Plains with those they found for the California events in the period 1990-1994. They found that, as is true for Great Plains tornadic supercells, the stronger the 0-6 km deep layer shear, the more likely the storm was to produce the stronger tornado events. But the deep layer shear in and of itself was insufficient. As in the Great Plains, this favorable deep layer shear must occur in concert with favorable low level shear (i.e., 0-1 km shear) for those supercells that proceed through the supercell cascade to tornadogenesis. In fact, they found that low level shear values for the California tornado events they studied exceeded those found

for Great Plains tornadic storms by a considerable margin, and they hypothesized that the larger values of low level shear in California might be related to the topographic effects summarized in Section 3.2 and 3.3.

The smaller sample of tornado events considered in their study consisted entirely of shear environments characterized by straight and anticyclonically curved hodographs, while hodographs developed for the larger dataset in the present study also included a few hodographs with cyclonic curvature. The curvature of the hodograph is important in determining the sense of rotation of the updraft but the magnitude of the shear value is of greater importance in determining whether the rotation, no matter what its sense, will exceed the threshold values for supercells. To circumvent problems in the arithmetic averaging procedure used to determine the positive shear values, the author converted any negative shear to absolute values. Thus, in the calculations summarized in this and succeeding sections, those analyses involving positive shear profiles really included some cases for which the absolute value of the shear was “counted” as positive. This shear will be hereafter in this study referred to as Absolute Value positive SHearR (ABVSHR). The calculations of bulk shear were unaffected by this issue.

An examination of the relationship of shear to the tornado intensity was performed using the mean ABVSHR and bulk shear values for each of the respective bins. Statistical analyses of the data indicated, as expected, that both ABVSHR and bulk shear values increases from F0 to F1 and from F1 to F2/F3. The largest increase in the

average values for 0-1 km ABVSHR and bulk shear occurred between the F1 to F2/F3 bins. In the 0-6 km layer ABVSHR the large increase in the average values was also found to be between the F1 to F2/F3 bins. However, in the 0-6 km layer bulk shear the largest increase occurred between the F0 to F1 bins with a small difference in the F1 and F2/F3 bins.

Box and whisker plots of ABVSHR (Figure 5.2) and bulk shear (Figure 5.3) values highlight the difference in shear environments between each bin. These plots show the difference between shear environments for the F2/F3 cases compared to those for the F0 and F1 events. The median value of 0-1 km and 0-6 km ABVSHR for the F2/F3 cases is about an entire quartile higher than for the F0 and F1 events. This difference in shear environments is also evident in the bulk shear but to a lesser extent, meaning that the median value for F2/F3 events in bulk shear is not as markedly different as it is in ABVSHR.

The ABVSHR in the 0–1 km layer for all tornado events (F0, F1, and F2/F3) exhibited higher magnitudes than the 0-6 km layer of ABVSHR. These 0-1 km values ranged from  $1.1 \times 10^{-3} \text{ s}^{-1}$  to  $34.2 \times 10^{-3} \text{ s}^{-1}$  for all tornado events. The mean values for the F0 events was  $10.8 \times 10^{-3} \text{ s}^{-1}$ , the mean value for the F1 events was  $11.4 \times 10^{-3} \text{ s}^{-1}$ , and the mean for the F2/F3 events was  $14.9 \times 10^{-3} \text{ s}^{-1}$ . While the mean for the F2/F3 and

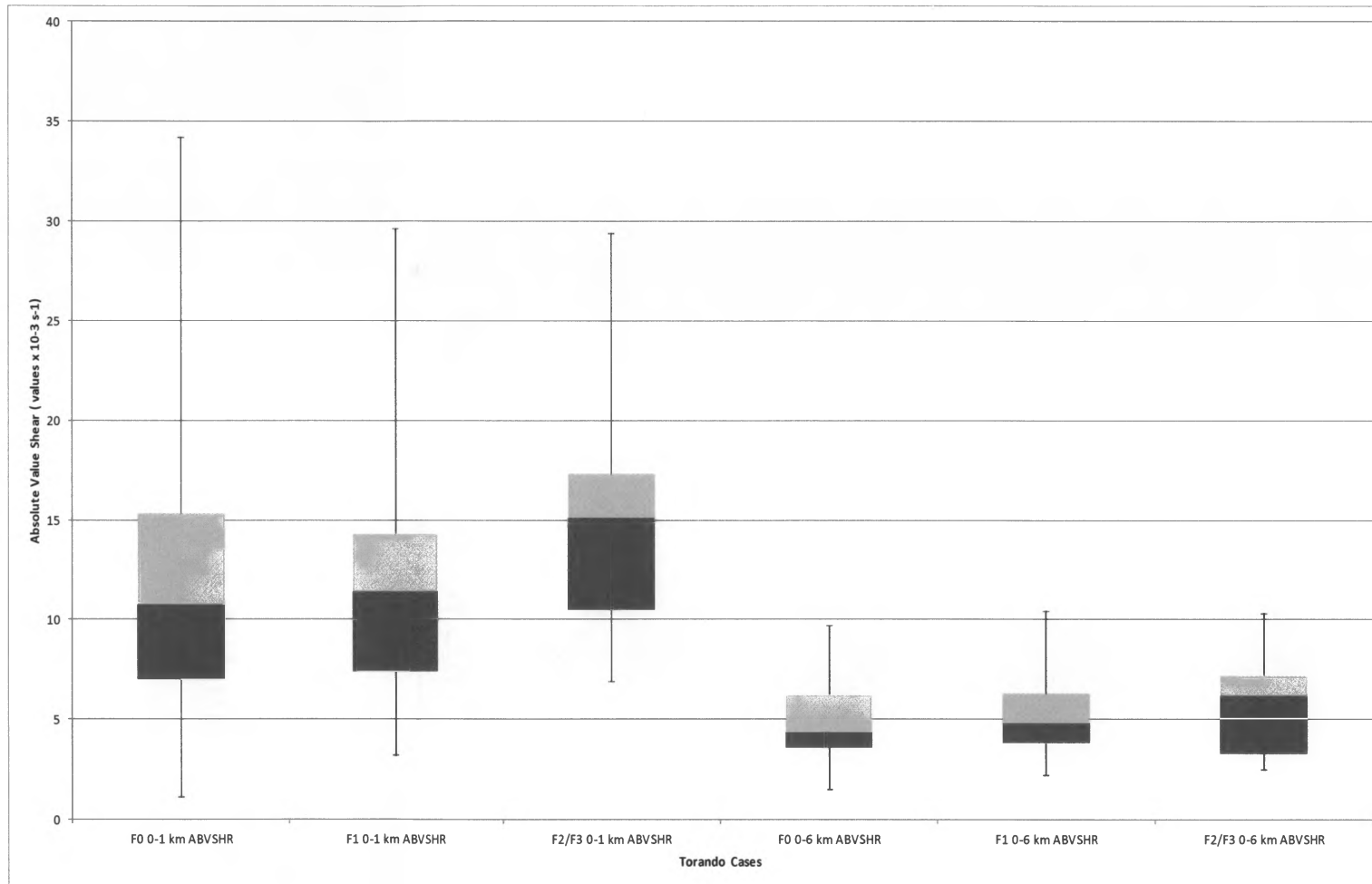


**Figure 5.2** Maximum, 75<sup>th</sup> percentile (green box), 25<sup>th</sup> percentile (red box), and minimum values of Absolute Value Shear observed for F0, F1, and F2/F3 bins

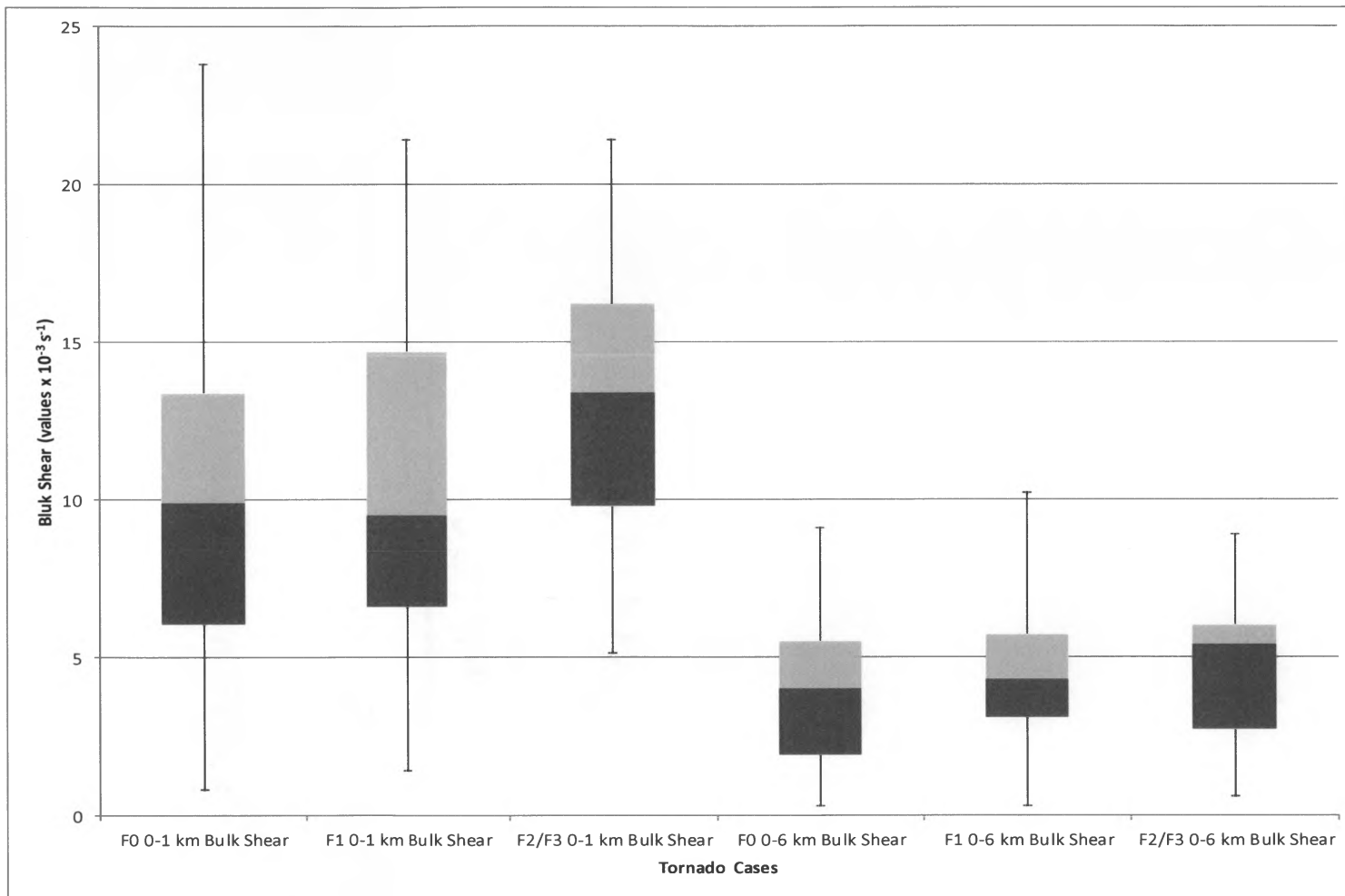


**Figure 5.3** Maximum, 75<sup>th</sup> percentile (green box), 25<sup>th</sup> percentile (red box), and minimum values of Bulk Shear observed for F0, F1, and F2/F3 bins



F1 events are smaller than those found by Monteverdi et al. (2003), they are still consistent with values found in supercell tornadic events in the Great Plains [Davies, 1993b], and low-topped supercell tornado events associated with land falling hurricanes [McCaul and Weisman, 1996].

The independent t-test was performed on the mean 0-1 km and 0-6 km ABVSHR and bulk shear values for each of the respective bins. There was no statistical difference between the mean values of 0-1 km ABVSHR or bulk shear for the F0 and F1 bins. However, the difference in mean values of ABVSHR and bulk shear for both the F0 and F1 bins compared to those for the F2/F3 was a statistically significant difference at the 5% and 1% level respectively. This suggests that the overall strength of the 0–1 km ABVSHR is a significant factor in the determination of the tornado intensity for all the California tornado events since 1951, a result that is consistent with the Monteverdi et al. (2003) results discussed in section 3.2.1. Furthermore, these values suggest that at least the F2/F3 California tornadoes were mesocyclone induced.

In analyzing the graphical distribution of the 0–1 km ABVSHR values (Figure 5.2) the median values and overall distribution of the shear values for the F0 and F1 events are similar and thus could be placed in the same bin. It is important to note that Monteverdi et al. (2003) found that the values of positive and bulk shear for the F1 and F2 events that occurred in their dataset exceeded the values found elsewhere for supercell tornadoes and, therefore, since there were just several F2 events, they grouped

the F1 and F2 events into one bin. However, in the present study, the shear values of the F0 and F1 bins are similar, and so that grouping does not appear to be justified in the larger data set considered here. Performing an independent t-test on this new grouping of F0 and F1 events against the means of the F2/F3 events produced a statistically significant difference between these two groups at the 5% level.

While the low level shear is important in the formation of lower level mesocyclones and tornadoes, the 0–6 km wind shear is crucial for two reasons: (a) the deep layer shear must exceed certain values in order for the storm not to be suppressed by its own precipitation and precipitation-induced downdraft; and (b) the deep layer shear must exceed similar values in order for horizontal shear vorticity to be tilted into the vertical and stretched by the updraft to produce a deep midlevel mesocyclone.

The median 0-6 km shear values (shown in Table 5.2) increase from F0, to F1 to F2/F3 bins. The mean value of 0-6 km ABVSHR for the F2/F3 events is similar to the value found in supercells in the Great Plains. This is significant when combined with relatively strong 0-1 km shear suggest that these stronger events in the California record were most likely supercells.

The box and whisker plots of 0-1 km and 0-6 km bulk shear as depicted in Figure 5.3 shows that the median values of 0-1 km bulk shear for F2/F3 events are much larger than those of the weaker F0 and F1 events. The median 0-1 km bulk shear values for the F0 and F1 events appear to be very similar. A similar pattern emerges in

the 0-6 km layer bulk shear with the median values of the F2/F3 events, which are much larger than the F0 and F1 events.

Performing the t-test on the 0-1 km bulk shear mean values reveals that there is a statistically significant difference between both the F0 and F2/F3 events and the F1 and F2/F3 events at the 1% level. The check for differences at the 0-6 km layer revealed that there are differences at the 5% level between F0 and F2/F3 events but no significant difference is found between the F1 and F2/F3 events. However, there is a difference at the 5% level between the F0 and F1 events.

These results suggest that at the lower levels of the atmosphere both ABVSHR and bulk shear were able to discriminate between thunderstorms that produced F2/F3 tornadoes and those that produced F0 or F1 tornadoes. While the F2/F3 cases are associated with larger shear values, one of the biggest differences was evident in the 0-1 km and 0-6 km layers. These findings agreed with those of Monteverdi et al. (2003) for a smaller dataset. This suggests that one of the controlling factors on development of stronger F2/F3 tornadoes is the strength of the low level wind shear (0-1 km); given that the deep layer shear (0-6 km) value is in the range of favorable values for the development of supercells.

It is important to note that the values of the 0-6 km bulk shear for the F2/F3 bin are consistent with those used in the modeling studies of supercell thunderstorms. The study conducted by Weisman and Klemp (1982) used 0-6 km bulk shear values between

$3 \times 10^{-3} \text{ s}^{-1}$  to  $5 \times 10^{-3} \text{ s}^{-1}$  and the modeled thunderstorms showed a favorable tendency to develop supercell characteristics. They noted that values above  $5 \times 10^{-3} \text{ s}^{-1}$  were associated with thunderstorms with strong and persistent mesocyclones. The means of the F0 and F1 bins show bulk shear suggesting that the parent thunderstorms may have exhibited supercell characteristics.

The control of low level and deep layer shear on tornado intensity during the study period is depicted in Figure 5.4. Each point represents an ABVSHR pair (0-1 km and 0-6 km) for a particular tornado event. There is a clustering or grouping of F0 events in this ABVSHR space around  $4 \times 10^{-3} \text{ s}^{-1}$  for 0-6 km deep layer shear and between  $10 \times 10^{-3} \text{ s}^{-1}$  and  $12 \times 10^{-3} \text{ s}^{-1}$ . This combination of low level shear and deep layer shear do fall into the lower range of values favorable for supercell development. There is a similar clustering of F1 events but they exhibit higher magnitudes of both lower level and deep layer shear. The F2/F3 events do not seem to converge on any particular values. However, looking at all of the tornadoes together there does appear to be an envelope or upper and lower bound of 0-1 km and 0-6 km ABVSHR. The upper bound is more visibly striking and apparent than the lower bound as shown in Figure 5.4.

About 71% of the tornado events exhibited 0-1 km ABVSHR values above the range favorable for supercells and 67% of the events exhibited 0-6 km ABVSHR value in the range supportive of supercells. The majority of tornado events display adequate

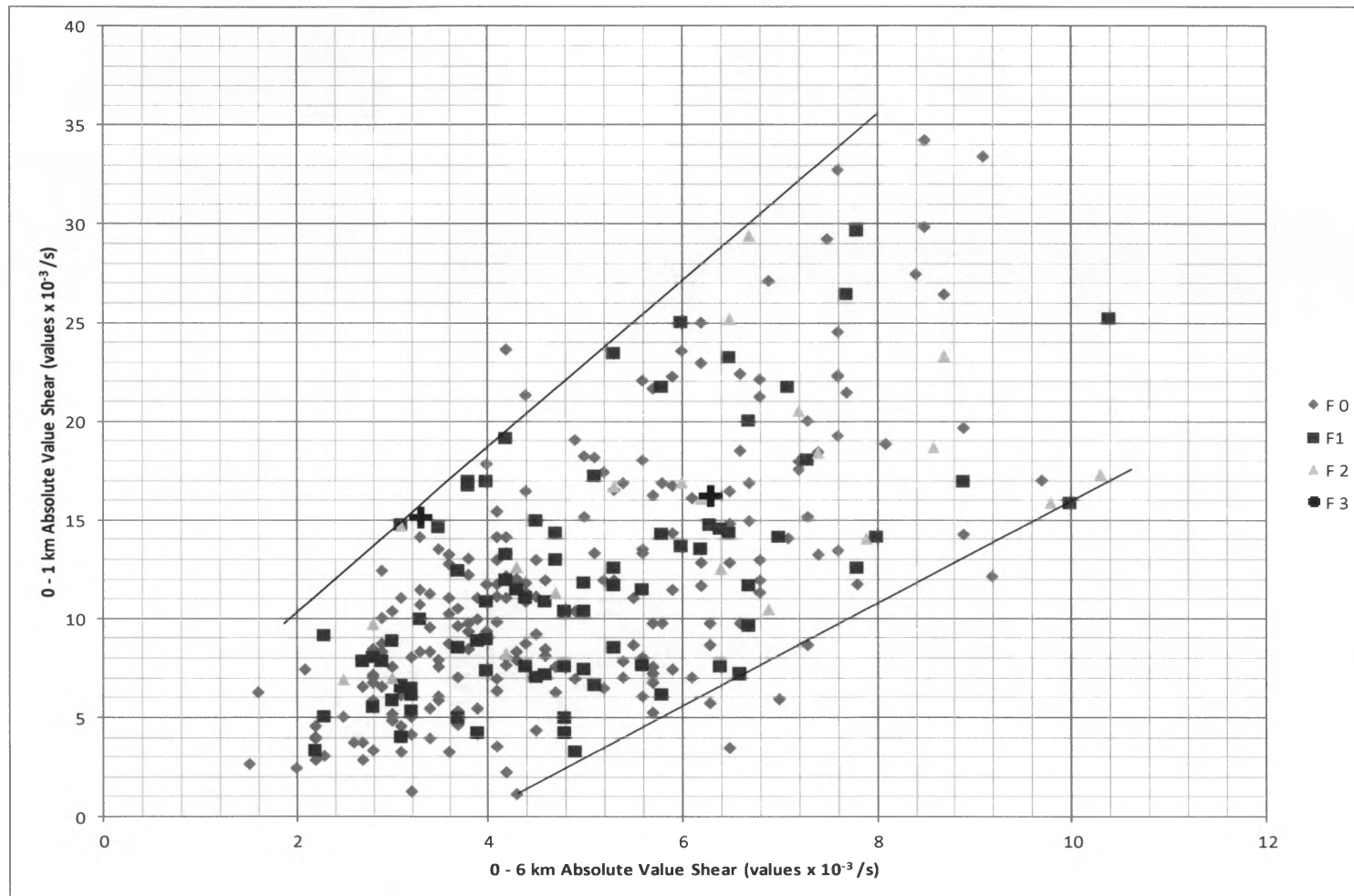


**Figure 5.4** Absolute value shears for 391 cases included in this study (diamonds = F0, filled squares = F1, triangles = F2, and black plus = F3. Black lines represent upper and lower bounds of shear values.

shear values both in the lower level and deep layer for supercell development and suggest that their parent thunderstorms exhibited supercellular characteristics.

### 5.1.3 Analysis of Environmental Storm-Relative Helicity

One way of assessing the potential of a thunderstorm to develop a mesocyclone is through use of the SRH index. Davies-Jones et al. (1990) and Moller et al (1994) suggest that a value of 0–3 km AGL SRH near  $150 \text{ m}^2\text{s}^{-2}$  is supportive of mesocyclone development in thunderstorms. Additionally, they suggest that 0–3 km SRH values of  $151\text{--}299 \text{ m}^2\text{s}^{-2}$  support weak tornadoes, SRH values of  $300\text{--}449 \text{ m}^2\text{s}^{-2}$  support strong tornadoes, and SRH values greater than  $450 \text{ m}^2\text{s}^{-2}$  support violent tornadoes. Since the threshold values of SRH associated with mesocyclone and tornado development were derived on the basis of clockwise turning hodographs, an evaluation of SRH for the tornado events considered here had the same issues that cropped up when the author was calculating positive shear. Thus, the author used the absolute value of the SRH (whether positive or negative) as an approximation of the total helicity in the 0-1 km and 0-3 km layers respectively

T-tests performed on the means of 0-1 km and 0-3 km SRH showed that there were statistically significant differences between the means of the F0 and F2/F3 events at the 95% level for both the 0-1 km and 0-3 km SRH. There were no significant differences found between the F0 and F1 or the F1 and F2/F3 events. These results

underscore the importance of the SRH in relation to the stronger tornado events when combined with adequate shear.

An evaluation of the SRH values calculated in this study shows that the values for 226 of the tornado events approached those values representative of potential for mesocyclone development ( $150 \text{ m}^2\text{s}^{-2}$ ). While this does not prove that 226 of the 391 tornadic thunderstorms were supercells this result strongly suggests that these tornadoes were mesocyclone induced. The tornado events characterized by SRH values between  $0\text{--}150 \text{ m}^2\text{s}^{-2}$  suggest the non-supercellular nature of the environment in which they occurred. The range suggested to encompass weak tornadoes ( $151\text{--}299 \text{ m}^2\text{s}^{-2}$ ) was made up of 121 tornado events and 32 events had values supporting strong tornadoes ( $> 300 \text{ m}^2\text{s}^{-2}$ ). However, of these strong tornado events only three of the F2/F3 events exhibited such large SRH.

Graphical depictions of the 0–1 km and 0–3 km SRH can be seen in Figure 5.5. This figure shows that the mean values of SRH for the F1 and F2/F3 bins are higher than that of the F0 events. This suggests that these stronger storms were able to ingest higher amounts of helicity than the weaker F0 events. These findings agree with those conducted by Monteverdi et al. (2003) for California tornadoes from 1990–1994 and although at a lesser extent agrees with the studies conducted in the Great Plains by Rasmussen (2003), Thompson et al. (2002), Edwards and Thompson (2000), and

Davies (2001), which found that increasingly larger values of SRH coincided with increasingly stronger tornado events.

An important source of error in the development of the SRH values used for this study should be underscored at this point. The SRH values quoted in the literature used actual storm motion vectors as part of the calculation. These can only be obtained from evaluation of the actual storm motions observed on Doppler Radar reflectivity plots, or when storms were very close to the older WSR-57 radars, with their limited geographic coverage. Before 1995, there was no Doppler radar sited in California, and the few WSR-57 radars were so widely and poorly spaced the inferring storm motions for each case was not feasible. Hence, the Bunkers technique (discussed in Section 4.3.6) was used to estimate storm motions. Thus, the values of SRH developed here may be slightly different than those that might have occurred if the actual storm motion vectors were known.



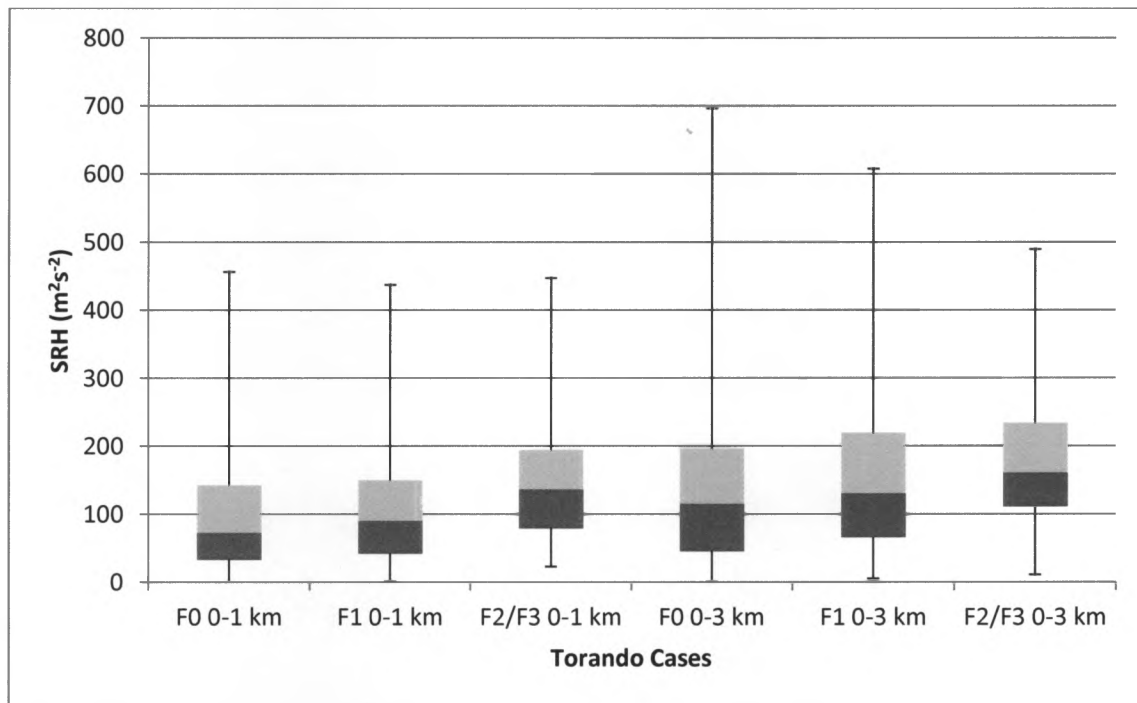


**Figure 5.5** Maximum, 75<sup>th</sup> percentile (green box), 25<sup>th</sup> percentile (red box), and minimum values of Absolute Storm-Relative Helicity observed for F0, F1, and F2/F3 bins.

#### 5.1.4 Analysis of Rotational Parameters (BRN, EHI, and VGP)

The BRN (see section 4.3.7) has been used in studies to discriminate between environments that are favorable for supercells and those that favor ordinary thunderstorms. The ranges of values which are suggestive of supercells are 2–45. Monteverdi et al. (2003) found that BRN values for twenty-three of the thirty tornado events they analyzed were in this range.

In the present study, the BRN calculated for 189 of the 391 tornado events was in the range of values found for supercell thunderstorms. Because the BRN is calculated by combining CAPE and shear, certain values can skew the values to very large or very small number outside the typical range. In some cases, moderate CAPE was found with negative shear values and the BRN number was found to be well outside the range of typical value associated with supercells. Thus, using the BRN number alone to diagnose or forecast the potential for supercells in California is not warranted and the forecaster should focus on the ingredients rather than the BRN.

A common index for assessing the potential for tornado intensity is the EHI (see section 4.3.8). As suggested in Lipari (2000) the EHI value as defined by Davies (1993a)  $EHI > 2$  for strong tornadoes, may be of little use in assessing the same potential for tornadoes in California because of its inclusion of CAPE values typical of Great Plains environments. Lipari (2000) found that EHI values of 1 and greater occurred with nearly 80% California tornado events he studied

The EHI was created to assess the potential for strong tornadoes to develop and it has been found that stronger tornadoes (F2 or greater) are associated with EHI values of 2 or greater. This index was developed in the Great Plains in environments consisting of moderate to large values of CAPE. Lipari (2000) suggested that an  $EHI=1$  is more representative of the low buoyancy environments found here in California. EHI values for tornado events in this study were calculated and compared against those found by

Lipari (2000). In the previous study the average EHI value for F1/F2 events was 0.65 and for all samples came out to 0.45. This study found that the F2/F3 values had an average of 0.56 and the average for all tornado events came out to 0.47. While the EHI value for stronger tornadoes (F2/F3) was slightly lower than those found by Lipari (2000) the average of all tornado events was similar. The smaller EHI number found for the F2/F3 events in this study suggests that  $EHI=1$  found by Lipari (2000) for the stronger tornado events in California should actually be lowered.

The VGP (see section 4.3.9) was developed for assessing the potential for supercell tornadoes. VGP values greater than 0.3 have been found to be associated with supercells and values exceeding 0.6 have been found to be associated with strong tornadoes in the Great Plains. The average VGP value for each tornado classification in this study was below 0.2. This suggests that the current range of VGP values as developed for Great Plains tornadic environments do not characterize or capture the same potential for rotation in California. The VGP value was devised for larger CAPE and deeper storm inflow environments and thus may not capture the sense of rotation for California storms.

## **5.2 Composite Soundings**

Composite profiles associated with the F0, F1 and F2/F3 tornado proximity environments were created using the methodology outlined in Section 4.2.1. The

composite soundings and composite hodographs for each F-rating proximity environments F0 events (Figure 5.6); F1 events (Figure 5.7); and F2/F3 events (Figure 5.8), reveal several important contrasts and similarities.

All three of the composite profiles are in an environment characterized by low CAPE with values for all three below  $250 \text{ J kg}^{-1}$ . The buoyancy in these soundings is confined to that part of the troposphere at or below 500 mb and resembles the composite profiles generated by Lipari (2000).

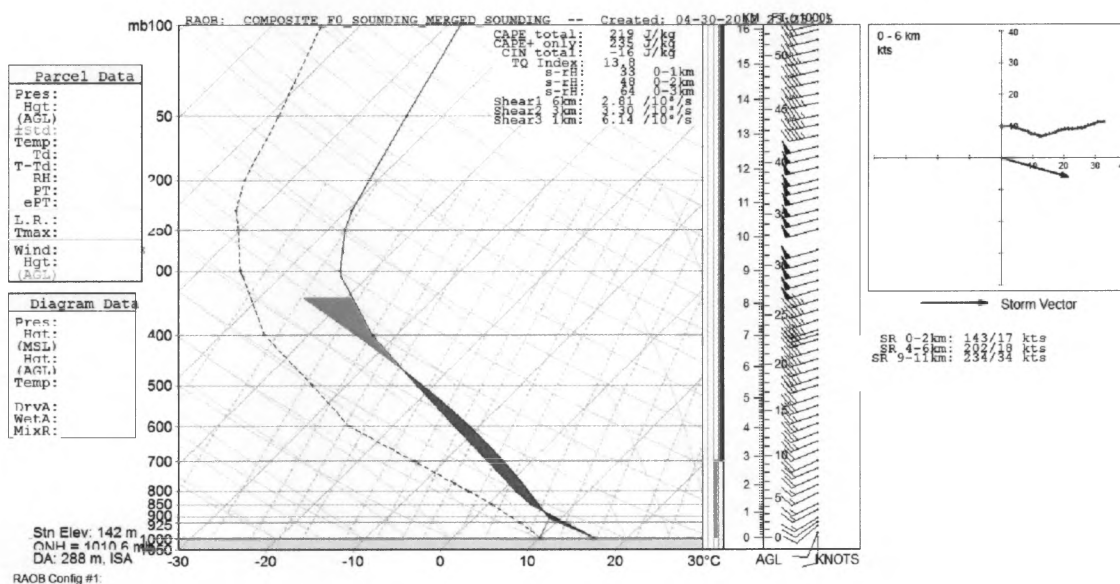


**Figure 5.6** Composite F0 profile of T,  $T_d$ , wind, and the composite hodograph derived from 232 tornado proximity soundings. The area denoted by red on the sounding profile shows CAPE present.

The composite hodographs for the F0 and F1 events display similar wind shear characteristics in that they are both mostly straight. The F2/F3 composite hodograph

however is of noticeable contrast to the F0 and F1 composites. Although not as dramatic as hodographs associated with Great Plains tornado events, this composite hodograph does show a moderate veering of the wind shear vector with height in the lowest 1.5 km. This does suggest that the stronger tornado events in California display similar shear profiles to that of supercells found in the Great Plains.

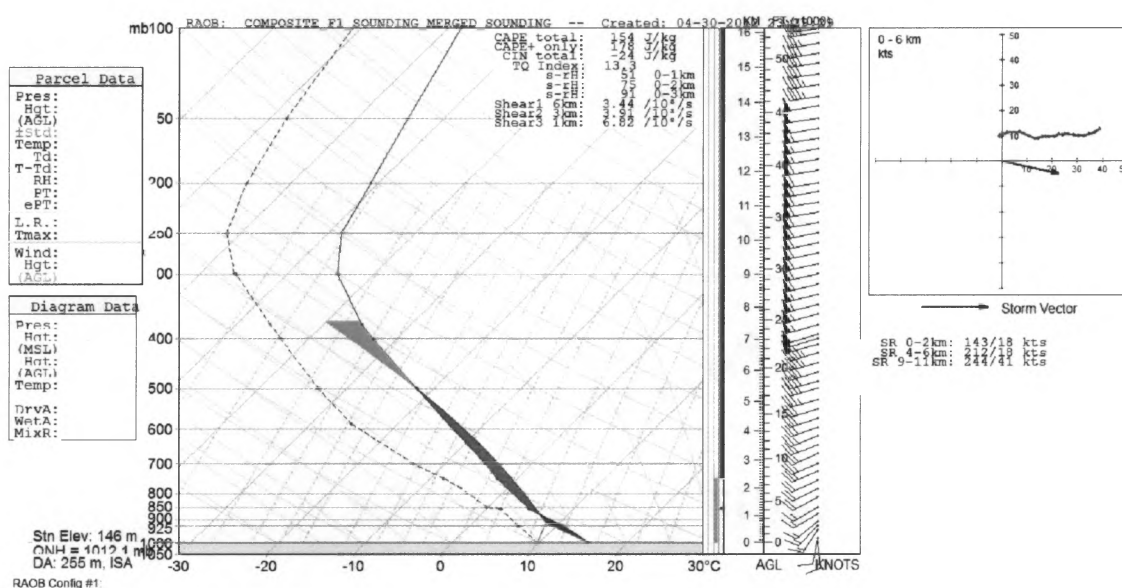


**Figure 5.7** Composite F1 profile of T, Td, wind, and the composite hodograph derived from 95 tornado proximity soundings. The area denoted by red on the sounding profile shows CAPE present.

The magnitudes of the ABVSHR calculated for the F1 and F2/F3 composite hodographs are larger than that of the F0 events. However, none of the composite hodographs display wind shear or storm-relative helicity values found in supercell environments. One explanation for this is that the tornado events in the record which

showed cyclonically turning hodograph or negative shear reduced the overall magnitude of these parameters. While there were only a handful of cases in which hodographs displayed these characteristics the author believes that these were able to reduce the shear values present in the composite hodographs.

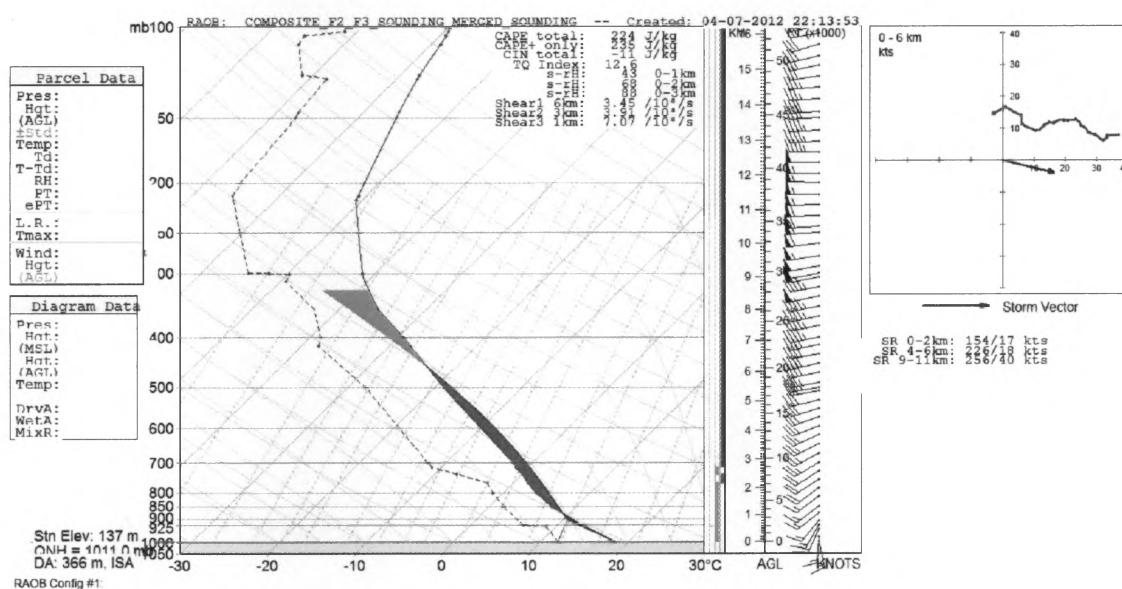


**Figure 5.8** Composite F2/F3 profile of T, T<sub>d</sub>, wind, and the composite hodograph derived from 25 tornado proximity soundings. The area denoted by red on the sounding profile shows CAPE present.

In Lipari (2000) the data set used only comprised of anticyclonically turning hodographs and there was a marked difference between the weaker F0 tornado events and the stronger F1/F2 tornado events. The hodographs for the stronger events displayed shear and helicity values consistent with supercell environments found elsewhere in the country. The inclusion of cyclonically turning hodographs in the

present study probably biased the results, and in more detailed future studies the shear environments of those somewhat unusual events will be studied.

### **5.3 Buoyancy and Shear Parameters Before 1980 and After 1980**

There are well recognized issues with the tornado record in the United States, chiefly in the period before the 1980s [*Doswell and Burgess, 1988*]. These include underreporting by the public of tornadoes in population-sparse portions of the country and misreporting of tornado damage as straight line wind damage. A separate issue is the rating of tornado intensity early in the period of record, chiefly before the 1980s.

SPC has been charged with the task of maintaining the tornado data base. This log has been maintained since 1954 based upon damage surveys. Before 1954, Kelly et al. (1978) point out that intensity ratings were estimated by SPC meteorologists using a combination of the reports made to Storm Data (available through NCDC) and anecdotal information from newspaper reports. Even more troublesome is that fact that they noted that many of the ratings for tornadoes from 1954–1976 also were obtained by SPC meteorologists from an examination of a combination of newspaper reports and photos submitted by the public. Doswell and Burgess (1988) suggest that many reports during this time may have been overestimated or overrated because newspapers are in the business of selling more newspapers, thus the intensity of a tornado may have been exaggerated in order to sell more newspapers.

Braun and Monteverdi (1991) and Monteverdi et al. (2003) point out that similar issues probably have plagued the California tornado record. Before 1980 it is possible that some tornadoes that occurred in California were not reported, reported as straight line wind damage or were not rated properly [*Braun and Monteverdi, 1991; Monteverdi et al., 2003*]. As is true in the tornado-prone section of the country, proper F-scale rating depends upon timely storm damage surveys. In the case of some of the earlier California tornado events, anecdotal evidence suggests that damage surveys occurred two to three days after the event, if at all. It is clear that unless the event is recognized as a tornado and/or damage surveys were accomplished before cleanup, proper F-scale rating could not be established. All of these factors suggest that the California tornado record before 1980 is somewhat suspect.

The reader will recognize that these issues could actually weaken the arguments made in previous sections regarding the correspondence of the shear and buoyancy values for the California events to those observed in the literature for tornadic events elsewhere in the country. Since the bins discussed in section 5 were defined on the basis of F-scale rating, any misratings that did occur early in the record might weaken or mischaracterize the relationships found in previous sections.

To address the impacts that there were possibly inaccurate F-ratings for tornado events in California before 1980, the buoyancy and shear data will be stratified on the basis of the F-rating that was observed for events occurring before 1980 and after. The



values obtained from the buoyancy and shear calculations are described in the section 4.3. The same data, previously grouped into F0, F1, and F2/F3 bins, will be stratified into pre and post 1980 groupings. The year 1980 was somewhat arbitrarily defined, since the author could find no firm estimates for the actual year or years in which tornado ratings became more trustworthy.

There was little to no difference between the buoyancy values stratified by F-scale rating for the two time periods (before 1980 and after 1980). Clearly, the buoyancy values associated with tornado events in California appear unrelated to the F-scale rating given, regardless of the accuracy of the rating.

An evaluation of the shear values associated with the F-scale bins grouped into the pre and post-1980 periods seems to corroborate the concerns of Doswell and Burgess (1988), Braun and Monteverdi (1991) and Monteverdi et al (2003). Independent t-tests showed that the ABVSHR values for the F0 and F1 bins in both the 0-1 km and 0-6 km layers differed significantly, at either the 5% or 1% level, for the period before 1980 from those calculated for the period since 1980.

Since 1980, the shear values for the different bins seem to be in line with those summarized in Monteverdi et al. (2003). The reader may recall that the analyses in previous sections suggested that the F0 and F1 events could be clumped together and that this result was in opposition to that of Monteverdi et al. (2003). The results here on the pre and post 1980 groupings now suggest that their conclusion that F1 and higher

rated tornadoes were probably mesocyclone-induced is consistent with the evidence found here in the longer term record.

The analysis of the 0-1 km and 0-6 km AGL ABVSHR quartiles shown in Figure 5.9 suggest that F0 and F1 before 1980 may have been over rated. The median ABVSHR values for the F0 and F1 events before 1980 are lower than the events after 1980. This suggests that the F-rating given to the F0 and F1 events before 1980 is greater than that which the shear profiles would indicate, given what is known about the relationship of shear values to tornado intensity. The median value and overall distribution of the shear values for the F2/F3 events before and after 1980 suggest that these events however are accurately rated. The larger mean ABVSHR value for the F2/F3 events occurring before 1980 compared to those after 1980 could be explained by the fact that only two F3 events occurred in the California record and both of these occurred before 1980.

In order to quantify the relationship between the lower level shear and the deep layer shear an ABVSHR shear space plot was constructed for each of the F-ratings. As suggested by the analysis of the ABVSHR quartiles the F0 and F1 events before 1980 were misrated. In the F0 ABVSHR space plot (Figure 5.10) there was some suggestion that tornadoes occurring before 1980 display weaker low level and deep layer ABVSHR than the events occurring after 1980. This combined with the median values shown in the quartiles would suggest that the F0 events before 1980 were possibly over rated.

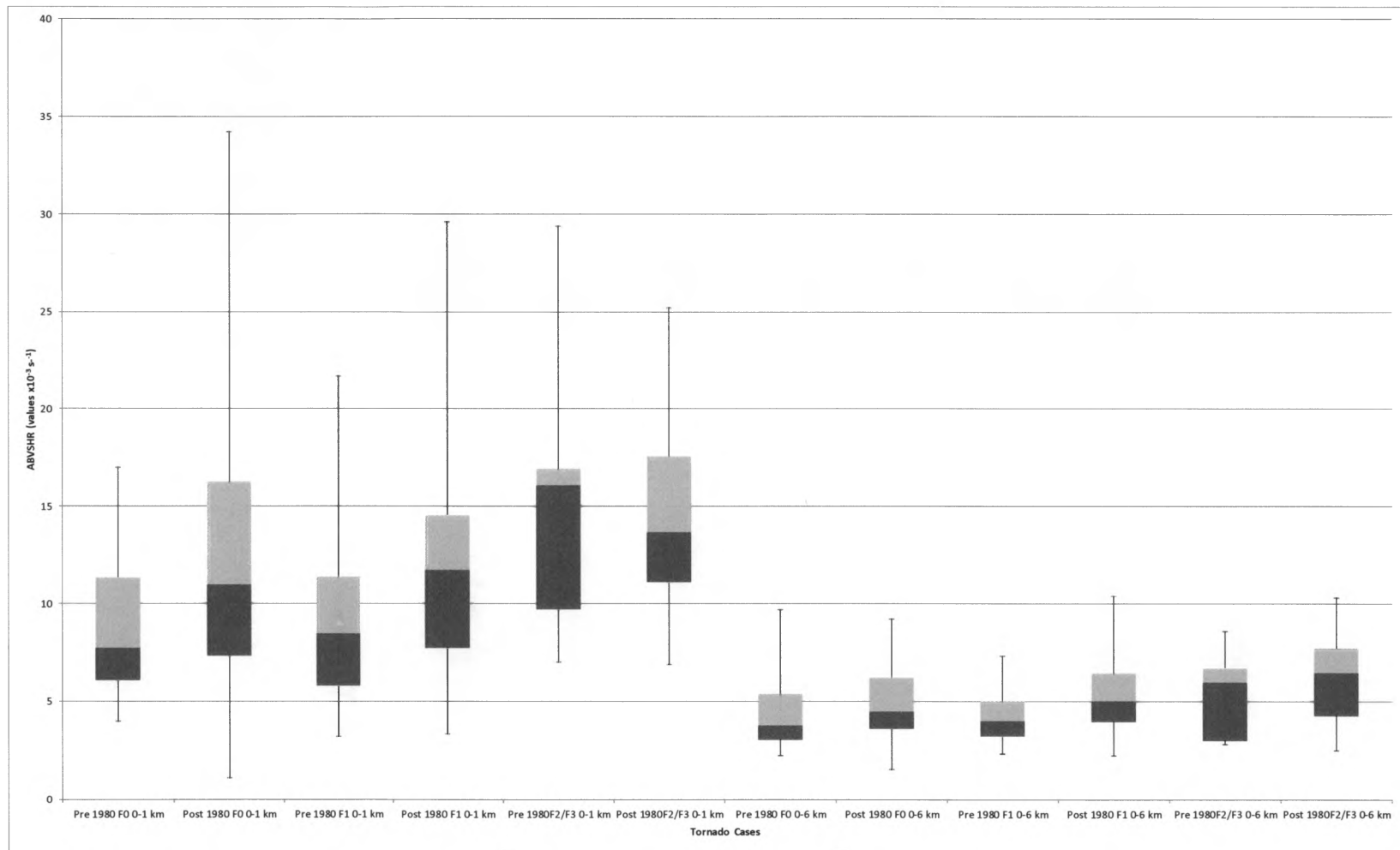


**Figure 5.9** ABVSHR quartiles for 0-1 km and 0-6 km shear for each F-rating before and after 1980.

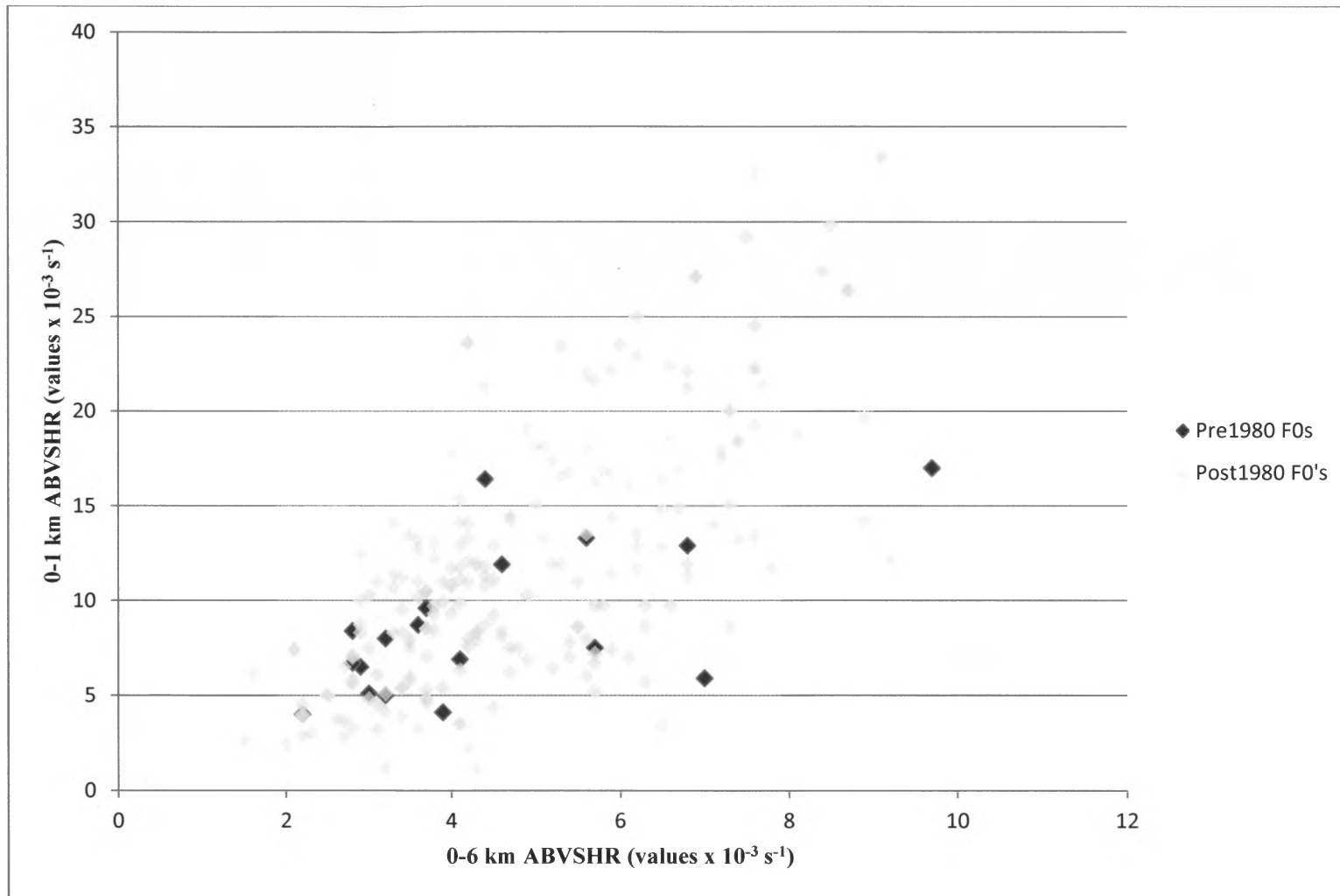


**Figure 5.10** ABVSHR shear space 0-1 km ABVSHR on the Y-axis and 0-6 km ABVSHR on the X-axis. The dark blue diamonds represent the F0 events before 1980 and the light blue diamonds represent the F0 events after 1980.

The ABVSHR space plot of F1 tornado events (Figure 5.11) shows a concentration or clustering of the F1 events occurring before 1980 in an area of smaller shear magnitudes in both low level and deep layer. The tornado events after 1980 appear to be of stronger magnitude and therefore accurately rated. Thus, this suggests F1 events before 1980 may have possibly been over rated.

This systematic over rating of the F0 and F1 events before 1980 lowered the average ABVSHR values found in the analysis of shear found in section 5.1.2. In Table 5.1 the mean values of 0-1 km and 0-6 km ABVSHR are shown for each F-rating for events before and after 1980. The tornado events occurring after 1980 display ABVSHR magnitudes that are more consistent than those values found by Monteverdi et al. (2003) for California supercell tornado events. These values also are consistent with those that are associated with tornadic supercells found in the Great Plains.

F-Rating	0-1 km ABVSHR Before 1980 ( $\times 10^{-3} \text{s}^{-1}$ )	0-1 km ABVSHR After 1980 ( $\times 10^{-3} \text{s}^{-1}$ )	0-6 km ABVSHR Before 1980 ( $\times 10^{-3} \text{s}^{-1}$ )	0-6 km ABVSHR After 1980 ( $\times 10^{-3} \text{s}^{-1}$ )
F0	8.7	12.3	4.4	5.0
F1	9.7	12.3	4.3	5.3
F2/F3	15.3	14.7	5.4	6.2

**Table 5.1** Shows 0-1 and 0-6 km ABVSHR values for (F0, F1, and F2/F3) tornado events before and after 1980.

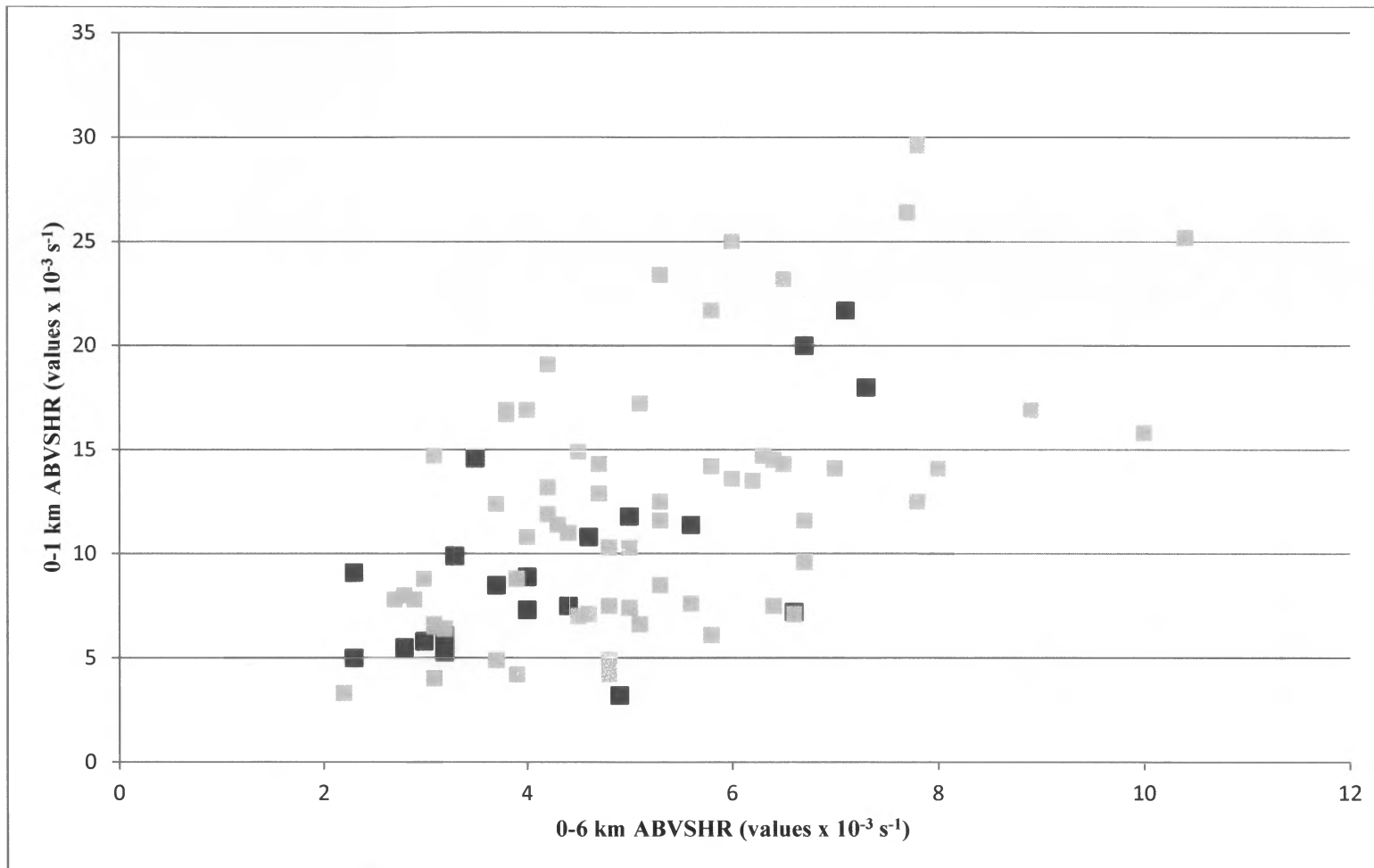


**Figure 5.11** Scatter plot of 0-1 km ABVSHR on the Y-axis and 0-6 km ABVSHR on the X-axis. The dark squares represent the Pre 1980 F1 tornadoes and the lighter squares represent the Post 1980 F1 tornado events.

## **6. Case Studies of the 1951 Sunnyvale F2 and the 1983 LA Convention Center**

### **Tornadoes**

Two of the strongest and most damaging tornadoes in the early record occurred on January 11, 1951 in Sunnyvale, CA and on March 1, 1983 in Los Angeles, CA. In Chapter 5, it was shown that there is a general correspondence of California tornado intensities to the same buoyancy and shear ingredients found for tornado intensity in the extensive studies that appear in the literature on Great Plains tornadic thunderstorms. But several issues emerged from the analyses presented in this thesis. One of the most important ones centered on the validity of establishing statistical bins defined on the basis of F-rating. If the ratings assigned to tornadoes in the early part of the record were done erroneously then any arguments about the relationship of tornado intensity to, particularly, shear environments would be difficult to make.

There was already enough evidence discussed in previous sections to suggest that this was an important issue for the early part of the California tornado record. But to investigate this issue further, the author has chosen to examine the controls on these two events in close detail. In so doing, the author also was able to examine the documentary evidence centered on the F-scale rating for each tornado. Using this evidence, the author then attempted to ascribe the damage with the guidelines given by

SPC on assigning EF-scale ratings currently. These issues are discussed in the next two sections.

### **6.1 The 1951 Sunnyvale F2 tornado**

On the morning of January 11, 1951 thunderstorms moved across central California with widespread reports of damage throughout the Bay Area. At least one of the thunderstorms was tornadic with SPC logging an F2-rated tornado at 8:25 AM LST in the town of Sunnyvale, California. This tornado was the first tornado recorded in the official SPC log for California. It was also one of the more damaging tornadoes on record for California.

The author used a number of sources to develop this case study. The synoptic maps used in the Sunnyvale case study were generated using the 6-Hourly National Center for Environment Prediction (NCEP)/National Center for Atmospheric Research (NCAR) Reanalysis Data Composites [ESRL, 2012]. The radiosonde data was obtained from the CD-ROM set entitled Radiosonde Data of North America [NCDC, 2012]. The hourly surface observations were obtained from a DVD set entitled Total Surface [Weather Graphics, 2012]. These hourly observations were plotted using a meteorological analysis software package called Digital Atmosphere [Weather Graphics, 2012]. The Sunnyvale Historical Society graciously provided photos and



newspaper clippings with information on the tornado event and other damage around the Bay Area.

#### **6.1.1 Synoptic and Mesoscale Environment**

There were several key features in the synoptic scale and mesoscale environment that contributed to both the initiation of thunderstorms and the development of the Sunnyvale tornado. In the middle and upper troposphere there was a long wave trough located over the Great Basin region of the United States. A shortwave trough was embedded in this flow and was approaching the northern California coast when the tornado formed. The location of this trough (shown in Figure 6.1) near the initiation time suggests that this was able to provide moderate to strong vertical motions in the middle troposphere, which allowed for destabilization of the atmosphere.

There were a number of factors that focused the synoptic and subsynoptic scale lift in the lower and mid troposphere over central California on January 11, 1951. First, the location of the trough in the hours leading up to the tornado event placed the Bay Area in the inflection point just to the east of the shortwave trough axis an area commonly associated with the strongest upper tropospheric divergence and upward motions in the middle troposphere.

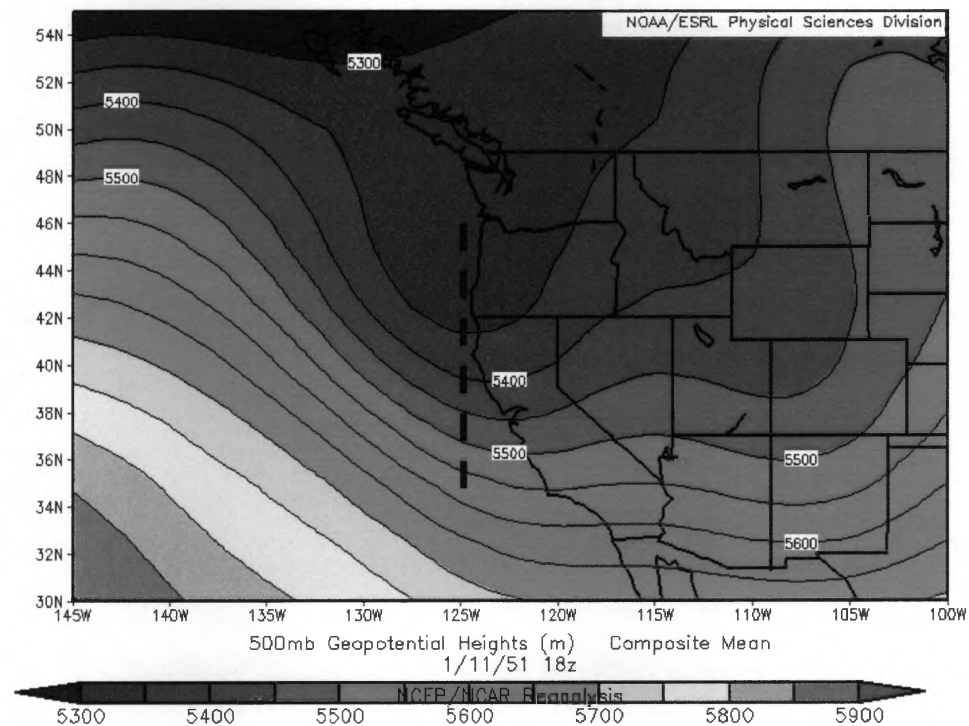


**Figure 6.1** The 500 mb Geopotential Height field at 1800 UTC on January 11, 1951. Shortwave trough axis (shown in black) is centered over northern California with the longwave trough axis centered over the Great Basin region.

Second, the location of the left exit region of an approaching jet streak (Figure 6.2) probably augmented the divergence in the upper troposphere for an area that appears to be focused over north-central California. The vertical motions associated with this feature in combination with the effects described above appeared to be centered over the San Francisco Bay region. The pattern in the middle and upper

troposphere resembled the prototypical synoptic pattern found for California tornado events as described in section 3.2.

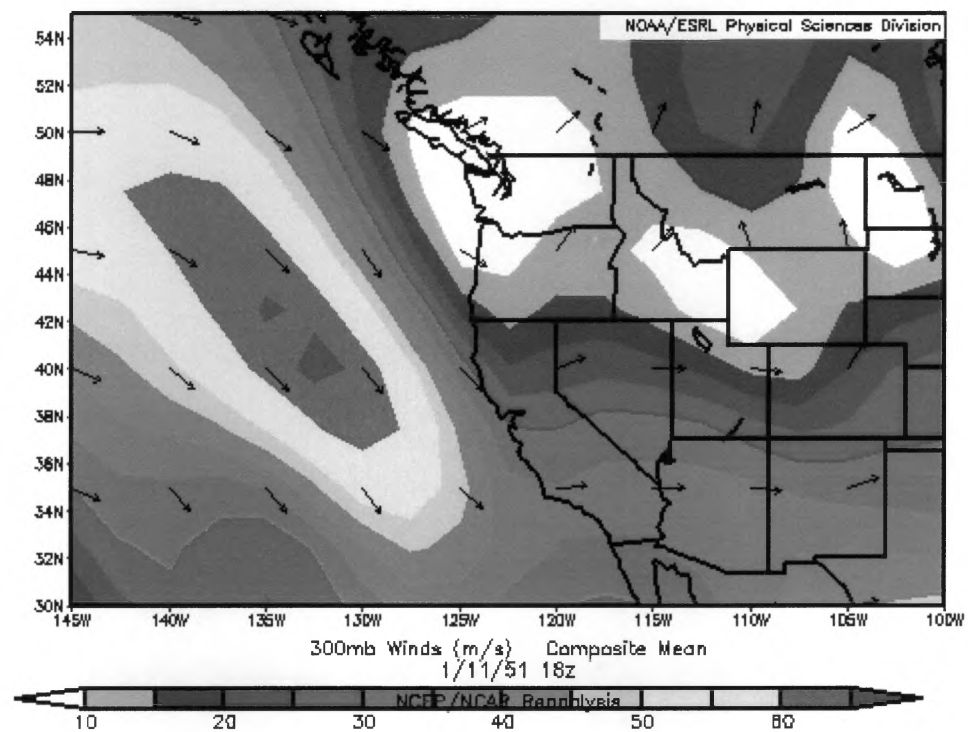


**Figure 6.2** The 300 mb vector wind speeds show a jet streak approaching the California coast. The Bay Area region was located in the left exit region of this jet streak

Third, subsynoptic features created regions of focused layer lifting of air and further destabilized the environment. These features were: 1. a postfrontal trough approaching the coast with subsynoptic low pressure system (shown in Figure 6.3); 2.

frictional convergence along the immediate coast; and 3. the coastal ranges to the west of Sunnyvale which extend vertically 400–600 m (1,300–2,000 ft.). Any one of these features would have provided the necessary lift to bring air parcels to the LFC and initiate convection.

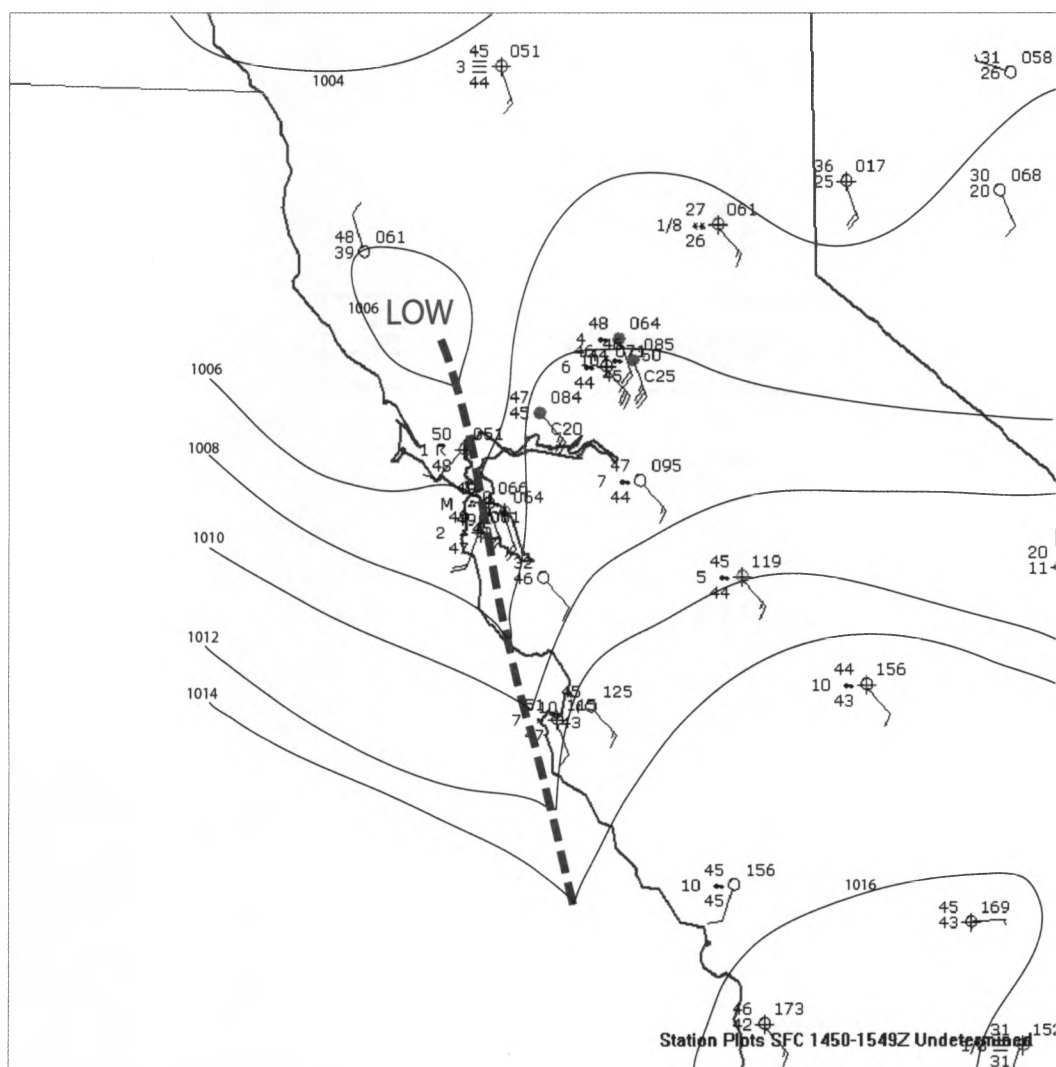


**Figure 6.3** Mesoscale analysis over central California, in the hour before the Sunnyvale tornado. Synoptic scale low and postfrontal trough located over the Bay Area.

The presence of strong winds in the middle and upper troposphere also helped create a favorable deep layer shear environment for supercells. The development of a weak leeside trough on the eastern side of the coastal ranges (located over the Sunnyvale area and over the San Francisco Bay) and the approaching postfrontal trough created a locally strong backed wind profile. Local low level channeling of the wind due to the mountainous coastal terrain helped to create additional strongly backed wind profiles over other parts of central California. This flow environment created low level shear values of large magnitudes, consistent with strongly rotating supercell thunderstorms found in the Great Plains and in other studies of California tornadoes.

#### **6.1.2 Buoyancy and Shear Environment**

An investigation of buoyancy and shear parameters associated with this tornado event is presented below. The procedure described in section 4.2.1 was used to construct this sounding. However, there were a few significant issues that needed to be addressed in constructing this sounding. The first is that the two soundings launched on this day did not accurately capture the near storm environment. The 0300 UTC radiosonde launched had a wind profile that resembles the synoptic conditions present on this day; however the temperature and dewpoint profile were not representative as there was no CAPE in this sounding. The 1700 UTC sounding displayed an accurate temperature and dewpoint profile with weak buoyancy appearing in the sounding but the wind profile was inaccurate because the wind shift line or the postfrontal trough had

moved through just before the sounding was taken. Thus, a combination of these two soundings was used by merging the 0300 UTC wind profile and 1700 UTC temperature and dewpoint profile. The next step was to substitute the surface conditions from the nearest surface (Moffett Field Naval Air Station, located in Mountain View, CA). The proximity sounding generated from this is shown in Figure 6.4 and is the most likely representation of what the atmospheric profile looked like over Sunnyvale on this day.

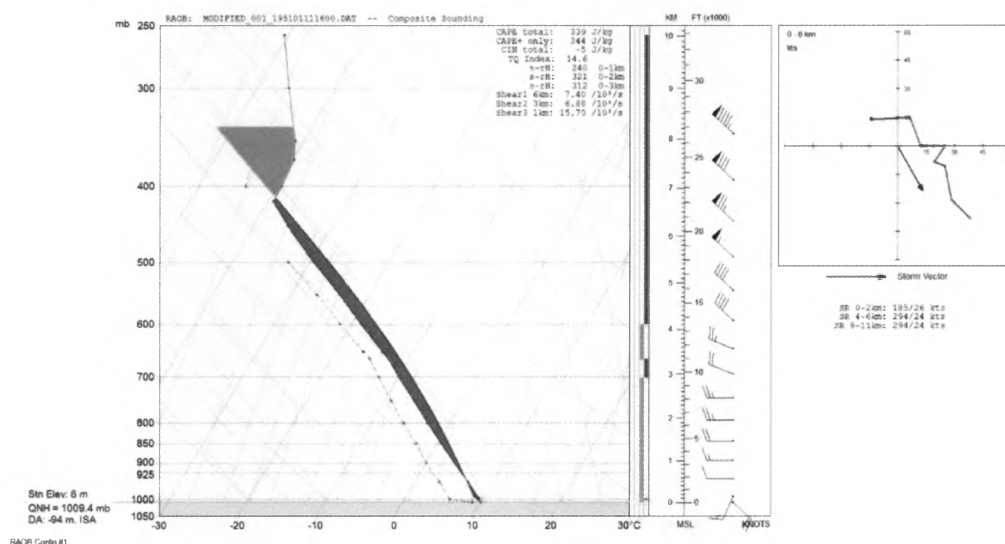


**Figure 6.4** Proximity sounding and hodograph generated for Sunnyvale at 15 UTC on January 11, 1951.

The atmosphere was weak to moderately unstable for typical California tornado events with a CAPE value of approximately  $400 \text{ J kg}^{-1}$ . This can be seen in Figure 6.4 as a vertically-extensive region in the troposphere characterized by buoyancy, but with small values of lofted parcel temperature excess relative to the environmental temperature (i.e., referred to as “tall skinny CAPE” by weather forecasters) highlighted

by the red region on the sounding. These CAPE values coincide with a strongly sheared low level and deep layer with values of  $18.7 \times 10^{-3} \text{s}^{-1}$  and  $8.6 \times 10^{-3} \text{s}^{-1}$  respectively. This shear can be seen in the anticyclonically curved hodograph found in Figure 6.4. These magnitudes of wind shear found in the environment over Sunnyvale are suggestive of moderate to strong supercells with moderate to strong tornadoes. The collocation of a strongly sheared low level and deep layer provided a shear environment necessary for the formation of supercells and ultimately tornadoes. The low level channeling of winds caused by the mountainous coastal terrain created a similar strongly sheared environment for other locations around the Bay Area.

### 6.1.3 Damage Assessment

The Sunnyvale tornado caused an estimated \$1.5 million dollars in damage as it traveled a distance of 5.7 miles (9 km) through the town as shown in Figure 6.5. Tornado damage in Sunnyvale started at the far southwest corner of town as a number trees were uprooted and broken. This damage is consistent with F0 rated wind speed estimates.



**Figure 6.5** Estimated damage path through Sunnyvale California on January 11, 1951

The evidence then suggests that the tornado intensified as it entered the main part of the town of Sunnyvale. Telephone and power line poles on this side of town were leaning and a few of them were broken or snapped half up the pole. This damage is consistent with wind speeds of 108 mph to an upper bound of 142 mph, which would mean a rating of F1 to F2. In addition to telephone poles being broken, many trees in the town were knocked over or uprooted and this damage is consistent with wind speeds of an F1 rated tornado.

In the next half mile, the evidence suggests that the tornado was at least of F2 intensity. Photographs show that the train station had a large section of the roof



completely removed (Figure 6.6). The train station appears to have been constructed similarly to the structures that SPC define as a two-story residence. This damage would indicate wind speeds expected to be around 122 mph with an upper bound 142 mph and would mean a tornado of F2 intensity. Additionally a few houses in the vicinity were shifted off their foundations, which would be expected with wind speeds of 121 mph up to 141 mph and a tornado of F2 intensity.



**Figure 6.6** Broken telephone pole in the foreground and large section of roof removed from the train station in Sunnyvale, CA on January 11, 1951.

The tornado became the most intense as it entered the center of town. Figure 6.7 shows the destruction of a corrugated iron and frame garage near the center of Sunnyvale. This damage resembles that of the Figure 6.8 from the Damage Classification guide [McDonald *et al.*, 2006] and would have wind speeds around 143

mph with an upper bound of 168 mph. These speeds would indicate a tornado of F3 strength. The most striking and suggestive of tornado rated F3 is the damage done to a 10 ton crane near the center of Sunnyvale. The crane was carried 100 feet away from its original location. While the Damage Classification guide [McDonald *et al.*, 2006] focuses solely on structural damage there is suggestion from Fujita's original work on the F-rating that damage of this extent would indicate F3 wind speeds (158-207 mph). This does suggest that the damage to the corrugated iron and frame garage and the 10 ton crane was caused by an F3 tornado.



**Figure 6.7** Corrugated iron and frame garage in Sunnyvale, CA knocked down on January 11, 1951.



**Figure 6.8** A Metal Building System as described by the Damage Classification guide. Damage to this building resembles the damage to the metal garage in Figure 6.7

Sunnyvale was not the only location in the Bay Area to experience damage related to a tornado. While not listed in the official SPC database as a tornado, the downtown area of San Jose (City Hall Area) experienced damage consistent with a tornado. There were numerous reports of a tornado and funnel cloud moving through San Jose. A few workers on the sixth floor of the Bank of America building saw the tornado as it moved through San Jose. There were 18 apartment units along Delmas Ave. in the San Jose area that had their roofs removed. This would indicate wind speeds of 138 mph up to 158 mph and be associated with either a strong F2 or weak F3

tornado. Figure 6.9 shows a two story home missing the top story wall. This would indicate wind speeds of 122 mph up to 142 mph and be associated with either a strong F2 or weak F3 tornado. There was additional damage throughout San Jose but these reports were of the strongest damage. Based on this damage, the author would recommend that a tornado of F2 intensity be entered into the official tornado record for San Jose on January 11, 1951. An estimated path of the tornado taken from a newspaper account and the reports of damage is shown in Figure 6.10.



**Figure 6.9** Second story exterior wall removed from home located near Delmas Ave. in San Jose on January 11, 1951.



**Figure 6.10** Estimated path of the San Jose tornado on January 11, 1951.

The cities of Sunnyvale and San Jose were they only locations around the Bay Area that had photographic evidence of damage. Additional damage was reported to the Cow Palace in San Francisco. This venue had the roof lifted off the main entrance way and the ticket booth in front of the building had the awning removed. While the exact building type can't be matched, the damage to the ticket booth awning suggests wind speeds were between 98 mph and 114 mph and may be associated with an F1 rated tornado. There were other reports of roof damage in the Presidio area of San Francisco and there was a report of a helicopter landing platform blown off the roof of the

Letterman building in the Presidio. This type of damage would suggest wind speeds from 98 mph up to 117 mph and be associated with a F1 rated tornado.

In the East Bay, there were numerous reports of roofs being removed from houses and collapsed chimneys following a two mile long, half mile wide path from El Cerrito to Richmond. There was a report in Richmond of a roof being removed from a construction company warehouse. In Oakland, there was a report of the roof being blown off the United Helicopter plant. Wind speeds associated with this type of damage would range from 97 mph up to 122 mph and be associated with either a F0 for some of the damage or a high end F1 tornado for the most severe damage. At the Benicia Airport, a roof was removed from the mess hall and there was a report of a plane flipped onto a nearby hanger. This damage may have been caused by a F0 to F1 rated tornado.

In Sonoma County there were reports of a 35 ft farm silo that was crumpled with a large section of the side of the barn near the silo torn away. Further east near the Two Rocks area there was a report of a two story home that was demolished. While it is impossible to know the exact strength of each of the structures and the exact damage done to each building, this damage would suggest wind speeds ranging from 112 mph up to 142 mph. Based on these wind speeds a tornado rated either F1 or F2 occurred in Sonoma County.

#### **6.1.4 Findings**

There were numerous accounts of damage consistent with that observed from tornadoes ranging from F0 to F3 throughout the Bay Area on January 11, 1951. The wind shear environment present on this day is suggestive of strong supercells and possibly moderate to strong tornadoes. The author would recommend that the Sunnyvale F2 tornado be reevaluated and rerated up to an F3 tornado and the San Jose tornado be entered into the log as an F2 tornado. Based on the damage reports across the Bay Area the author recommends that there be an additional six tornadoes entered into the log. The locations and strength of each of these tornadoes can be found in (Figure 6.11 on the next page) as well as the recommend strength of the Sunnyvale and San Jose tornadoes.



**Figure 6.11** Locations and suggested F-rating for tornadoes occurring on January 11, 1951.



## 6.2 The Los Angeles Convention Center F2 Tornado

At approximately 7:40 AM LST on March 1, 1983 an F2 rated tornado touched down and moved through the city of Los Angeles (LA). The tornado caused significant structural damage to buildings in the downtown vicinity. The LA Convention Center was one of the hardest hit structures in the area. The forecasts on this day never mentioned anything about possible severe weather because the synoptic environment did not resemble the tornado events typically associated with Great Plains tornadoes. Thus, the author believes that the misunderstanding of the environmental characteristics on this day lead to a possible under rating of this tornado.

The author used a number of sources to develop this case study. The synoptic maps used in the LA Convention Center case study were generated using the NARR [NCDC, 2012]. The radiosonde data was obtained from the CD-ROM set entitled Radiosonde Data of North America [NCDC, 2012]. The hourly surface observations were obtained from a DVD set entitled Total Surface [Weather Graphics, 2012]. These hourly observations were plotted using a meteorological analysis software package called Digital Atmosphere [Weather Graphics, 2012]. The photos and additional synoptic maps used in this case study were obtained from the *Los Angeles, California Tornado of March 1, 1983* provided by the National Academy of Sciences.

### 6.2.1 Synoptic and Mesoscale environment

There were several key features in the synoptic scale and mesoscale environment that contributed to storm initiation and the development of the LA Convention Center tornado. The synoptic environment present on this day was similar to the model proposed by Hales (1985) for southern California tornado events. There was a surface low pressure system centered off the coast of central California with a 500 mb low stacked almost directly above the surface low. The only difference between the environment on this day and the model proposed by Hales (1985) was that a cold front had not moved through the area before the tornado occurred. The cold front was still located off the coast.

A number of factors focused the synoptic and subsynoptic scale vertical motions in the lower and mid troposphere over southern California on March 1, 1983. First, differential cyclonic vorticity advection and weak WAA were associated with quasigeostrophic forcing for mid-tropospheric layer lifting over southern California. This layer lifting destabilized the atmosphere by increasing the lapse rates and providing a more buoyant atmosphere above the surface.

As shown in Figure 6.12 southern California was in the left exit region of a jet streak, this area has been found to be associated with upper tropospheric divergence and upward vertical motions in the mid-troposphere. The vertical motions associated with

the divergence in the upper troposphere was in concert with the quasigeostrophic forcing for upward motions (CVA and WAA) already present to create strong synoptic scale vertical motions.

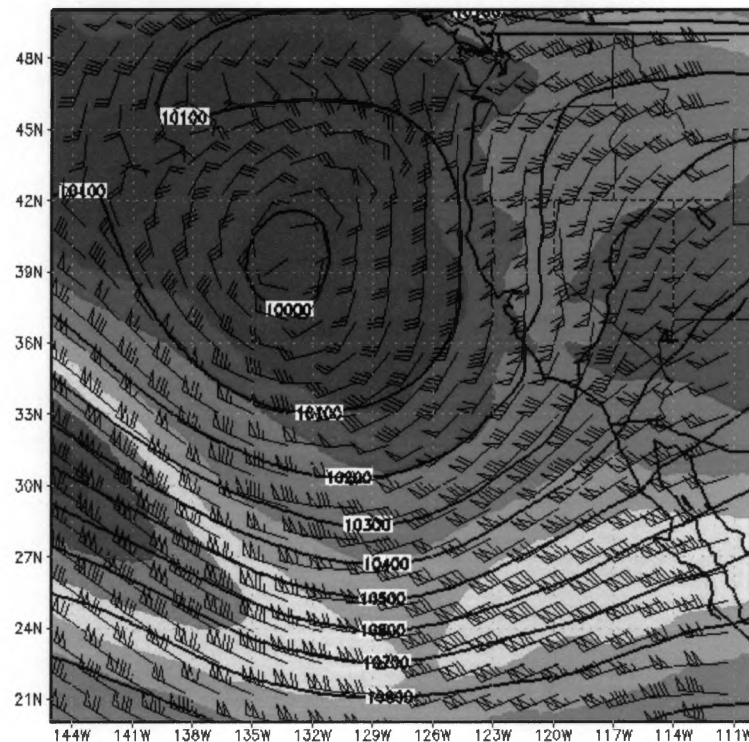


**Figure 6.12** Upper air and jet stream diagram for 1200 UTC on March 1, 1983. 250 mb Geopotential height solid black lines, 250 mb isotachs color fill, and wind barbs for 250 mb wind.

There were a few mechanisms present on this day which provided additional lift or lofting of air. The first was an approaching cold front (shown in Figure 6.13), which

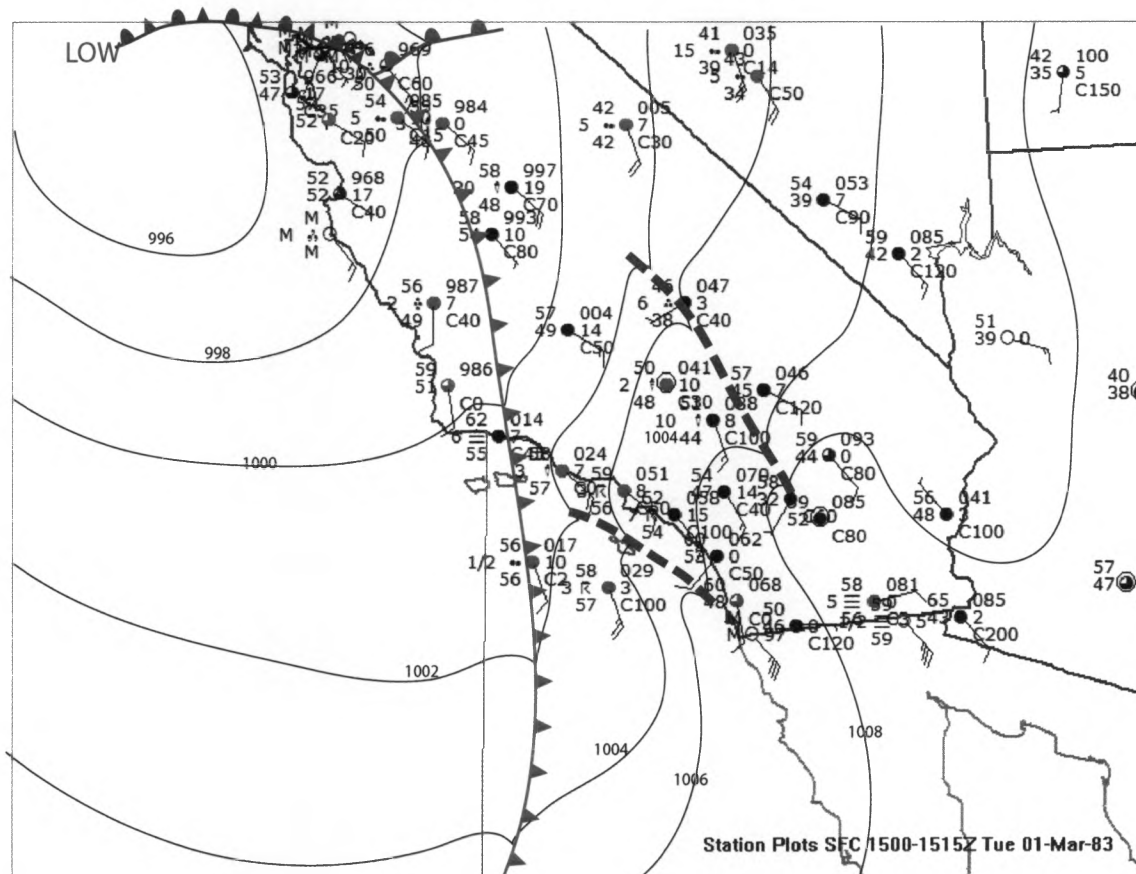


**Figure 6.13** Mesoscale analysis over southern California at 1500 UTC, the hour before the tornado. Cold front located off the coast with a mesoscale trough out ahead of the cold front.

layer lifted air vertically and destabilized the environment. Just ahead of the cold front there was a small mesoscale trough (shown in Figure 6.13) located immediately off the coast. As winds moved off the ocean and on shore they experienced a deceleration due

to friction and because of this, frictional convergence developed along the immediate coast. This convergence at the coast provided a source of lift for air parcels to reach their LFC. The interaction of the atmosphere with the islands located off the coast of southern California created local areas of lift.

The tornado touched down just downstream from the Palos Verdes Peninsula, which has a vertical extent of close to 370 m (1200 ft). As discussed in section 3.3.2 the downstream side of this topographic feature has been found to be associated with a convergence zone. In addition to providing an area of enhanced surface convergence this feature has also been found to generate areas of helicity on the downwind side of the island. This additional helicity created by the island was able to be tilted vertically, which increased the strength of the rotating updraft and was most likely associated with the development of the tornado.

The presence of strong winds in the middle to upper troposphere created a deep layer shear environment favorable for the development of supercell thunderstorms. The interaction of the synoptic scale winds with the transverse range provided a locally backed wind profile that extended vertically up to around 850 mb and a strong low level shear environment. This low level shear environment had values that are consistent with strongly rotating supercell thunderstorms found both in California and in the Great Plains.

### 6.2.2 Buoyancy and Shear Parameters

The generation of the tornado proximity sounding for the LA Basin on this date followed the procedure discussed in section 4.2.1. However, there were a few issues in the generation of this proximity sounding that will be discussed. The 1200 UTC San Diego, CA (KNKX) sounding profile displayed a significant marine inversion present at 850 mb. This did not support the development of convection. However, the atmospheric profile from the 0000 UTC Vandenberg, CA (KVBG) sounding had no such marine inversion. There was a special sounding released from the UCLA campus at 6:00 AM LST. This sounding was for the California Air Resources Board and was not expected to be followed higher than 700 mb [*Hart*, 1985]. The atmospheric profile associated with this sounding resembled the profile of the KVBG sounding at 0000 UTC. However, the wind profile associated with the KVBG sounding did not represent the lower tropospheric wind profile suggested by the analysis of the synoptic and mesoscale environment. As a result, the wind profile from the KNKX at 1200 UTC was combined with the temperature and dewpoint profile of the KVBG sounding. The surface conditions taken from the Los Angeles Airport (KLAX) in the hour before the tornado were inserted and replaced the observations from the base of the sounding. Then, the wind profile was smoothed vertically from the surface up to the height of the transverse range just southeast of the LA area.

This procedure produced the near storm buoyancy and shear environment for the developing thunderstorms that seems conceivable. The atmosphere had  $226 \text{ J kg}^{-1}$  of CAPE present in the hour before the tornado and is visible in Figure 6.14. The WSR-57 radar located in the LA Basin reported storm top heights of around 5,500 m (18,000 ft), which matches well with the vertical extent of CAPE found in the sounding.

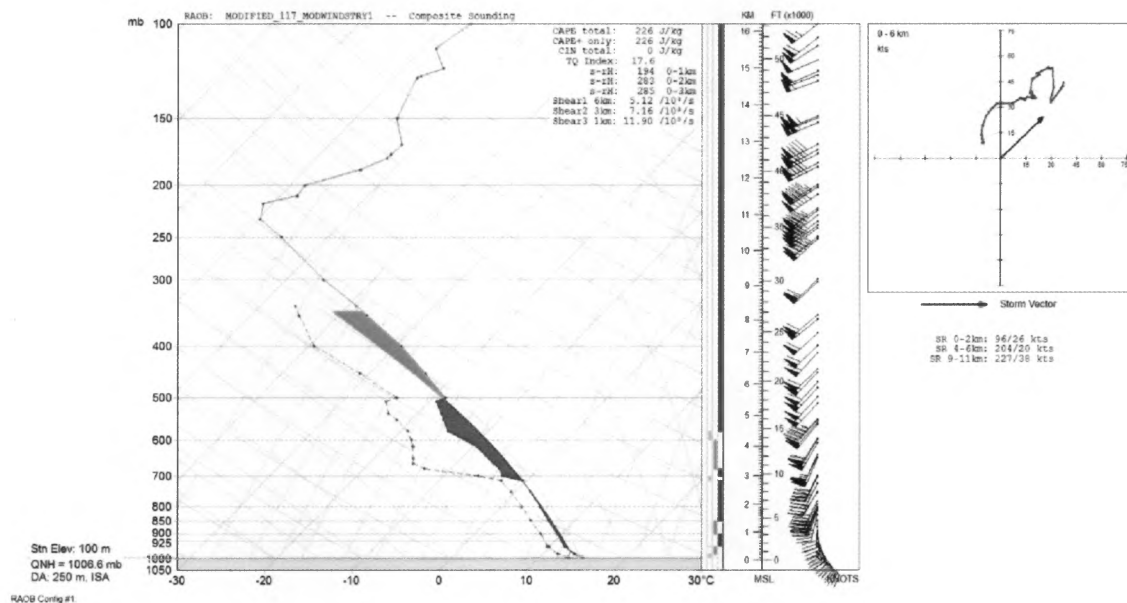


**Figure 6.14** Tornado proximity sounding for the LA Convention Center tornado. The red area indicates CAPE present in the sounding and the blue area indicated CIN present in the sounding. Modest buoyancy is present but the 0-6 km hodograph in the upper right corner shows strong curvature in the lower levels of the atmosphere.

This modest amount of CAPE coincided with a moderate to strongly sheared low level and deep layer shear environment. The value of low level shear (0-1 km) AGL was  $12.5 \times 10^{-3} \text{ s}^{-1}$  and  $6.4 \times 10^{-3} \text{ s}^{-1}$  respectively. This is evident in the anticyclonically

turning hodograph found in Figure 6.14. These values for wind shear are suggestive of moderate to strong supercells with moderate to strong tornadoes possible.

### 6.2.3 Damage Assessment

The shear values found in the section above suggest that the original report of an F2 tornado is plausible; however, there is some suggestion via the damage done that a tornado of a higher magnitude may have been possible. This section provides a detailed look at the damage done and uses the Damage Classification guide [*McDonald et al.*, 2006] provided by SPC to determine the strength of the wind speeds and ultimately the rating of the tornado.

The telephone and power lines in the path of the tornado consisted of wood poles. There were numerous photos showing poles that were leaning and a few poles were snapped or broken (shown in Figure 6.15). The damage indicates that wind speeds are expected to be around 108 to 118 mph with an upper bound of 130 to 142 mph respectively. Wind speeds of this magnitude would suggest an F2 rating with possible F3 damage in the stronger wind gusts.



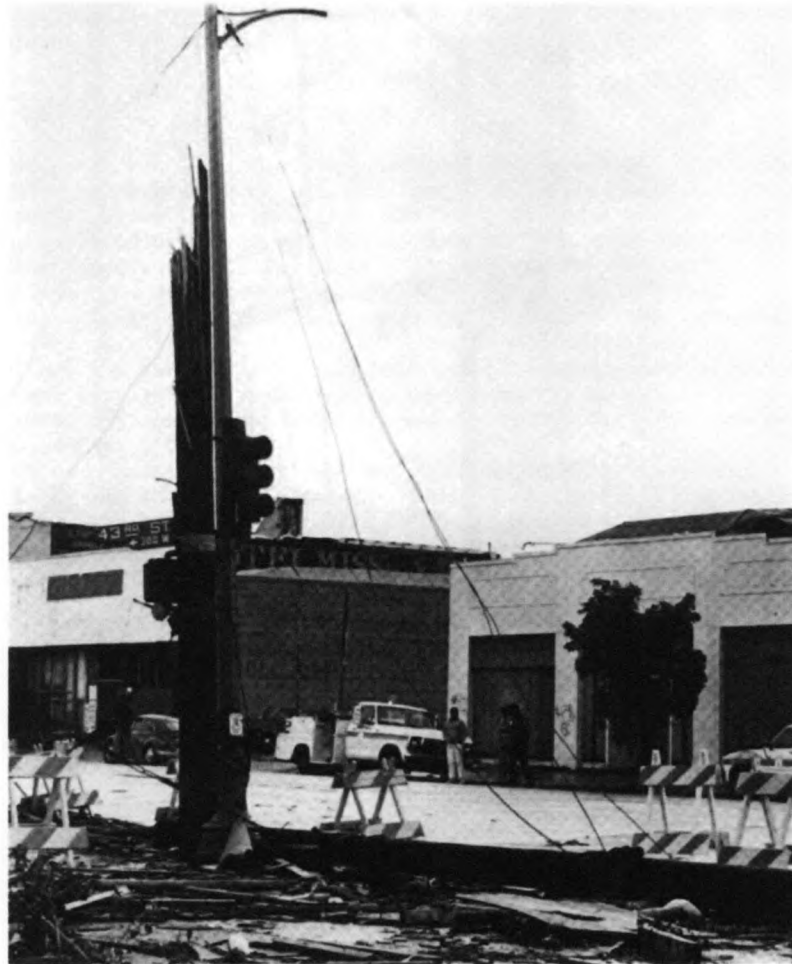


**Figure 6.15** Telephone pole snapped about half way up the pole

Most masonry buildings in the path of the tornado had damage to glass storefront windows as shown in Figure 6.16. There was also roof and parapet damage that is expected with unreinforced masonry buildings. The masonry buildings which showed less extensive damage were those that had reinforced walls. The estimated wind speeds exhibited by damage to glass windows is 89 mph with an upper bound



**Figure 6.16** Damage to storefront windows. Collapse of masonry parapet and part of roof.

of 107 mph, which would mean an F0 or F1. The damage to the unreinforced masonry walls would indicate wind speeds of 103 mph expected and an upper bound of 125 mph, which would mean an F1 to F2 tornado.

The damage to single story wood frame houses in the path of the tornado was quite severe. Many of the houses had portions of the roofs removed (Figure 6.17) and a few homes suffered a complete collapsing of the roof (Figure 6.18). The removal of sections of the roofs but while most walls remain standing, this would indicate expected



**Figure 6.17** Section of roof removed from house located near the Convention Center



**Figure 6.18** Collapse of entire roofing structure, house located near the Convention Center

wind speeds of 122 mph with an upper bound of 142 mph. The collapsing and removal of the roof structure would be consistent with the upper bound of 142 mph wind speeds but stronger winds may be possible. This would then suggest a tornado rated F3.

In the Damage Classification guide [*McDonald et al.*, 2006] there are no estimates for structures like the Convention Center. Based upon an assessment of the damage to comparable structures presented in the guide, the author used those associated with a well-constructed shopping mall. At the time of construction the convention center represented the state of the art design for such buildings and was reinforced to withstand earthquakes. Figures 6.19 and 6.20 show the damage to the convention center with significant roof damage evident in Figure 6.19. Many of the panels along the exterior walls were removed (visible in Figure 6.20).



**Figure 6.19** Damage to the Los Angeles Convention Center shortly after tornado moved through.



**Figure 6.20** Removal of side panels along exterior walls from the Los Angeles Convention Center

The removal of sections of the roof as shown in Figure 6.19 would indicate expected wind speeds around 108 mph with an upper bound of 128 mph. However, the removal of the side panels along the exterior walls (Figure 6.20) would indicate wind speeds around 111 mph with an upper bound of 131 mph. These wind speed estimates would suggest a tornado rated F2. However, it is possible that the design of the structure to withstand earthquakes may have meant that the convention center was exposed to wind speeds greater than what the current damage suggests.

#### **6.2.4. Findings**

The convention center was located immediately downwind from the single story homes that displayed damage consistent with an F2-F3 rated tornado. Thus, the convention was most likely exposed to the wind speeds in the range of F3 tornadoes but the state of the art design of the structure allowed the minimal amount of damage to be done. The author would therefore recommend that the LA tornado of March 1, 1983 be rated as a very strong F2 or low end F3 tornado.

## 7. Discussions and Conclusions

### 7.1 Synopsis

This study of all California tornado events during the period 1951–2011 verified many of the results of other studies on the nature of tornadic storms in California [Braun and Monteverdi, 1991; Blier and Batten, 1994; Monteverdi and Quadros, 1994; Monteverdi *et al.*, 2003]. These earlier studies concluded that while California tornadic storms generally were low-topped and associated with low buoyancy environments, the shear environments in which they developed were rich with low and deep layer shear. Vertical accelerations associated with the shear-induced pressure perturbations augmented the buoyancy accelerations by a factor of 2 to 4.

The buoyancy environment for most the tornadic storms studied here developed in an environment with low Equilibrium Levels, consistent with low tops. The magnitude of the buoyancy was low to moderate. Statistical analyses showed that buoyancy alone could not be used as a discriminator between storms that produced weaker tornadoes from those that produced the strongest, since there was no statistically significant difference in buoyancy values between the F0, F1, and F2/F3 bins defined for this study.

On the other hand this evaluation of a much larger data set than that examined by Lipari (2000) corroborated the fact that values of 0-1 km AGL and 0-6 km AGL ABVSHR, and the 0-3 km AGL SRH, can distinguish the weaker F0 and some F1

events from the stronger F1 and F2/F3 tornado events. This result was expected since the shear environments for the stronger events were associated with wind profiles that have been identified as consistent with both supercellular updrafts and the development of low level rotation preceding tornadogenesis elsewhere in the country.

Clearly, the weak buoyant updrafts (suggested by average CAPE values less than  $1000 \text{ J kg}^{-1}$  for most California tornadic storms) were mitigated by accelerations associated with the moderate to strong shear related vertical pressure perturbations related to the vertical wind and wind shear profiles of the tornadic storm environments. These shear related vertical pressure perturbations, intrinsic to some degree in all supercell circulations, can account for the statistical significance between tornado intensity and low-level (0-1 km AGL) ABVSHR considered in this study.

Additionally it can be concluded that the local and regional topography found in California plays a crucial role in the development of tornadic thunderstorms as suggested by Blier and Batten (1994), Monteverdi and Quadros (1994), and Lipari (2000). The orientation of the topography in California can provide a local low level channeling of wind flow to create strongly sheared low level environments. Many of the stronger if not all of the stronger F1 and F2/F3 tornadoes in this study occurred in favorable low level shear environments apparently related to topographic channeling and when the deep layer shear environments were already favorable for the development of supercell thunderstorms.



An important difference between the present results from those summarized in Lipari (2000) and Monteverdi et al. (2003) centers on the circumstantial evidence regarding the nature of the parent thunderstorm. In those earlier studies, there was clear statistical justification for assuming that the F1 and F2 bins (in their studies) suggested that the parent thunderstorms were supercells and the tornadoes mesocyclone-induced. Simply stated, the shear values associated with the F1 bin in the earlier studies corresponded to the values widely regarded as consistent with supercellular convection. In the examination of the shear data from the entire data set in this study, the author found that there were no statistically significant differences between the shear values in the F0 and F1 bins, though values were slightly larger in the latter. In fact, there were considerably more statistical similarities between those two bins and differences between them and those for the F2/F3 cases.

The author suspected that although this might be true, there might be a non-meteorological reason for the differences in the present results with respect to the F1 bin. In particular, the overrating of tornado intensity that has been identified in the tornado literature might be responsible for the inclusion of mistakenly higher rated tornado events into the lower intensity bins. In fact, other issues with the assigning of ratings before 1980 may create a flawed analysis for the early period.

To test this, the author separated out all events pre and post 1980 and did a separate analysis of the shear and buoyancy for each of those two groupings. From 1950 to 1980 there appears to be a systematic over rating of the F0 and F1 tornado events that

occurred in California. The ABVSHR for these events both in the 0-1 km and 0-6 km levels was weaker than that of the tornado events that occurred after 1980. By separating the shear parameters into before and after 1980 it is apparent that the events occurring after 1980 exhibit low level and deep layer shear values consistent with supercell tornado events occurring in California found by Monteverdi et al. (2003) and by other studies of tornadoes conducted in the Great Plains. This suggests that a large majority (65-70%) of the tornado events occurring after 1980 were supercellular. It also suggests that similar results would be found for the earlier period, and that serious errors might have occurred in the assigning of ratings before 1980.

The author made an attempt to investigate these issues a bit by completing short case studies of two of the more damaging events in the very early California tornado record: the Sunnyvale tornado of January 11, 1951 and the Los Angeles Convention Center tornado of March 1, 1983, which are listed in the record as F2 tornadoes. The buoyancy and shear environments were evaluated for both of these events. The low level and deep layer shear magnitudes were at the upper end of the envelope of shear values for tornadic supercell events, and suggested that both events might be associated with strong and violent tornadoes, F3 and higher intensity.

The author attempted to categorize the damage with both events by an investigation of the documentary evidence and associating it with the EF-damage scale guidelines that are in use currently. The investigation suggests that the Sunnyvale tornado should be re-rated to an F3 tornado. Additional damage around the Bay Area on

this day suggests that there were as many as seven other tornadoes that occurred with F-ratings ranging from F0 to F3 intensity. In short, the San Francisco Bay Area experienced what would be considered a major tornado outbreak in other areas of the country.

The evidence regarding the damage done by the March 1, 1983 Los Angeles tornado is more difficult to evaluate and is somewhat ambiguous. Damage in the neighborhoods surrounding the Los Angeles Convention Center appeared to suggest high end F2 and low end F3 tornado intensity. However, the damage to the convention center itself does appear to be consistent with the F2 rerating. Thus, more thoughtful analysis would need to be accomplished before the author would recommend rerating this tornado event.

## **7.2 Limitations of Methodology**

The use of constructed tornado proximity soundings, as explained in section 4.2.1, is the method favored in situations when a proximity radiosonde is not available. While there are inherent limitations of the constructed soundings and hodographs, the author believes these limitations did not diminish the quality and accuracy of the results of this study in any important way. The availability, and/or lack of, observational data may always be a contention in performing analysis and research. As meteorological events become more localized, the ability for of numerical forecast models and surface

observation network to diagnose such environments becomes increasingly dependent on the availability of surface observations located near the developing storms [Davies, 1993a].

One factor that may have affected the results is the occurrence of both anticyclonically and cyclonically turning hodographs. The combination of both of these shear environments into the composite soundings and shear environments may provide either a positive or negative bias to the results found within this study. But the author argues that any bias was marginal and did not influence the overall results of the study.

### **7.3 Future Work**

The author plans to validate of the methods and results of this study by studying the shear environments of California tornadic events since 2002 by analyzing the NWS's Rapid Update Cycle (RUC) and Rapid Refresh (RAP) model generated proximity soundings and hodographs. Additionally, the Weather Research and Forecasting (WRF) model could be used to develop proximity soundings for all tornado events (1951–2011) using the synoptic and surface environment present near the time of each tornado event as the initialization parameters of the model. The use of these three numerical models to generate proximity soundings may provide a more accurate representation of the buoyancy and shear environment present for each tornado event. The comparison of these results with those obtained by use of the proximity soundings

obtained by the methods described in section 4.2.1 would be a contribution not only to the literature on California tornadic storms, but to that on tornadic storm environments in general.

## References

- Aldrich, J. H., 1970: Convergence Zones in Southern California. *Weather*, 25, 140-146
- Adlerman, E. J., K. K. Droegemeir, and R. Davies-Jones, 1999: A numerical simulation of cyclic mesocyclogenesis. *J. Atmos. Sci.*, 56, 2045-2069.
- American Meteorological Society Glossary of Meteorology, 2012: "Convective Inhibition", [online] Available from: <http://amsglossary.allenpress.com/glossary/search?p=1&query=convective+inhibition&submit=Search> (Accessed 24 April 2012).
- American Meteorological Society Glossary of Meteorology, 2012: "Misocyclone", [online] Available from: <http://amsglossary.allenpress.com/glossary/search?p=1&query=misocyclone&submit=Search> (Accessed 24 April 2012)
- American Meteorological Society Glossary of Meteorology, 2012: "Tornado", [online] Available from: <http://amsglossary.allenpress.com/glossary/search?id=tornado1> (Accessed 24 April 2012)
- Blanchard, D.O., 1998: Assessing the vertical distribution of convective available potential energy. *Weather and Forecasting*, 13, 870-877.
- Blier, W., and K. A. Batten, 1993 (a): A case study of a northern California tornado accompanied by unusually thorough photographic documentation. Preprints, 17<sup>th</sup> Conf. on Severe Local Storms, St. Louis, MO, Amer. Meteor. Soc., 342-346.
- Blier, W., and K. A. Batten, 1993 (b): Climatological analysis of California tornadoes, Preprints, 17<sup>th</sup> Conf. on Severe Local Storms, St. Louis, MO, Amer. Meteor. Soc., 15-19.
- Blier, W., and K. A. Batten, 1994: On the incidence of tornadoes in California. *Wea. Forecasting*, 9, 301-315.
- Bluestein, H. B., 1979: A mini-tornado in California. *Mon. Wea. Rev.*, 107, 1227-1229.
- Bluestein, H. B., 1985: The formation of a "landspout" in a "broken-line" squall line in Oklahoma. Preprints, 14<sup>th</sup> Conf. on Severe Local Storms, Indianapolis, IN, Amer. Meteor. Soc., 267-270.

- Bluestein, H. B., 1993: *Synoptic-Dynamic Meteorology in Midlatitudes*, Vol. II. Oxford, 594 pp.
- Bluestein, H. B., and K. Thomas, 1984: Diagnosis of a jet streak in the vicinity of a severe weather outbreak in the Texas Panhandle. *Mon. Wea. Rev.*, 112, 2499-2519.
- Brady, R. H., and E. Szoke, 1988: The landspout – a common type of northeast Colorado tornado. Preprints, *15<sup>th</sup> Conf. on Severe Local Storms*, Baltimore, MD, Amer. Meteor. Soc., 312-315.
- Braun, S. A. and J. P. Monteverdi, 1991: An analysis of a mesocyclone-induced tornado occurrence in northern California. *Wea. Forecasting*, 6, 13-31.
- Brandes, E. A., 1978: Mesocyclone evolution and tornadogenesis: Some observations. *Mon. Wea. Rev.*, 106, 995-1011.
- Brooks, H. E., C. A. Doswell III, and R. Davies-Jones, 1993: Environmental helicity and the maintenance and evolution of low-level mesocyclones. *The Tornado: Its Structure, Dynamics, Prediction, and Hazards* (C. Church et al., Eds.), *Geophys. Monogr.* 79, Amer. Geophys. Union, 97-104.
- Brooks, H.E., Doswell III, and C.A., Cooper, J., 1994. On the environments of tornadic and nontornadic mesocyclones. *Weather Forecast.* 9, 606–618
- Brooks, H.E., Doswell III, and R. B. Wilhelmson, 1994b, On the role of midtropospheric winds in the evolution and maintenance of low-level mesocyclones. *Mon. Wea. Rev.*, 122, 126-136.
- Brooks, H. E., and J. P. Craven, 2002: A database of proximity soundings for significant severe thunderstorms, 1957-1993. Preprints, *21<sup>st</sup> Conf. on Severe Local Storms*, San Antonio, TX, Amer. Meteor. Soc., 639-642.
- Brooks, H. E., J. W. Lee, and J. P. Craven, 2003: The spatial distribution of severe thunderstorm and tornado environments from global reanalysis data. *Atmos. Res.*, 67-68, 73-94.
- Browning, K. A., and C. R. Landry, 1963: Air flow within a tornadic storm. Preprints, *10<sup>th</sup> Weather Radar Conf.*, Boston, MA, Amer. Meteor. Soc., 116-122.

- Bunkers, M. J., B. A. Klimowski, J. W. Zeitler, R. L. Thompson, and M. L. Weisman, 2000: Predicting supercell motion using a new hodograph technique, *Wea. Forecasting*, 15, 61-79.
- Burgess, D. W., 1976: Single Doppler radar vortex recognition. Part I: Mesocyclone signatures. *Preprints, 17th Conf. on Radar Meteorology*, Seattle, WA, Amer. Meteor. Soc., 97-103.
- Burgess, D. W., and R. J. Donaldson, 1979: Contrasting tornadic storms types. *Preprints, 11<sup>th</sup> Conf. on Severe Local Storms*, Kansas City, MO, Amer. Meteor. Soc., 189-192.
- Carbone, R. E., 1982: A severe frontal rainband: part I – stormwide hydrodynamic structure. *J. Atmos. Sci.*, 39, 258-279.
- Carbone, R. E., 1983: A severe frontal rainband: part II – tornado parent vortex circulation. *J. Atmos. Sci.*, 40, 2639-2654.
- Cooley, J., 1978: Cold air funnel clouds. *Mon. Wea. Rev.*, 106, 1368-1372.
- Craven, J. P., 2001: A baseline climatology of sounding derived parameters associated with deep, moist convection. Unpublished manuscript, 56 pp. [Available from Storm Prediction Center, 1313 Halley Circle, Norman, OK 73069].
- Craven, J. P., H. E. Brooks, and J. A. Hart, 2002: Baseline climatology of sounding derived parameters associated with deep, moist convection. *Preprints, 21st Conference on Severe Local Storms*, San Antonio, TX, American Meteorological Society.
- Darkow, G. L., 1969: An analysis of over sixty tornado proximity soundings. *Preprints, 6<sup>th</sup> Conf. on Severe Local Storms*, Chicago, IL, Amer. Meteor. Soc., 218-221.
- Davies, J. M., 1989: On the use of shear magnitudes and hodographs in tornado forecasting. *Preprints, 12<sup>th</sup> Conf. on Weather Analysis and Forecasting*. Monterey, CA, Amer. Meteor. Soc., 219-224.
- Davies, J. M., 1993 (a): Hourly helicity, instability, and EHI in forecasting supercell tornadoes. *Preprints, 17<sup>th</sup> Conf. on Severe Local Storms*, St. Louis, MO, Amer. Meteor. Soc., 107-111.



- Davies, J. M. 1993 (b): Small tornadic supercells in the central plains. Preprints. *17<sup>th</sup> Conf. on Severe Local Storms*, St. Louis, MO, Amer. Meteor. Soc., 305-309.
- Davies, J. M., and R. H. Johns, 1993: Some wind and instability parameters associated with strong and violent tornadoes: part I – wind shear and helicity. *The Tornado: Its Structure, Dynamics, Prediction, and Hazards* (C. Church et al., Eds.), *Geophys. Monogr.* 79, Amer. Geophys. Union, 573-582.
- Davies, J. M., 2001: Supercell and tornado parameters from a large dataset of simple forecast soundings. *2001 Central Iowa Severe Storms Conference*, Des Moines, IA, National Weather Association.
- Davies, J. M., 2004: Estimations of CIN and LFC associated with tornadic and nontornadic supercells. *Wea. Forecasting*, 19, 714-726.
- Davies-Jones, R. P., 1986: Tornado dynamics. In *Thunderstorm Morphology and Dynamics*, E. Kessler, ed., 2nd ed. (Vol. 2 of *Thunderstorms: A Social, Scientific, and Technological Documentary*). University of Oklahoma Press, 411 pp.
- Davies-Jones, R., D. Burgess, and M. Foster, 1990: Test of helicity as a tornado forecast parameter. Preprints, *16th Conf. on Severe Local Storms*, Kananaskis Park, AB, Canada, Amer. Meteor. Soc., 588-592.
- Davies-Jones, R. P., and H. E. Brooks, 1993: Mesocyclogenesis from a theoretical perspective. Tornadoes and tornadic storms: A review of conceptual models. *The Tornado: Its Structure, Dynamics, Prediction, and Hazards*. Geophys. Monogr. No. 79, Amer. Geophys. Union, 105-114.
- Davies-Jones, R. P., R. J. Trapp, and H. B. Bluestein, 2001: *Tornadoes and Tornadic Storms*. Meteor. Monogr., No. 50, Amer. Meteor. Soc., 167-221.
- Doswell, C. A., III, 1982: The operational meteorology of convective weather—Volume I: Operational mesoanalysis. NOAA Tech. Memo. NWS NSSFC-5, 170 pp. [Available from the National Severe Storms Laboratory, 1313 Halley Circle, Normal, OK 73069].
- Doswell, C. A. III, and D. W. Burgess, 1988: On some issues of United States tornado climatology. *Mon. Wea. Rev.*, 116, 495-501.

- Doswell, C. A., III, 1991: A review for forecasters on the application of hodographs to forecasting severe thunderstorms. *Natl. Wea. Dig.*, 16, 2-16.
- Doswell, C. A., III, and D. W. Burgess, 1993: Tornadoes and tornadic storms: A review of conceptual models. *The Tornado: Its Structure, Dynamics, Prediction, and Hazards* (C. Church et al., Eds.), *Geophys. Monogr.* 79, Amer. Geophys. Union, 161-172.
- Doswell, C. A., III, and E. N. Rasmussen, 1994: The effect of neglecting the virtual temperature correction on CAPE calculations. *Wea. Forecasting.*, 9, 625-629.
- Doswell, C. A. III, and J. S. Evans, 2003: Proximity sounding analysis for derechos and supercells: An assessment of similarities and differences. *Atmos. Research*, 67-68, 117-133.
- Doswell, C. A. III, 2012: On the role of deep columnar convective vortices within the atmosphere, [online] Available from: <http://www.flame.org/~cdoswell/SuptorRoles/SuptorRoles.html> (Accessed 24 April 2012).
- Edwards, R., and R. L. Thompson, 2000: RUC-2 supercell proximity soundings, Part II: An independent assessment of supercell forecast parameters. Preprints, 20<sup>th</sup> Conf. on Severe Local Storms, Orlando, FL, Amer. Meteor. Soc., 435-438.
- Edwards, R. E., 2008: The online tornado FAQ: Frequently asked questions about tornadoes. Storm Prediction Center. Available from: <http://www.spc.noaa.gov/faq/tornado/ef-scale.html> (Accessed 24 April 2012).
- Edwards, R. E., 2008: The online tornado FAQ: Frequently asked questions about tornadoes. Storm Prediction Center. Available from: <http://www.spc.noaa.gov/faq/tornado/> (Accessed 24 April 2012).
- ESRI 2012. ArcGIS Desktop: Release 10. Redlands, CA: Environmental Systems Research Institute.
- ESRL 2012, 6-Hourly NCEP/NCAR Reanalysis Data Composites, [online] Available from: <http://www.esrl.noaa.gov/psd/data/composites/hour/> (Accessed 5 March, 2012).

- Fujita, T. T., 1971: Proposed characterization of tornadoes and hurricanes by area and intensity. SMRP Res. Pap. No. 91, Dept. of Geophysical Science, University of Chicago, 42 pp.
- Fujita, T. T., 1981: Tornadoes and downbursts in the context of generalized planetary scales. *J. Atmos. Sci.*, 38, 1511-1534.
- Glickman, T. S., Ed., 2000: *Glossary of Meteorology*, 2d ed. Amer. Meteor. Soc., 782 pp.
- Grasso, L. D., and W. R. Cotton, 1995: Numerical Simulations of tornado vortex. *J. Atmos. Sci.*, 52, 1192-1203.
- Golden, J. H., 1971: Waterspouts and tornadoes over south Florida. *Mon. Wea. Rev.*, 99, 146-154.
- Golden, J. H., 1973: Some statistical aspects of waterspout formation. *Weatherwise*, 26, 108-117.
- Grasso, L. D., and W. R. Cotton, 1995: Numerical simulation of tornado vortex. *J. Atmos. Sci.*, **52**, 1192-1203.
- Grzych, M. L. B. D. Lee, and C. A. Finley, 2007: Thermodynamic analysis of supercell rear-flank downdrafts from Project ANSWERS. *Mon. Wea. Rev.*, **135**, 240-246.
- Hales, J. E., 1972: Surges of maritime tropical air northward over the Gulf of California, *Mon. Wea. Rev.*, 100, 298 – 306.
- Hales, J. E., Jr., and C. A. Doswell III, 1982: High resolution diagnosis of instability using hourly surface lifted parcel temperatures. Preprints, *12<sup>th</sup> Conf. on Severe Local Storms*, San Antonio, TX, Amer. Meteor. Soc., 172-175.
- Hales, J. E., Jr., 1985: Synoptic features associated with Los Angeles tornado occurrences. *Bull. Amer. Meteor. Soc.*, 66, 657-661
- Hamill, T. M., and A. Church, 2000: Conditional tornado probabilities From RUC-2 forecasts, *Wea. Forecasting*, **15**, 461-475.
- Hart, G. C., L. E. Escalante, W. J. Petale, C. W. Pinkham, E. Schwartz, and M. Wurtele, 1985: *The Los Angeles, California Tornado of March 1, 1983*. National Academy Press, 39 pp.

- Holton, J. R., 2004: *An Introduction to Dynamic Meteorology*. 4th ed. San Diego: Academic Press, 535 pp.
- Houze, R. A., Jr., 1993: *Cloud Dynamics*. San Diego, Academic Press, 573 pp.
- Johns, R.H., J.M. Davies, and P.W. Leftwich, 1990: An examination of the relationship of 0-2 km AGL “positive” wind shear to potential buoyant energy in strong and violent tornado situations. Preprints, *16<sup>th</sup> Conf. on Severe Local Storms*, Kananaskis Park, AB, Canada, Amer. Meteor. Soc., 593-598.
- Johns, R. H., and C. A. Doswell III, 1992: Severe local storms forecasting. *Wea. Forecasting*, 7, 588-612.
- Johns, R. H., J. M. Davies, and P. W. Leftwich, 1993: Some wind and instability parameters associated with strong and violent tornadoes: part II – variations in the combinations of wind and instability parameters. *The Tornado: Its Structure, Dynamics, Prediction, and Hazards* (C. Church et al., Eds.), *Geophys. Monogr.* 79, Amer. Geophys. Union, 583-590.
- Kelly, D. L., J. T. Schaefer, R. P. McNulty, C. A. Doswell III, and R. F. Abbey, Jr., 1978: An augmented tornado climatology. *Mon. Wea. Rev.*, 106, 1172-1183.
- Kerr, B. W., and G. L. Darkow, 1996: Storm-relative winds and helicity in the tornadic thunderstorm environment. *Wea. Forecasting*, 11, 489-505.
- Klemp, J. B., and R. B. Wilhelmson, 1978: Simulations of right- and left-moving thunderstorms produced through storm splitting. *J. Atmos. Sci.*, **35**, 1097-1110.
- Kocin, P. C., L. W. Uccellini, and R. A. Peterson, 1986: Rapid evolution of a jet streak circulation in a pre-convective environment. *Meteor. Atmos. Phys.*, 35, 103-138.
- Korotky, J., R. W. Przybylinski, and J. A. Hart, 1993: The Plainfield , Illinois, tornado of August 28, 1990 – the evolution of synoptic and mesoscale environments. *The Tornado: Its Structure, Dynamics, Prediction, and Hazards* (C. Church et al., Eds.), *Geophys. Monogr.* 79, Amer. Geophys. Union, 611-624.
- LaDochy, S. and J. Brown, 2001: Topographic and synoptic influences on cold season California severe weather: Regional patterns in convective storms, Preprints, *20<sup>th</sup> Conf. on Severe Local Storms*, Amer. Meteor. Soc., Orlando, FL, 485-488.

- Lemon, L. R., and C. A. Doswell, 1979: Severe thunderstorm evolution and mesocyclone structure as related to tornadogenesis. *Mon. Wea. Rev.*, **107**, 1184-1197.
- Lipari, G. S. and J. P. Monteverdi, 2000: Convective and shear parameters associated with Northern and Central California tornadoes during the period 1990-1994. Preprints, *20<sup>th</sup> Conf. on Severe Local Storms*, Orlando, FL, Amer. Meteor. Soc., 518-521.
- Markowski, P. M., E. N. Rasmussen, and J. M. Straka, 1998a: The occurrence of tornadoes in supercells interacting with boundaries during VORTEX-95. *Wea. Forecasting*, **13**, 852-859.
- Markowski, P. M., J. M. Straka, E. N. Rasmussen, and D. O. Blanchard, 1998b: Variability of storm-relative helicity during VORTEX. *Mon. Wea. Rev.*, **11**, 2959-2971.
- Markowski, P. M., 2002: Hook echoes and rear-flank downdrafts: A review. *Mon. Wea. Rev.*, **130**, 852-876.
- Markowski, P. M., and Y. P. Richardson, 2008: Tornadogenesis: Our current understanding, forecasting considerations, and questions to guide future research. *Atmos. Res.*, **93**, 3-10.
- Markowski, P. M., J. M. Straka, and E. N. Rasmussen, 2002: Direct surface thermodynamic observations within the rear-flank downdrafts of nontornadic and tornadic supercells. *Mon. Wea. Rev.*, **130**, 1692-1721.
- Markowski, P. M., J. M. Straka, and E. N. Rasmussen, 2003: Tornadogenesis resulting from the transport of circulation by a downdraft. *J. Atmos. Sci.*, **60**, 795-823.
- Markowski, P., and Y. Richardson, 2010: *Mesoscale Meteorology in Midlatitudes*. Oxford: Wiley-Blackwell, 407 pp.
- McCaul, E. W., Jr., 1990: Simulations of convective storms in hurricane environments. Preprints, *16<sup>th</sup> Conf. on Severe Local Storms*, Kananaskis Park, AB, Canada, Amer. Meteor. Soc., 334-339.
- McCaul, E. W., Jr., 1991: Buoyancy and shear characteristics of hurricane-tornado environments. *Mon. Wea. Rev.*, **119**, 1951-1978.

- McCaul, E. W., Jr., 1993: Observations and simulations of hurricane-spawned tornadoes. *The Tornado: Its Structure, Dynamics, Prediction, and Hazards* (C. Church et al., Eds.), *Geophys. Monogr.* 79, Amer. Geophys. Union, 119-142.
- McCaul, E. W., Jr., and M. L. Weisman, 1996: Simulations of shallow supercell storms in landfalling hurricane environments. *Mon. Wea. Rev.*, 124, 408-429.
- McDonald, J. R., K. C. Mehta, and S. Mani, 2006: A recommendation for an enhanced Fujita scale (EF-Scale), revision 2. Wind Science and Engineering, Texas Tech. Univ., Lubbock, TX, 111 pp. [Available at [www.wind.ttu.edu/EFScale.pdf](http://www.wind.ttu.edu/EFScale.pdf)].
- McNulty, R., 1978: On upper tropospheric kinematics and severe weather occurrence. *Mon. Wea. Rev.*, 106, 662-672.
- Meier, K., 1993: Jet streak dynamics: effects of curvature. Western Region Technical Attachment 93-03, 3 pp. [Available from the National Weather Service Western Region, P.O. Box 11188, Salt Lake City, UT 84146].
- Mesinger, Fedor, and Coauthors, 2006: North American Regional Reanalysis. *Bull. Amer. Meteor. Soc.*, 87, 343-360.
- Moller, A. R., C. A. Doswell III, M. P. Foster, and G. R. Woodall, 1994: The operation recognition of supercell thunderstorm environments and storm structures. *Wea. Forecasting*, 9, 237-347.
- Monteverdi, J.P., S. A. Braun, and T. Trimble, 1988: Funnel clouds in the San Joaquin Valley, California, *Mon. Wea. Rev.*, 116, 787-789.
- Monteverdi, J. P., 1993: A case study of the operational usefulness of the SHARP workstation in forecasting a mesocyclone-induced cold sector tornado event in California. NOAA Tech. Memo. NWS WR-219, 22 pp. [Available from National Weather Service Western Region, P.O. Box 11188, Salt Lake City, UT, 84146].
- Monteverdi, J.P., and J. Quadros, 1994: Convective and rotation parameters associated with three tornado episodes in northern and central California. *Wea. Forecasting*, 9, 285-300.
- Monteverdi, J.P., and S. Johnson, 1996: A supercell with hook echo in the San Joaquin Valley of California. *Wea. Forecasting*, 11, 246-261.

- Monteverdi, J. P., W. Blier, G. Stumpf, W. Pi, and K. Anderson, 2001: First WSR-88D documentation of an anticyclonic supercell with anticyclonic tornadoes: The Sunnyvale/Los Altos, California tornadoes of 4 May 1998, *Mon. Wea. Rev.*, **129**, 2805-2814.
- Monteverdi, J. P., C. Doswell III, and G. S. Lipari, 2003: Shear parameter thresholds for forecasting tornadic thunderstorms in Northern and Central California. *Wea. Forecasting*, **18**, 357-370.
- Parish, T. R., 1982: Barrier winds along the Sierra Nevada Mountains. *J. Appl. Meteor.*, **21**, 925-930.
- NOAA NCDC Storm Data Publication, 2012, [online] Available from: <http://www.ncdc.noaa.gov/oa/climate/sd/> (Accessed 2 January 2012).
- NOAA NCDC 2012, Radiosonde Data of North America CD-ROM (1946–1996)
- NOAA NWS 2012, National Weather Service Glossary, [online] Available from: <http://www.weather.gov/glossary/index.php?word=severe+thunderstorm> (Accessed 24 April 2012).
- RAOB: The Rawinsonde Observation Program for Windows. Weather Graphics Technologies. Version 6.3 Beta. Released 2011.
- Rasmussen, E. N., and R. B. Wilhelmson, 1983: Relationships between storm characteristics and 1200 GMT hodographs, low-level shear, and stability. Preprints, *13<sup>th</sup> Conf. on Severe Local Storms*, Tulsa, OK, Amer. Meteor. Soc., J5-J8
- Rasmussen, E. N., J. M. Straka, R. P. Davies-Jones, C. A. Doswell III, F. H. Carr, M.D. Eilts, and D. R. MacGorman, 1994: Verification of the Origins of Rotation in Tornadoes Experiment: VORTEX, *Bull. Amer. Meteor. Soc.*, **75**, 995-1006.
- Rasmussen, E. N., and D. O. Blanchard, 1998: A baseline climatology of sounding derived supercell and tornado forecast parameters. *Wea. Forecasting*, **13**, 1148-1164., **18**, 530-535.
- Rasmussen, E. N., 2003: Refined supercell and tornado forecast parameters. *Wea. Forecasting*, **18**, 530-535.

- Reed R., and W. Blier, 1986: A case study of comma cloud development over the eastern Pacific. *Mon. Wea. Rev.*, **114**, 1681-1695.
- Rotunno, R., and J. B. Klemp, 1982: The influence of shear-induced pressure gradient on thunderstorm motion. *Mon. Wea. Rev.*, **110**, 136-151.
- Rotunno, R., and J. B. Klemp, 1985: On the rotation and propagation of simulated supercell thunderstorms. *J. Atmos Sci.*, **45**, 463-485.
- Rotunno, R., 1986: Tornadoes and tornadogenesis. *Mesoscale Meteorology and Forecasting*, P. S. Ray, Ed., Amer. Meteor. Soc., 414-436.
- Shabbott, C. J., and P. M. Markowski, 2006: Surface in situ observations within the outflow of forward-flank downdrafts of supercell thunderstorms. *Mon. Wea. Rev.*, **134**, 1422-1441.
- Small, I., Mackechnie, T., and Bower, B., 2000: Mesoscale Interactions Triggering Severe Thunderstorms and Flash Flooding in Southwestern California July 1999. Western Regional Technical Attachment, 00-01, [online] Available online from: <http://www.wrh.noaa.gov/wrh/00TAs/0001/index.html> (Accessed 24 April 2012).
- Small, I., T. Mackechnie, and S. Vanderburg, 2009: The Dramatic Effect of Tornadic Severe Weather on a Rapidly Growing Urban Interface. Symposium on Urban High Impact Weather, The 89<sup>th</sup> American Meteorological Society Annual Meeting, Phoenix, AZ, [online] Available from: <http://ams.confex.com/ams/pdfpapers/144420.pdf> (Accessed 24 April 2012).
- Smith, R. K., and L. M. Leslie, 1979: A numerical study of tornadogenesis in a rotating thunderstorm. *Quart. J. Roy. Meteor. Soc.*, **105**, 107-127.
- Smith, T. B., and V. A. Mirabella, 1972: Characteristics of California tornadoes. Report to the University of California Lawrence Livermore Laboratory by Meteorological Research Inc., 25 pp.
- Storm Prediction Center Severe Weather GIS, 2012, [online] Available from: <http://www.spc.noaa.gov/gis/svrgis/> (Accessed 3 March 2012).
- Stensrud, D. J., J. V. Cortinas Jr., and H. E. Brooks, 1997: Discriminating between tornadic and nontornadic thunderstorms using mesoscale model output. *Wea. Forecasting*, **12**, 613-632.



- Thompson, R. L., R. Edwards, and J. A. Hart, 2002: Evaluation and interpretation of the supercell composite and significant tornado parameters at the Storm Prediction Center. Preprints, *21st Conference on Severe Local Storms*, San Antonio, TX, American Meteorological Society.
- Trapp, R. J., and R. Davies-Jones, 1997: Tornadogenesis with and without a dynamic pipe effect. *J. Atmos. Sci.*, **54**, 113-133.
- Trapp, R.J., S.A. Tessendorf, E.S. Godfrey, and H.E. Brooks, 2005: Tornadoes from Squall Lines and Bow Echoes. Part I: Climatological Distribution. *Wea. Forecasting*, **20**, 23-34.
- Walko, R. L., 1993: Tornado spin-up beneath a convective cell: Required basic structure of the near-field boundary layer winds. *The Tornado: Its Structure, Dynamics, Prediction, and Hazards*. Geophys. Monogr. No. 79, Amer. Geophys. Union, 89-95.
- Wakimoto, R. M., 1983: The West Bend, Wisconsin storm of 4 April 1981: A problem in operational meteorology. *J. climate Appl. Meteor.*, **22**, 181-189.
- Wakimoto, R.M., and J.W. Wilson, 1989: Non-supercell Tornadoes. *Mon. Wea. Rev.*, **117**, 1113-1140.
- WeatherGraphics Inc., 2012: Total Surface and Upper Air Observation Sets, 1951-2011. Available from Weather Graphics, P.O. Box 450211, Garland TX.
- Weisman, M. L., and J. B. Klemp, 1982: The dependence of numerically simulated convective storms on vertical wind shear and buoyancy. *Mon. Wea. Rev.*, **110**, 504-520.
- Weisman, M.L., and J.B. Klemp, 1984: The Structure and Classification of Numerically Simulated Convective Storms in Directionally Varying Wind Shears. *Mon. Wea. Rev.*, **112**, 2479-2498.
- Weisman, M. L., and J. B. Klemp, 1986: Characteristics of isolated convective storms (Chap. 15). In *Mesoscale Meteorology and Forecasting* (P. Ray, ed.), Amer. Meteor. Soc., Boston, 331-358.

- Wicker, L. J., and R. B. Wilhelmson, 1995: Simulation and analysis of tornado development and decay within a three-dimensional supercell thunderstorm. *J. Atmos. Sci.*, **52**, 2675-2703.
- Wicker, L. J., and L. Cantrell, 1996: The role of vertical buoyancy distributions in miniature supercells. *Preprints, 18th Conf. on Severe Local Storms*, San Francisco, CA, Amer. Meteor. Soc., 225-229.
- Wilson, J. W., 1986: Tornadogenesis by nonprecipitation induced wind shear lines. *Mon. Wea. Rev.*, **114**, 270-284.

## Appendix 1: Compilation of Buoyancy and Shear Parameters for 391 Tornado events from 1951–2011

**Table A1 Compilation of results from 22 tornado proximity soundings for the 1950s**

Tornado Number	County of Occurrence	Date	Time (LST)	F-Rating	Latitude (°N)	Longitude	Width (Yards)	Length (Miles)	0-1 km ABVSHR (x10 <sup>-3</sup> s <sup>-1</sup> )	0-6 km ABVSHR (x10 <sup>-3</sup> s <sup>-1</sup> )	0-1 km Bulk Shear (x10 <sup>-3</sup> s <sup>-1</sup> )	0-6 km Bulk Shear (x10 <sup>-3</sup> s <sup>-1</sup> )	0-3 km CAPE (J/kg)	Total CAPE (J/kg)	CIN (J/kg)	0-1 km Total SRH (m/s) <sup>2</sup>	0-3 km Total SRH (m/s) <sup>2</sup>	EH1	BRN	VGP
torid #001	Santa Clara	1/11/1951	0825	F2	37.37	-122.12	5.7	10	18.7	8.6	15.7	7.4	92	339	-5	239.9	311.5	0.7	3	0.199
torid #002	Los Angeles	12/20/1952	1200	M	34.4	-118.53	0.1	10	4.4	2.8	4.4	3.8	180	288	-2	0	149.4	0.2	5	0.151
torid #003	Stanislaus	4/27/1953	1315	F2	37.65	-121	0.1	10	16.9	6	16.6	5.3	221	322	0	250.9	341.3	0.3	8	0.137
torid #004	Glenn	5/19/1953	1330	F2	39.75	-122.18	2	10	20.5	7.2	17.5	8.1	170	330	0	149.8	154.5	0.4	2	0.18
torid #005	San Bernardino	6/25/1954	1000	F2	34.63	-117.2	0.1	10	7	3	5.1	0.9	-94	47	-207	22.7	10.9	0	72	0.093
torid #006	Los Angeles	1/18/1955	1101	M	34.05	-118.3	3	23	4.5	4.5	4.8	6.2	28	28	0	45.8	100	0	0	0.204
torid #007	Riverside	4/6/1955	1330	M	34	-117.25	1	50	3.8	2.9	2.7	3.1	36	121	0	20.7	13.3	0	5	0.102
torid #008	Merced	4/18/1955	1200	M	37.3	-120.25	0.1	10	16.2	3.2	14.6	4.5	82	218	-9	171.7	185.7	0.3	7	0.1
torid #009	San Diego	4/13/1956	1455	F1	32.63	-117.08	0.1	20	7.3	4	6.8	3.9	188	521	0	106.5	246	0.7	5	0.177
torid #010	Los Angeles	5/9/1956	0830	F0	34.08	-118.18	0.1	17	6.5	2.9	6.4	3.9	258	660	0	73.7	88.1	0.4	19	0.151
torid #011	Fresno	5/19/1957	0822	F1	36.7	-119.83	0.1	10	21.7	7.1	19.7	7.7	350	52	-14	242.5	355.4	0	2	0.052
torid #012	Del Norte	1/10/1958	0245	F0	41.75	-124.2	0.8	60	4.1	3.9	6.5	3.4	183	674	0	49.5	212.5	0.6	6	0.204
torid #013	Mendocino	2/3/1958	1000	M	38.75	-123.53	0.1	10	17.3	4.6	9.6	3.1	65	104	-21	142	137.4	0.1	2	0.304
torid #014	Madera	2/28/1958	0500	M	37.12	-119.7	0.5	90	6.8	4.4	5.2	4.4	369	777	0	10.2	9	0.2	17	0.22
torid #015	Madera	3/12/1958	1100	F0	36.97	-120.07	0.2	10	16.4	4.4	13.5	2.3	96	240	0	154.9	171	0.2	9	0.102
torid #016	Humboldt	3/29/1958	1340	F2	40.95	-124.1	2	200	14	7.9	13.4	6.9	61	61	0	158.5	233.7	0.1	0	0.064
torid #017	San Mateo	4/1/1958	0025	M	37.62	-122.35	0.2	67	5.3	3.7	6.8	4.4	133	136	0	59.9	142.8	0	3	0.073
torid #018	Stanislaus	4/1/1958	0500	F1	37.47	-120.78	2	20	20	6.7	19.7	7.7	350	350	0	184.6	297.9	0.6	2	0.189
torid #019	Orange	4/1/1958	0930	M	33.52	-117.77	0.5	30	20.7	4.6	18.4	4.4	48	438	-17	288.7	252.3	0.8	6	0.118
torid #020	Siskiyou	5/22/1958	1800	F1	41.92	-121.47	2.7	50	11.8	5	5	3.8	-51	376	-62	35.3	145.3	0.2	5	0.161
torid #021	Sonoma	6/1/1958	0555	F2	38.28	-122.98	15	50	16.1	6.2	6.3	3.1	59	400	-29	87.5	95.3	0.3	62	0.186
torid #022	Sonoma	2/17/1959	0445	M	38.52	-123.25	0.5	50	14.7	4.3	9.4	5.2	214	284	-5	183.1	316.7	0.5	2	0.155

## Appendix 1: Compilation of Buoyancy and Shear Parameters for 391 Tornado events from 1951–2011

**Table A2 Compilation of results from 26 tornado proximity soundings for the 1960s**

Tornado Number	County of Occurrence	Date	Time (LST)	F-Rating	Latitude (°N)	Longitude	Width (Yards)	Length (Miles)	0-1 km ABVSHR (x10 <sup>-3</sup> s <sup>-1</sup> )	0-6 km ABVSHR (x10 <sup>-3</sup> s <sup>-1</sup> )	0-1 km Bulk Shear (x10 <sup>-3</sup> s <sup>-1</sup> )	0-6 km Bulk Shear (x10 <sup>-3</sup> s <sup>-1</sup> )	0-3 km CAPE (J/kg)	Total CAPE (J/kg)	CIN (J/kg)	0-1 km Total SRH (m/s) <sup>2</sup>	0-3 km Total SRH (m/s) <sup>2</sup>	EH1	BRN	VGP
torid #023	Del Norte	5/13/1960	1300	M	41.55	-124	0.1	10	9.3	4	7.9	4.2	192	246	0	23.6	<b>88.3</b>	<b>0.1</b>	<b>7</b>	<b>0.183</b>
torid #024	San Diego	10/8/1961	0930	F1	33.17	-117.35	0.1	10	18	7.3	17.3	9.4	188	471	-9	64.7	81.1	0.2	3	0.174
torid #025	Orange	2/19/1962	0330	F0	33.7	-117.8	2	10	17	9.7	14.6	4.9	6	54	-4	313.6	566.2	0.2	0	0.1
torid #026	Orange	2/19/1962	1600	F1	33.68	-117.78	0.6	250	9.1	2.3	7.1	2.3	-21	291	-1	65.6	83.4	0.1	36	0.071
torid #027	Fresno	3/22/1962	1200	F2	36.8	-119.8	0.5	10	29.4	6.7	21.4	5.4	216	684	0	446.9	489.4	2.2	4	0.313
torid #028	Los Angeles	5/14/1962	1200	F1	33.87	-118.3	0.1	10	5.5	2.8	6.1	5.2	167	267	0	24.6	59.5	0.1	6	0.067
torid #029	Fresno	1/21/1964	0200	F0	36.82	-119.7	0.2	10	12.9	6.8	13.3	5.4	402	816	0	178.3	373.1	1.8	6	0.304
torid #030	Kings	11/1/1964	1520	M	35.88	-119.52	1	50	8.7	5.6	7.8	6	106	106	0	27.3	153.8	0.1	1	0.24
torid #031	Los Angeles	11/9/1964	0700	F1	33.93	-118.42	1	10	6.1	3.2	6	5.1	80	113	-10	42.1	67	0	1	0.076
torid #032	Sonoma	11/10/1964	0134	M	38.53	-122.8	1	30	22.3	6.2	21.4	5.7	31	43	-17	113.2	29.9	0	1	0.198
torid #033	Santa Cruz	4/1/1965	1030	F1	36.98	-121.8	0.1	100	9.9	3.3	3.6	1.4	95	328	0	37.7	50.1	0.1	0	0.076
torid #034	Orange	4/8/1965	1100	M	33.65	-117.9	0.1	30	5.5	3.1	5.5	4.2	188	192	0	59.4	151.1	0	2	0.231
torid #035	Yuma	7/5/1965	1215	F1	32.73	-114.63	2	10	11.4	5.6	10.8	1.3	-516	771	-557	22.2	11.5	0	88	0.251
torid #036	Imperial	7/5/1965	1300	M	32.8	-114.83	0.1	10	3.5	1.9	3.4	0.3	-395	17	-523	1.9	0.7	0.1	0	0.071
torid #037	Los Angeles	11/25/1965	1430	F1	34.12	-117.77	2	50	3.2	4.9	3.3	5.8	180	413	0	25.5	65	0.1	8	0.082
torid #038	San Bernardino	7/22/1966	1645	M	34.5	-117.3	0.1	10	5.3	1.8	3.4	0.5	9	814	0	3.8	17.2	0.1	313	0.24
torid #039	Orange	11/7/1966	0909	M	33.62	-117.88	0.5	10	8.5	3.2	7.4	4	125	188	0	89.3	70.8	0.1	6	0.081
torid #040	Los Angeles	11/7/1966	1300	F2	33.9	-118.3	0.1	10	9.7	2.8	9.8	2.7	34	347	-13	89.8	88.4	0.2	39	0.088
torid #041	Los Angeles	11/7/1966	1300	F2	33.85	-118.33	10.3	50	9.7	2.8	9.8	2.7	34	347	-13	89.8	88.4	0.2	39	0.088
torid #042	Orange	11/7/1966	1315	F2	33.65	-117.92	0.2	10	9.7	2.8	9.8	2.7	34	347	-13	89.8	88.4	0.2	39	0.088
torid #043	Los Angeles	4/18/1967	1800	F0	34.02	-118.5	0.3	10	7.5	5.7	7.1	6.4	347	589	0	104.3	196.8	0.6	4	0.22
torid #044	Madera	4/21/1967	1645	F1	36.97	-120.07	0.1	10	5.3	3.2	4.4	2.7	100	469	0	29.9	54.3	0.2	7	0.135
torid #045	Fresno	<b>24584</b>	<b>1707</b>	F1	36.7	-120.67	0.1	10	5.3	3.2	4.4	2.7	100	214	0	29.9	54.3	0.1	15	0.048
torid #046	Merced	<b>24584</b>	<b>1815</b>	F1	37.1	-120.75	1	10	8.5	3.7	6.5	3.1	151	214	0	54.3	65.5	0.1	15	0.048
torid #047	San Joaquin	<b>24623</b>	<b>1750</b>	F1	37.97	-121.3	0.1	100	5.8	3	6.8	4.1	58	476	0	16.7	84.1	0.2	11	0.139
torid #048	San Joaquin	<b>25492</b>	<b>1500</b>	M	37.67	-121.3	0.1	10	5.2	4.5	4.3	6.5	148	219	0	63.9	144.7	0.2	2	0.136

## Appendix 1: Compilation of Buoyancy and Shear Parameters for 391 Tornado events from 1951–2011

**Table A3 Compilation of results from 42 tornado proximity soundings for the 1970s**

Tornado Number	County of Occurrence	Date	Time (LST)	F-Rating	Latitude (°N)	Longitude	Width (Yards)	Length (Miles)	0-1 km ABVSHR (x10-3 s-1)	0-6 km ABVSHR (x10-3 s-1)	0-1 km Bulk Shear (x10-3 s-1)	0-6 km Bulk Shear (x10-3 s-1)	0-3 km CAPE (J/kg)	Total CAPE (J/kg)	CIN (J/kg)	0-1 km Total SRH (m/s)^2	0-3 km Total SRH (m/s)^2	EH1	BRN	VGP
torid #049	San Joaquin	4/27/1970	1630	F0	37.9	-121.3	1.5	50	9.6	3.7	8.2	1.9	75	256	0	50.8	38.4	0.1	25	0.073
torid #050	Butte	6/28/1970	1415	F1	39.35	-121.8	2.3	10	10.8	4.6	9.7	4.5	45	291	0	97.8	109.7	0.2	3	0.116
torid #051	San Diego	2/23/1971	0930	F0	32.6	-117	0.1	10	5.9	7	4.3	6.6	163	170	0	61.5	44.4	0.1	2	0.118
torid #052	San Joaquin	4/24/1971	1535	F0	37.95	-121.35	0.2	10	13.3	5.6	4.7	2.6	105	419	0	7.9	5.3	0.1	15	0.155
torid #053	Imperial	6/7/1972	1340	F0	33.3	-115.05	0.1	10	6.7	2.8	4.6	1	179	2937	0	23.6	28.8	0.6	533	0.183
torid #054	El Dorado	10/1/1972	1200	F0	38.8	-120.5	0.1	10	8	3.2	6.8	2.6	332	1162	0	58.5	13.4	0.4	51	0.24
torid #055	Tuolumne	10/15/1972	1224	F0	37.8	-119.83	0.1	10	8.4	2.8	7.7	2.1	316	1345	0	57.6	97.1	0.7	100	0.198
torid #056	Placer	10/15/1972	1226	F0	38.75	-121.35	0.1	10	5.1	3	9.7	2.5	317	1182	0	71.9	54.4	0.7	37	0.231
torid #057	Riverside	8/16/1973	2100	F3	33.62	-114.63	0.1	10	15.1	3.3	13.1	2.6	-241	4395	-241	139.3	155.1	4.6	333	0.337
torid #058	Riverside	7/20/1974	1349	F1	33.75	-116.95	1	20	5	2.3	4.3	0.7	-48	400	-48	34.8	66.3	0	0	0.111
torid #059	San Bernardino	10/22/1974	1355	F1	34.18	-116.37	0.1	10	7.5	4.4	8.4	1.4	189	1638	-10	5.3	65.2	0.6	92	0.337
torid #060	San Diego	10/29/1974	0400	F0	33.05	-117.3	0.1	10	4	2.2	4.4	1.9	91	242	0	6.9	45.1	0.1	11	0.071
torid #061	Fresno	3/13/1975	1517	F0	36.5	-119.67	0.3	10	11.9	4.6	11.1	8	280	624	0	228.6	318.7	1.1	2	0.24
torid #062	Merced	4/5/1975	1000	F0	37.07	-120.85	0.3	10	8.7	3.6	7.6	6.1	93	142	-12	105.9	167.6	0.1	1	0.081
torid #063	Fresno	4/5/1975	1632	F0	36.78	-119.93	0.3	10	5	3.2	6.3	4.6	366	744	0	9.2	45	0.1	15	0.136
torid #064	San Bernardino	9/4/1976	1745	M	34.62	-117.6	0.1	10	6.9	3.9	3.3	1.4	161	3135	0	3.5	129.8	2.4	94	0.111
torid #065	San Bernardino	9/5/1976	1719	M	34.68	-117.5	0.1	10	12.5	6.1	5.6	2.2	235	3730	0	12	0.2	1.7	84	0.071
torid #066	San Bernardino	9/6/1976	1600	M	34.28	-117.6	0.1	10	6.8	3.4	5.3	1.2	558	4338	0	36.9	95.9	2.4	190	0.25
torid #067	San Bernardino	9/6/1976	1719	M	34.58	-117.57	0.1	10	14	4.6	6.3	0.3	236	2748	0	24.9	33.4	1.4	153	0.019
torid #068	San Bernardino	9/6/1976	1725	M	34.63	-117.62	0.1	10	14	4.6	6.3	0.3	236	2748	0	24.9	33.4	1.4	153	0.101
torid #069	San Bernardino	9/6/1976	1730	M	34.65	-117.63	0.1	10	14	4.6	6.3	0.3	236	2748	0	24.9	33.4	1.4	153	0.221

# Appendix 1: Compilation of Buoyancy and Shear Parameters for 391 Tornado events from 1951–2011

## Table A3 (Continued) Compilation of results from 42 tornado proximity soundings for the 1970s

Tornado Number	County of Occurrence	Date	Time (LST)	F-Rating	Latitude (°N)	Longitude	Width (Yards)	Length (Miles)	0-1 km ABVSHR (x10-3 s-1)	0-6 km ABVSHR (x10-3 s-1)	0-1 km Bulk Shear (x10-3 s-1)	0-6 km Bulk Shear (x10-3 s-1)	0-3 km CAPE (J/kg)	Total CAPE (J/kg)	CIN (J/kg)	0-1 km Total SRH (m/s) <sup>2</sup>	0-3 km Total SRH (m/s) <sup>2</sup>	EH1	BRN	VGP
torid #070	Santa Barbara	1/3/1977	2215	M	34.43	-119.82	0.1	10	8.3	3	8.3	3	25	52	-43	97.5	162.8	0.1	2	0.162
torid #071	Orange	3/16/1977	1830	F1	33.85	-118	10.9	10	7.2	6.6	6.9	10.2	181	420	0	45.3	18.9	0.1	2	0.12
torid #072	Los Angeles	5/8/1977	1000	M	33.78	-118.2	0.1	100	3.3	2.4	3.4	2.4	143	404	0	31.7	67.3	0.1	21	0.231
torid #073	Los Angeles	1/4/1978	1515	M	34.12	-117.82	0.1	10	7	3.7	9.4	4.3	100	100	0	120.3	173.8	0.1	1	0.16
torid #074	Sacramento	2/7/1978	1326	F2	38.7	-121.45	1.9	20	16.7	5.3	15.8	6.9	297	429	0	79.6	160.4	0.4	3	0.213
torid #075	Orange	2/9/1978	0155	F3	33.67	-117.78	2	67	16.2	6.3	15.9	5.6	239	458	0	176.9	234	0.5	5	0.166
torid #076	Los Angeles	2/10/1978	2230	M	33.93	-118.42	1	10	8.9	4.2	8	6.2	19	112	-19	125.9	107.3	0.1	1	0.168
torid #077	Stanislaus	3/1/1978	1400	M	37.67	-120.93	1.5	100	7.2	3.6	7.2	1.1	29	30	0	48.5	99.3	0	3	0.24
torid #078	Butte	3/4/1978	1400	M	39.83	-121.92	1.5	53	10.2	2.9	10.2	2.3	257	927	0	54.9	74.8	0.4	29	0.274
torid #079	Stanislaus	3/4/1978	1430	M	37.63	-120.83	2.5	100	14.6	3.5	14.8	3	251	915	0	77.9	101.7	0.6	29	0.091
torid #080	Merced	3/4/1978	1435	F1	37.42	-120.85	1	880	14.6	3.5	14.8	3	251	915	0	77.9	101.7	0.6	29	0.206
torid #081	Tehama	3/5/1978	1400	M	40.05	-122.37	0.1	10	11.6	4.6	11.2	2.7	378	1322	0	110	144.9	1.4	35	0.172
torid #082	Tehama	3/5/1978	1600	M	40.33	-122.17	0.1	10	11.6	4.6	10.8	2.5	376	1284	0	109.2	144.1	1.3	34	0.09
torid #083	Tehama	3/5/1978	1600	M	40	-122.17	0.1	10	11.6	4.6	10.8	2.5	376	1284	0	109.2	144.1	1.3	34	0.445
torid #084	Butte	3/23/1978	1420	M	39.77	-121.62	0.1	10	13	6.3	12.4	6.8	122	122	0	198.1	265.3	0.2	1	0.16
torid #085	San Joaquin	3/31/1978	1340	M	37.93	-121.21	0.5	10	10.8	3.9	9.9	2.9	349	846	0	92.3	48.6	0.1	55	0.133
torid #086	San Diego	12/18/1978	1030	M	33.2	-117.38	0.8	80	9.2	5.3	8.6	6.5	414	1072	0	98.5	14.5	0.1	10	0.163
torid #087	San Diego	1/18/1979	0502	F0	32.8	-117.1	0.1	30	6.9	4.1	7	4.7	158	158	0	92.1	173.3	0.1	2	0.111
torid #088	Los Angeles	1/31/1979	1045	M	34.17	-118.37	0.1	10	5.6	4	6.2	5.6	334	797	0	15.1	77	0.5	8	0.074
torid #089	Orange	1/31/1979	1130	F1	33.75	-117.88	2	10	8.9	4	4.3	5.3	399	1042	0	72.2	134.1	0.9	10	0.243
torid #090	Fresno	3/14/1979	1250	M	36.6	-119.67	2	10	7.3	3.1	5	1.6	39	39	-19	1.1	21.1	0	4	0.15

## Appendix 1: Compilation of Buoyancy and Shear Parameters for 391 Tornado events from 1951–2011

**Table A4** Compilation of results from 63 tornado proximity soundings for the 1980s

Tornado Number	County of Occurrence	Date	Time (LST)	F-Rating	Latitude (°N)	Longitude	Width (Yards)	Length (Miles)	0-1 km ABVSHR (x10 <sup>-3</sup> s <sup>-1</sup> )	0-6 km ABVSHR (x10 <sup>-3</sup> s <sup>-1</sup> )	0-1 km Bulk Shear (x10 <sup>-3</sup> s <sup>-1</sup> )	0-6 km Bulk Shear (x10 <sup>-3</sup> s <sup>-1</sup> )	0-3 km CAPE (J/kg)	Total CAPE (J/kg)	CIN (J/kg)	0-1 km Total SRH (m/s) <sup>2</sup>	0-3 km Total SRH (m/s) <sup>2</sup>	EH1	BRN	VGP
torid #091	Alameda	1/14/1980	1330	F1	37.48	-121.88	0.3	67	14.9	4.5	13.1	2.9	280	652	0	146.1	181.1	0.6	16	0.211
torid #092	Los Angeles	1/28/1980	1315	F0	33.88	-118.3	0.4	10	4.6	3.7	3	4.5	117	140	0	32.9	135.9	0.1	2	0.071
torid #093	Tulare	2/15/1980	1500	F0	36.55	-119.38	1	10	23.5	6	22.3	4.4	197	604	0	366.3	436.8	1.4	4	0.25
torid #094	Fresno	2/19/1980	1405	F1	36.77	-119.72	1.7	10	12.4	3.7	10.9	1.9	122	428	-4	109.9	132.3	0.4	19	0.123
torid #095	San Diego	2/20/1980	1800	F1	32.78	-117.2	0.1	10	4.2	3.9	6.5	3.3	370	1378	0	88.9	202.6	1.2	15	0.265
torid #096	Kings	4/5/1980	0940	F2	36.37	-119.7	15	10	11.3	4.7	10.3	5.8	104	104	0	94	143.2	0.1	1	0.08
torid #097	Tehama	5/9/1980	1705	F2	40.13	-122.22	0.1	10	10.5	6.9	16.2	8.8	192	264	0	200.7	257.3	0.4	1	0.163
torid #098	Calaveras	7/29/1980	1500	M	38.12	-120.88	0.1	10	5.5	2.9	7.1	1.8	-149	0	-326	7.2	24.7	0.1	34	0.289
torid #099	Butte	1/22/1981	0730	F0	39.73	-121.88	0.1	10	14.2	8.9	13.3	6.7	47	0	-8	73.5	24.6	0	0	0.019
torid #100	San Joaquin	1/23/1981	1045	F0	37.97	-121.3	0.1	10	14.4	4.7	12.2	4	72	125	-9	57.3	67.3	0	3	0.101
torid #101	San Joaquin	3/19/1981	1530	F0	37.98	-121.05	0.1	10	10.3	3	10	3.5	324	1182	0	72.2	82.5	0.6	36	0.221
torid #102	Riverside	1/20/1982	0205	F0	33.95	-117.4	0.3	60	16.7	5.9	14.4	6.7	165	223	-3	125.1	211.7	0.3	1	0.162
torid #103	San Diego	3/17/1982	1715	F0	32.73	-117.18	0.1	10	6.4	5.2	9	5.8	404	575	0	88.3	153.9	0.5	4	0.231
torid #104	Fresno	3/28/1982	1700	F1	36.57	-119.62	5	20	26.4	7.7	18.2	3.5	236	457	0	274.4	271.2	0.8	4	0.226
torid #105	Alameda	3/29/1982	1525	F0	37.68	-121.77	0.1	10	11.9	6.8	12.5	7.6	165	302	-4	127.5	176.5	0.3	2	0.16
torid #106	Los Angeles	3/29/1982	2130	F1	34.08	-118.1	2	67	14.7	6.3	11.2	6.4	103	135	0	59.6	117.8	0.1	1	0.119
torid #107	San Joaquin	6/29/1982	1320	F0	38.1	-121.43	0.5	20	11	3.6	4	0.5	141	811	0	1.9	7.8	0.2	126	0.168
torid #108	San Bernardino	9/7/1982	1330	F2	34.23	-116.37	0.5	20	6.9	2.5	7.1	0.6	25	1808	0	40.1	19	0.1	1384	0.171
torid #109	Los Angeles	11/9/1982	0930	F1	34.03	-118.68	0.2	20	21.7	5.8	19.9	6.5	65	307	-42	291.2	347.5	0.7	3	0.204
torid #110	Los Angeles	11/9/1982	1130	F2	34.18	-118.45	1	150	12.6	4.3	13.3	5.5	79	292	-18	136.6	194.4	0.3	4	0.153
torid #111	Los Angeles	11/9/1982	1200	F2	33.78	-118.2	10	1300	8.2	4.2	9.2	4.9	253	966	-2	70.7	130.4	0.6	12	0.242

## Appendix 1: Compilation of Buoyancy and Shear Parameters for 391 Tornado events from 1951–2011

**Table A4 (Continued) Compilation of results from 63 tornado proximity soundings for the 1980s**

Tornado Number	County of Occurrence	Date	Time (LST)	F-Rating	Latitude (°N)	Longitude	Width (Yards)	Length (Miles)	0-1 km ABVSHR (x10-3 s-1)	0-6 km ABVSHR (x10-3 s-1)	0-1 km Bulk Shear (x10-3 s-1)	0-6 km Bulk Shear (x10-3 s-1)	0-3 km CAPE (J/kg)	Total CAPE (J/kg)	CIN (J/kg)	0-1 km Total SRH (m/s)²	0-3 km Total SRH (m/s)²	EH1	BRN	VGP
torid #112	Los Angeles	11/9/1982	1200	F0	33.97	-118.3	0.1	20	7.9	4.3	11.1	5.2	245	923	0	51	107.2	0.5	12	0.24
torid #113	Orange	11/9/1982	1300	F0	33.78	-117.92	0.1	150	6.3	4.1	8.3	4.8	357	1412	0	47.9	104.1	0.8	18	0.274
torid #114	Orange	11/9/1982	1300	F1	33.58	-117.67	0.2	33	11.9	4.2	5.8	4.1	238	993	0	82.8	142.6	0.7	13	0.253
torid #115	Ventura	11/9/1982	1515	F0	34.12	-119.12	0.1	33	7.5	4.7	12.3	4.8	34	111	-5	112.3	123.3	0	2	0.091
torid #116	Sonoma	2/27/1983	0520	F1	38.45	-122.7	0.8	100	11	4.4	7.4	3.6	48	334	-22	86.6	202.7	0.4	5	0.173
torid #117	Los Angeles	3/1/1983	0740	F2	33.98	-118.37	3.5	100	12.5	6.4	11.9	5.1	30	226	0	194.4	285	0.4	1	0.164
torid #118	Los Angeles	3/1/1983	0815	F0	34.13	-118.12	0.2	100	8	5.6	9.9	4.9	10	171	-58	158.1	242.9	0.4	1	0.172
torid #119	Placer	3/3/1983	1715	F0	38.75	-121.28	0.1	50	3	2.3	3.1	0.6	139	491	0	15.3	40	0.2	78	0.09
torid #120	Sacramento	3/22/1983	1410	F1	38.72	-121.35	2	50	19.1	4.2	15.5	5	203	301	-23	192.1	201	0.4	3	0.154
torid #391	Sacramento	3/22/1983	1400	F1	38.73	-121.33	0	0	8	2.8	7.3	3.6	102	133	0	55.6	17.9	0	3	0.077
torid #121	San Bernardino	8/1/1983	1050	F0	34.28	-116.45	0.3	30	7	2.8	4	1.2	183	5929	0	22.7	13.1	2.2	1706	0.445
torid #122	Los Angeles	9/30/1983	0700	F0	33.92	-118.28	0.3	100	5	2.5	4.8	1.8	233	749	0	25.6	81.6	0.3	26	0.16
torid #123	Los Angeles	10/1/1983	2235	F1	33.92	-118.35	0.3	100	6.4	3.2	6.8	3.3	57	187	-11	30.5	73.5	0.1	5	0.066
torid #124	Mendocino	12/11/1983	1030	F0	39.15	-123.22	2	300	18	5.6	17.5	6.8	64	165	0	140.3	172.1	0.2	1	0.133
torid #125	Orange	1/13/1984	1819	F0	33.67	-118	0.1	10	7.2	5.7	4.8	6	167	303	0	51.3	125.8	0.2	3	0.163
torid #126	Los Angeles	5/30/1984	0915	F0	34.12	-117.82	0.3	70	5.6	2.8	2.9	1.4	-35	0	-214	36.3	34.9	0	7	0.074
torid #127	San Diego	2/4/1985	0840	F0	32.8	-117.1	0.1	17	5.4	3.4	1.6	3	333	416	-1	1.7	61.9	0.2	9	0.15
torid #128	San Benito	3/11/1985	1000	F2	36.85	-121.4	0.5	20	25.2	6.5	11.5	2.7	34	137	-29	222.5	216.6	0.2	6	0.116
torid #129	Riverside	9/18/1985	0955	F0	33.52	-115.93	0.1	10	6.7	5.7	4.5	4.3	186	928	0	42.9	7.8	0.5	31	0.289
torid #130	Santa Cruz	2/3/1986	1300	F0	36.97	-121.9	0.2	50	18.5	6.6	11.9	4.8	148	148	0	33.7	53.2	0.1	2	0.161
torid #131	Tulare	2/15/1986	1450	F0	36.53	-119.38	0.5	100	29.2	7.5	22.6	5.7	271	1278	0	456	459.1	3.7	6	0.448



# Appendix 1: Compilation of Buoyancy and Shear Parameters for 391 Tornado events from 1951–2011

## Table A4 (Continued) Compilation of results from 63 tornado proximity soundings for the 1980s

Tornado Number	County of Occurrence	Date	Time (LST)	F-Rating	Latitude (+N)	Longitude	Width (Yards)	Length (Miles)	0-1 km ABVSHR (x10-3 s-1)	0-6 km ABVSHR (x10-3 s-1)	0-1 km Bulk Shear (x10-3 s-1)	0-6 km Bulk Shear (x10-3 s-1)	0-3 km CAPE (J/kg)	Total CAPE (J/kg)	CIN (J/kg)	0-1 km Total SRH (m/s)^2	0-3 km Total SRH (m/s)^2	EH1	BRN	VGP
torid #132	Merced	2/19/1986	1430	F0	37.23	-120.25	0.2	10	21.2	6.8	19.2	6.4	249	925	0	195.2	202.4	1.2	7	0.327
torid #133	Fresno	3/8/1986	2035	F1	36.55	-119.65	4	50	16.9	3.8	13.5	3.6	423	1581	0	166.9	192.8	1.8	28	0.283
torid #134	San Mateo	3/10/1986	1345	F0	37.52	-122.52	0.2	50	8.4	3.8	3.8	0.9	102	255	-3	36.8	115.6	0.1	6	0.092
torid #135	Orange	3/16/1986	0730	F1	33.83	-117.92	1.2	40	16.9	4	14.2	4.1	103	308	-11	186.8	249.1	0.5	3	0.122
torid #136	San Bernardino	7/21/1986	1245	F0	34.72	-117.03	0.2	10	6.9	4.9	5.6	3.1	92	3522	0	28.7	134.3	1.9	138	0.579
torid #137	Tehama	9/24/1986	1415	F2	39.93	-122.05	2	100	15.9	9.8	15	5.4	248	532	0	292.3	413.4	1.3	3	0.384
torid #138	Tehama	3/14/1987	1805	F0	39.92	-122.4	0.2	70	22.2	5.9	19.4	4.2	32	32	-3	49.3	40.2	0	1	0.078
torid #139	Monterey	4/3/1987	1014	F0	36.77	-121.63	0.1	30	11.7	4.1	11.1	1.9	137	311	0	82.9	59.6	0	96	0.116
torid #140	Los Angeles	6/5/1987	1515	F0	34.63	-118.1	0.2	20	8.3	3.3	2	1.4	0	469	0	9.1	51.5	0.2	96	0.121
torid #141	San Bernardino	7/27/1987	1851	F0	34.13	-116.05	1.5	50	2.8	2.7	1.7	0.8	-28	1322	-2	5.5	58.6	0.4	174	0.196
torid #142	Orange	1/18/1988	1130	F0	33.6	-117.63	1.5	13	8.3	4.3	8.4	4	45	57	0	92.7	38.3	0	7	0.073
torid #143	Orange	1/18/1988	1200	F0	33.42	-117.62	0.2	10	8.3	4.3	8.4	4	45	57	0	92.7	38.3	0	7	0.073
torid #144	Tulare	3/1/1988	1840	F0	36.55	-119.28	0.2	10	11.7	7.8	7.9	4.7	320	871	0	110.2	90.7	0.7	39	0.327
torid #145	San Joaquin	4/19/1988	1435	F1	38.17	-121.15	0.2	23	7.1	6.6	9	5.3	309	603	0	85.6	65.2	0.4	12	0.194
torid #146	Sacramento	4/19/1988	1458	F1	38.68	-121.17	1	30	9.6	6.7	10	5.6	144	206	-7	119.4	93.3	0.2	4	0.128
torid #147	Kern	4/20/1988	1240	F0	35.07	-118.63	0.2	10	11.1	4.1	10	2.2	115	115	0	49.7	14.6	0	10	0.084
torid #148	Fresno	3/2/1989	1620	F0	36.78	-119.77	0.1	10	32.7	7.6	20	5.3	472	907	0	405.8	395.1	2.4	7	0.412
torid #149	Contra Costa	9/18/1989	1510	F0	37.97	-122.03	0.2	10	8.5	3.7	0.8	0.5	261	789	0	5.7	15.1	0.2	87	0.172
torid #150	Contra Costa	9/18/1989	1710	F0	37.97	-122.03	0.2	10	8.5	3.7	0.8	0.5	261	789	0	5.7	15.1	0.2	87	0.172
torid #151	Yolo	9/18/1989	1840	F0	38.55	-121.75	0.2	10	5.8	2.8	1.9	0.9	59	108	-8	15	5	0	13	0.064
torid #391	Sacramento	3/22/1983	1400	F1	38.73	-121.33	0	0	8	2.8	7.3	3.6	102	133	0	55.6	17.9	0	3	0.077

## Appendix 1: Compilation of Buoyancy and Shear Parameters for 391 Tornado events from 1951–2011

**Table A5 Compilation of results from 137 tornado proximity soundings for the 1990s**

Tornado Number	County of Occurrence	Date	Time (LST)	F-Rating	Latitude (°N)	Longitude	Width (Yards)	Length (Miles)	0-1 km ABVSHR (x10 <sup>-3</sup> s <sup>-1</sup> )	0-6 km ABVSHR (x10 <sup>-3</sup> s <sup>-1</sup> )	0-1 km Bulk Shear (x10 <sup>-3</sup> s <sup>-1</sup> )	0-6 km Bulk Shear (x10 <sup>-3</sup> s <sup>-1</sup> )	0-3 km CAPE (J/kg)	Total CAPE (J/kg)	CIN (J/kg)	0-1 km Total SRH (m/s) <sup>2</sup>	0-3 km Total SRH (m/s) <sup>2</sup>	EH1	BRN	VGP
torid #152	San Diego	1/14/1990	0330	F0	32.75	-117.1	0.1	10	12.9	4.5	10.1	6.2	229	601	0	96.9	102.9	0.5	9	0.204
torid #153	Los Angeles	1/16/1990	2120	F0	33.95	-118.05	0.2	33	12	4.3	9.5	4.1	46	61	-11	47.6	110.4	0	2	0.074
torid #154	Placer	4/23/1990	1530	F0	38.85	-121.17	0.2	10	11.9	5.3	12	6.2	136	282	-1	138.9	187.9	0.3	2	0.178
torid #155	San Bernardino	8/14/1990	1645	F0	34.85	-116.85	0.1	10	3.2	3.1	5.7	2.6	37	3023	0	54.4	131.3	2.5	71	0.359
torid #156	San Bernardino	9/29/1990	1600	F0	34.85	-116.88	0.2	10	4.1	3.2	3.3	0.8	0	800	0	9.4	18.4	0.1	384	0.127
torid #157	Orange	2/28/1991	1445	F0	33.73	-117.8	0.5	50	11.8	4.4	16.3	5.2	406	1517	0	121.1	158.1	1.7	32	0.325
torid #158	Kings	2/28/1991	1815	F1	36.35	-119.45	0.2	10	12.9	4.7	12	5.4	126	147	0	185.9	223.6	0.2	1	0.085
torid #159	Kern	3/17/1991	2130	F1	35.13	-119.48	0.1	40	25.2	10.4	17.5	7.4	192	277	0	377.9	501.1	0.7	1	0.237
torid #160	Los Angeles	3/19/1991	0200	F0	33.85	-118.13	0.5	50	34.2	8.5	23.1	4	177	500	0	339.1	377.7	1.1	37	0.332
torid #161	San Diego	3/19/1991	0430	F1	32.75	-117.1	1	440	29.6	7.8	21.4	3.5	245	722	0	225.2	277.6	1.1	152	0.369
torid #162	Riverside	3/20/1991	1130	F0	33.95	-117.4	0.2	10	7.5	3.5	6.2	1.8	84	248	-2	51.3	35.2	0	27	0.09
torid #163	San Bernardino	3/20/1991	1245	F0	34.17	-117.35	1	50	9.3	3.8	9.7	1.7	109	325	-2	37.5	36.7	0	29	0.11
torid #164	Madera	3/20/1991	1430	F0	37.05	-120.35	0.1	10	13.2	3.6	8.6	0.9	191	451	0	113.8	123.9	0.4	24	0.131
torid #165	Kern	3/25/1991	1420	F0	35.68	-117.68	0.2	10	9.7	6.6	9.7	7.6	75	77	0	45.7	61.6	0	1	0.06
torid #166	Kern	3/26/1991	1407	F0	35.63	-117.68	0.1	10	9.2	4.5	5.2	3.8	31	45	0	38.1	8.6	0	3	0.048
torid #167	San Joaquin	3/26/1991	1715	F0	38.13	-121.37	0.1	10	3.7	2.7	6	1.1	82	248	0	36.9	109	0.1	9	0.067
torid #168	Merced	3/26/1991	1740	F0	37.23	-120.32	0.1	10	10.2	3.6	6.9	0.6	109	278	0	48.7	126.4	0.2	10	0.083
torid #169	Orange	3/27/1991	2235	F1	33.67	-118	3	53	10.3	5	9.6	6.4	334	588	0	64.4	112.9	0.4	5	0.204
torid #170	San Diego	3/27/1991	0200	F1	33.15	-117.17	0.2	10	7	4.5	7.9	6.1	139	209	-23	69.7	118.3	0.1	2	0.114
torid #171	Kings	10/12/1991	0015	F0	36.17	-119.65	0.1	10	2.4	2	2.7	2.2	-335	147	-376	22.4	56.6	0.1	25	0.099
torid #172	Santa Barbara	12/29/1991	1200	F0	34.63	-120.3	0.1	10	14	7.1	12.7	3.2	184	587	-1	152.8	216.2	0.8	8	0.256
torid #173	San Diego	2/15/1992	1330	F0	33.33	-117.3	0.5	20	6.5	2.7	8.6	4.6	110	111	-2	49.2	87.3	0	1	0.061
torid #174	Los Angeles	3/20/1992	2100	F1	34.1	-118.18	0.2	20	7.8	2.9	4.7	1.5	126	182	0	14.4	16.4	0	32	0.065

**Appendix 1: Compilation of Buoyancy and Shear Parameters for 391 Tornado events from 1951–2011**  
**Table A5 (Continued) Compilation of results from 137 tornado proximity soundings for the 1990s**

Tornado Number	County of Occurrence	Date	Time (LST)	F-Rating	Latitude (°N)	Longitude	Width (Yards)	Length (Miles)	0-1 km ABVSHR (x10-3 s-1)	0-6 km ABVSHR (x10-3 s-1)	0-1 km Bulk Shear (x10-3 s-1)	0-6 km Bulk Shear (x10-3 s-1)	0-3 km CAPE (J/kg)	Total CAPE (J/kg)	CIN (J/kg)	0-1 km Total SRH (m/s) <sup>2</sup>	0-3 km Total SRH (m/s) <sup>2</sup>	EH1	BRN	VGP
torid #175	Imperial	5/5/1992	1830	F0	32.85	-115.57	0.2	10	8.1	4.6	4.1	1.5	-23	1593	-38	11.9	31.4	0.6	168	0.246
torid #176	Sonoma	12/2/1992	1700	F1	38.4	-122.9	7.5	100	11.6	5.3	18.5	5.7	53	96	-11	120.9	170.9	0.1	1	0.078
torid #177	Sonoma	12/2/1992	1700	F1	38.4	-122.83	1	23	11.6	5.3	18.5	5.7	53	96	-11	120.9	170.9	0.1	1	0.078
torid #178	Sonoma	12/2/1992	1700	F1	38.55	-122.82	3	23	11.6	5.3	18.5	5.7	53	96	-11	120.9	170.9	0.1	1	0.078
torid #179	Monterey	12/6/1992	1900	F1	36.55	-121.92	7	73	14.1	7	15.5	4.5	76	92	-3	237.5	209.6	0.1	1	0.128
torid #180	Monterey	12/6/1992	1900	F1	36.6	-121.88	1	23	14.1	7	15.5	4.5	76	92	-3	237.5	209.6	0.1	1	0.128
torid #181	Ventura	12/7/1992	0700	F0	34.28	-118.88	0.1	10	13.5	5.6	7.9	5.7	83	382	-2	145.7	114.8	0.4	7	0.17
torid #182	Orange	12/7/1992	0730	F1	33.75	-118	0.1	10	6.1	5.8	5	5.2	83	454	-3	76.7	45.7	0.3	10	0.15
torid #183	Orange	12/7/1992	1030	F1	33.83	-117.92	0.1	10	7.6	5.6	3.8	5	65	382	-2	58	27	0.2	9	0.141
torid #184	San Diego	12/7/1992	1700	F0	33.17	-117.35	0.1	10	13.2	7.4	13	4.2	10	53	-6	91.9	157.2	0.1	1	0.091
torid #185	Del Norte	12/11/1992	1315	F1	41.75	-124.2	0.2	23	6.5	3.1	11.5	3.1	345	1128	0	121.1	252.7	1.7	13	0.241
torid #186	Monterey	12/11/1992	1845	F0	36.68	-121.77	0.1	10	6.2	1.6	6.7	2.3	127	312	-15	55	86.7	0.1	15	0.071
torid #187	Fresno	12/11/1992	1850	F0	36.65	-119.77	0.1	10	13.3	4.2	10.1	3.1	102	238	-18	173.6	289.3	0.4	3	0.122
torid #188	Alameda	12/17/1992	1230	F0	37.73	-122.15	0.2	23	9.7	6.3	13.4	5.8	31	34	0	273.8	412	0.1	0	0.062
torid #189	Butte	12/17/1992	1620	F1	39.52	-121.57	1	100	14.3	6.5	14.7	6.8	239	456	-2	98.2	97.9	0.4	2	0.239
torid #190	Yuba	12/17/1992	1730	F1	39.32	-121.38	5	23	14.3	6.5	14.7	6.8	239	456	-2	98.2	97.9	0.4	2	0.239
torid #191	Orange	12/29/1992	1330	F0	33.42	-117.62	0.1	10	11.9	5.2	11.9	6.4	423	710	0	134.9	94.9	0.5	6	0.29
torid #192	Del Norte	12/30/1992	0330	F1	41.75	-124.2	0.2	23	7.4	5	9.1	4.1	76	123	-9	139.5	328.3	0.1	0	0.057
torid #193	Butte	1/7/1993	1700	F1	39.42	-121.72	0.1	10	11.6	6.7	10.2	4.5	156	105	0	93.3	130.5	0.2	1	0.081
torid #194	Orange	1/14/1993	0140	F1	33.88	-117.95	1	30	12.5	5.3	9.3	4.6	155	450	-12	130.6	106.5	0.1	2	0.121
torid #195	Orange	1/17/1993	1930	F0	33.67	-117.75	0.1	10	12.7	3.6	13.6	5	269	757	-2	147	173.9	0.8	16	0.152
torid #196	Los Angeles	1/18/1993	2345	F0	34.03	-118.3	0.7	50	10.7	3.3	11.3	4.6	142	398	-11	132.5	158.1	0.4	9	0.101
torid #197	Orange	1/18/1993	1405	F0	33.67	-118	0.1	10	17.8	4	13.9	2.8	129	423	-2	176.7	199.3	0.5	12	0.141

# Appendix 1: Compilation of Buoyancy and Shear Parameters for 391 Tornado events from 1951–2011

## Table A5 (Continued) Compilation of results from 137 tornado proximity soundings for the 1990s

Tornado Number	County of Occurrence	Date	Time (LST)	F-Rating	Latitude (°N)	Longitude	Width (Yards)	Length (Miles)	0-1 km ABVSHR (x10 <sup>-3</sup> s <sup>-1</sup> )	0-6 km ABVSHR (x10 <sup>-3</sup> s <sup>-1</sup> )	0-1 km Bulk Shear (x10 <sup>-3</sup> s <sup>-1</sup> )	0-6 km Bulk Shear (x10 <sup>-3</sup> s <sup>-1</sup> )	0-3 km CAPE (J/kg)	Total CAPE (J/kg)	CIN (J/kg)	0-1 km Total SRH (m/s) <sup>2</sup>	0-3 km Total SRH (m/s) <sup>2</sup>	EBI	BRN	VGP
torid #198	Orange	2/8/1993	1220	F0	33.92	-117.88	0.5	10	2.6	1.5	2.5	0.6	280	1165	0	10.9	17	0.3	258	0.09
torid #199	Tulare	2/19/1993	1915	F0	36.07	-119.32	0.1	30	4.5	3.1	4.5	4.6	141	276	0	49.4	124.5	0.1	5	0.073
torid #200	Kern	2/23/1993	1445	F0	35.68	-119.23	0.1	30	3.2	3.6	4.6	4.7	220	545	0	17.4	22.4	0.1	8	0.122
torid #201	Glenn	4/17/1993	1540	F1	39.53	-122.13	0.5	200	13.5	6.2	17.1	7.8	243	358	-10	180.3	219.3	0.5	8	0.24
torid #202	Butte	4/17/1993	1820	F0	39.73	-121.83	0.1	23	13.5	6.2	17.1	7.8	243	358	0	180.3	219.3	0.5	1	0.234
torid #203	Fresno	6/5/1993	1405	F0	36.78	-119.77	0.1	23	12.4	2.9	9.8	1.7	215	957	0	122.3	183.9	1	28	0.205
torid #204	Imperial	8/29/1993	1530	F1	32.85	-115.57	0.1	10	11.4	4.3	13.1	2.6	10	3376	0	84.2	95.5	0.5	1	0.234
torid #205	Orange	11/11/1993	1130	F0	33.68	-117.82	0.1	10	7	5.4	3.8	6.3	135	135	0	43.2	115.1	0.1	1	0.108
torid #206	Los Angeles	2/7/1994	1745	F0	34.25	-118.35	0.1	10	11.6	6.2	17.2	6.7	184	536	-4	199.4	235.8	1	5	0.309
torid #207	Orange	2/7/1994	2015	F0	33.62	-117.93	9	73	12.8	6.5	10.1	5.3	322	1002	0	145.5	181.9	1.5	11	0.379
torid #208	Butte	2/10/1994	1428	F2	39.52	-121.57	0.3	20	23.3	8.7	19.5	6	256	331	0	151.1	165.2	0.3	2	0.264
torid #209	Kings	3/5/1994	1445	F0	36.3	-119.78	0.1	30	4.8	3.7	4.3	4.7	215	1401	0	15.4	40.4	0.2	22	0.22
torid #210	Butte	3/10/1994	1930	F0	39.52	-121.57	0.2	30	5.7	6.3	6.8	5.2	233	527	0	77	132.8	0.3	7	0.22
torid #211	Santa Barbara	3/24/1994	1740	F0	34.43	-119.7	0.1	10	17.5	7.2	22	4.2	419	621	0	11.1	42	0.2	11	0.329
torid #212	Alameda	4/25/1994	1150	F0	37.68	-121.77	0.7	30	4.8	3	4.7	1.8	116	147	-1	47.1	73.6	0.1	6	0.071
torid #213	Butte	4/25/1994	2010	F0	39.33	-121.53	0.1	20	22	5.6	16	3.5	164	318	-7	275.8	303.1	0.6	4	0.178
torid #214	Riverside	8/12/1994	1500	F0	33.75	-116.9	0.1	10	1.2	3.2	1.3	1.6	-423	920	-434	8.5	66.2	0.3	84	0.169
torid #215	Madera	1/14/1995	1715	F1	37.12	-120.27	1	10	4.9	3.7	6.1	4.1	219	466	-21	38.7	119.1	2.5	204	0.484
torid #216	Sacramento	3/23/1995	1830	F0	38.23	-121.52	0.2	10	18.1	5.1	18.3	4.3	62	237	0	374.6	449.6	0.6	2	0.168
torid #217	Fresno	5/1/1995	1745	F0	36.78	-119.73	0.1	10	12.9	4.1	12.3	4.4	181	419	-1	23.6	36.8	0.2	7	0.169
torid #218	Tulare	5/13/1995	1100	F0	35.98	-119.12	2.5	10	17.9	7.2	11.6	8.9	92	145	0	45.8	43.8	0.1	1	0.115
torid #219	Fresno	5/13/1995	1315	F0	36.7	-120.03	1	33	16.4	6.5	17.4	7.3	139	279	0	184.1	164.8	0.3	4	0.155
torid #220	Los Angeles	6/16/1995	1255	F0	33.93	-118.02	0.1	10	16.2	5.7	9.2	3.7	272	336	0	75.9	34.5	0.3	9	0.205

**Appendix 1: Compilation of Buoyancy and Shear Parameters for 391 Tornado events from 1951–2011**  
**Table A5 (Continued) Compilation of results from 137 tornado proximity soundings for the 1990s**

Tornado Number	County of Occurrence	Date	Time (LST)	F-Rating	Latitude (°N)	Longitude	Width (Yards)	Length (Miles)	0-1 km ABVSHR (x10-3 s-1)	0-6 km ABVSHR (x10-3 s-1)	0-1 km Bulk Shear (x10-3 s-1)	0-6 km Bulk Shear (x10-3 s-1)	0-3 km CAPE (J/kg)	Total CAPE (J/kg)	CIN (J/kg)	0-1 km Total SRH (m/s) <sup>2</sup>	0-3 km Total SRH (m/s) <sup>2</sup>	EH1	BRN	VGP
torid #221	Kern	6/26/1995	1650	F0	34.98	-117.97	2	17	11	3.1	3.7	1.2	-187	1600	-192	5.7	29.3	1	95	0.309
torid #222	Del Norte	1/20/1996	1130	F0	41.95	-124.17	0.3	30	20	7.3	20.3	6.4	40	41	-1	197	171.5	0	0	0.078
torid #223	Del Norte	1/20/1996	1200	F0	41.75	-124.2	0.1	20	20	7.3	20.3	6.4	40	41	-1	197	171.5	0	0	0.078
torid #224	Sonoma	2/22/1996	0100	F1	38.55	-122.73	1	50	7.1	4.6	8.5	5.4	62	74	0	60.3	111.5	0.3	7	0.148
torid #225	Kings	3/12/1996	1407	F0	36.35	-119.68	0.1	10	23.6	4.2	18.5	4.3	283	929	0	303	313.6	1.8	9	0.234
torid #226	Kings	3/12/1996	1425	F0	36.38	-119.65	0.1	10	23.6	4.2	18.5	4.3	283	927	0	303	313.6	1.8	9	0.233
torid #227	Stanislaus	4/1/1996	1440	F0	37.32	-121.02	0.1	50	29.8	8.5	23	0.3	223	759	0	96.9	174.8	0.2	66	0.424
torid #228	San Joaquin	4/1/1996	1500	F0	37.98	-121.32	0.8	50	33.4	9.1	22.3	1.2	176	564	0	59.4	112.3	0.4	20	0.387
torid #229	San Joaquin	4/1/1996	1500	F0	38.08	-121.3	0.3	150	33.4	9.1	22.3	1.2	176	564	0	59.4	112.3	0.4	20	0.387
torid #230	San Joaquin	4/1/1996	1500	F0	38.13	-121.25	0.1	100	33.4	9.1	22.3	1.2	176	564	0	59.4	112.3	0.4	20	0.387
torid #231	San Joaquin	4/1/1996	1500	F0	38.13	-121.27	0.1	100	33.4	9.1	22.3	1.2	176	564	0	59.4	112.3	0.4	20	0.387
torid #232	Merced	4/1/1996	1545	F0	37.13	-120.48	0.5	10	24.5	7.6	20.6	0.5	240	896	0	142.6	204	0.2	123	0.421
torid #233	Tulare	4/1/1996	1630	F0	36.17	-119.32	0.3	10	5.1	3.2	4.7	4.8	261	329	0	75.6	50.5	0.1	3	0.148
torid #234	Madera	4/16/1996	1350	F0	36.88	-119.88	0.5	10	14.8	6.5	15.5	8.5	484	799	-97	96.4	125.5	0.7	7	0.287
torid #235	Fresno	10/30/1996	1250	F0	36.77	-119.78	0.2	10	21.3	4.4	15.8	2.6	277	820	0	213.1	214.4	1.1	12	0.222
torid #236	Merced	11/22/1996	1350	F1	37.33	-120.45	0.2	10	25	6	15.6	4	78	293	0	343.4	385.6	0	1	0.048
torid #237	Fresno	11/22/1996	1427	F0	36.33	-119.93	1	30	14.3	4.7	11.4	4.3	282	832	0	155.3	204.9	1	8	0.223
torid #238	Fresno	11/22/1996	1505	F1	36.33	-119.93	0.8	20	14.3	4.7	11.4	4.3	282	832	-1	155.3	204.9	0.7	2	0.189
torid #239	Kern	11/22/1996	1543	F0	35.42	-118.85	2	10	3.3	2.8	5.2	3.7	175	554	0	48.3	158.6	0.3	7	0.128
torid #240	Stanislaus	12/12/1996	1550	F1	37.77	-120.85	0.6	25	8.5	5.3	10.4	6.1	116	116	0	168.9	245.9	1	8	0.223
torid #241	Riverside	12/22/1996	0900	F1	33.92	-116.78	0.1	25	23.2	6.5	20.5	5.6	569	655	-9	436.8	607.6	0.2	1	0.127
torid #242	Marin	12/23/1996	1000	F1	38.25	-122.93	6	20	10.3	4.8	10	6.6	61	61	0	188.8	251.9	2	3	0.275
torid #243	Solano	12/23/1996	1130	F0	38.28	-122.08	0.3	20	8.7	4.4	6.1	3.2	115	115	0	50.8	76.3	0	3	0.089

# Appendix 1: Compilation of Buoyancy and Shear Parameters for 391 Tornado events from 1951–2011

## Table A5 (Continued) Compilation of results from 137 tornado proximity soundings for the 1990s

Tornado Number	County of Occurrence	Date	Time (LST)	F-Rating	Latitude (°N)	Longitude	Width (Yards)	Length (Miles)	0-1 km ABVSHR (x10 <sup>-3</sup> s <sup>-1</sup> )	0-6 km ABVSHR (x10 <sup>-3</sup> s <sup>-1</sup> )	0-1 km Bulk Shear (x10 <sup>-3</sup> s <sup>-1</sup> )	0-6 km Bulk Shear (x10 <sup>-3</sup> s <sup>-1</sup> )	0-3 km CAPE (J/kg)	Total CAPE (J/kg)	CIN (J/kg)	0-1 km Total SRH (m/s) <sup>2</sup>	0-3 km Total SRH (m/s) <sup>2</sup>	EH1	BRN	VGP
torid #244	Tulare	1/20/1997	1535	F0	36.32	-119.13	3	10	7.6	4.2	9.1	4.1	115	319	-8	78.9	109.2	0.2	5	0.139
torid #245	Kern	2/17/1997	1415	F0	35.37	-119	0.3	10	11	3.9	10.3	4.4	135	227	-1	89.6	197.1	0.2	2	0.11
torid #246	Kern	3/22/1997	1637	F0	35.67	-119.42	0.2	10	8	4.2	6.4	3.2	60	896	-26	32.2	68.9	0.3	42	0.193
torid #247	San Bernardino	5/11/1997	1330	F1	34.52	-117.2	0.2	40	16.7	3.8	8.5	1.2	0	4332	0	88.2	82.7	0.1	0	0.087
torid #248	San Bernardino	5/18/1997	1537	F1	34.63	-117.23	3.5	100	8.8	3.9	6.6	0.3	5	1680	0	34.4	5	2.9	310	0.492
torid #249	San Bernardino	5/18/1997	1550	F1	34.6	-117.18	9	40	8.8	3.9	6.6	0.3	5	1680	0	34.4	5	0.1	157	0.335
torid #250	San Diego	5/20/1997	1645	F0	33.25	-116.27	0.1	23	6	3.5	4.5	0.5	-173	526	-176	44.1	11.8	0.2	0	0.153
torid #251	San Bernardino	6/6/1997	1700	F0	34.42	-117.3	0.2	20	11.3	6.8	11.4	4.7	-159	250	-233	99.6	37.8	0.4	3	0.228
torid #252	Los Angeles	7/21/1997	1555	F0	34.58	-118.12	0.1	10	5.8	3.5	5.8	1.3	-181	7	-199	15.8	73.8	0.1	21	0.071
torid #253	San Bernardino	8/7/1997	1733	F0	34.6	-114.6	0.1	23	5.4	3.4	2.9	0.5	0	3773	0	11.1	0.8	0.1	0	0.342
torid #254	Imperial	9/24/1997	1514	F0	32.78	-115.67	1.5	23	5.3	3.7	5.2	0.8	-364	1130	-374	9.9	18.5	0.1	184	0.288
torid #255	Orange	11/11/1997	1240	F1	33.68	-117.82	0.2	200	8.8	3	5.4	2.7	252	539	0	17.3	14.5	0.1	157	0.335
torid #256	Merced	11/13/1997	1530	F0	37.03	-120.85	3	10	11.7	4	9.9	2.6	178	627	-6	103.7	132.5	0.5	17	0.191
torid #257	Fresno	11/26/1997	1300	F0	36.93	-119.68	0.1	10	27.1	6.9	21.8	2.3	121	259	-16	311.7	292.1	0.6	5	0.173
torid #258	Fresno	11/26/1997	1410	F0	36.93	-119.58	0.3	10	27.1	6.9	21.8	2.3	121	259	-16	311.7	292.1	0.6	5	0.173
torid #259	Santa Clara	12/8/1997	1435	F0	37.33	-121.88	0.2	100	5.4	3.9	6.2	2.9	2	132	-14	59.7	57.7	0.1	10	0.07
torid #260	Orange	12/21/1997	1340	F1	33.67	-118	1	30	13.6	6	4.9	3.7	4	4	0	116.5	116.8	0.1	47	0.155
torid #261	Los Angeles	1/9/1998	1400	F1	33.78	-118.17	1.5	30	17.2	5.1	12.5	4.1	171	752	-3	171.5	347.3	0	0	0.039
torid #262	San Diego	1/29/1998	1112	F1	33.05	-117.3	0.5	40	16.9	8.9	19.6	5.8	137	148	0	150.9	45.7	1	13	0.302
torid #263	Santa Clara	2/6/1998	1600	F0	37.37	-122.03	0.1	30	19	4.9	16.7	2.3	57	69	-11	202.5	211.2	0.1	3	0.072
torid #264	San Mateo	2/7/1998	1400	F0	37.47	-122.43	0.2	50	11.1	4.5	11.5	4.6	177	118	-12	177.1	276.9	0.2	1	0.087
torid #265	San Diego	2/8/1998	0000	F0	33.03	-117.28	3	30	5.2	5.7	9.1	5	45	45	-1	84.2	10.9	0	0	0.063
torid #266	Merced	2/14/1998	1325	F0	37.07	-120.77	0.1	30	7.5	4.8	8.8	4.8	270	453	0	98.9	281.7	0.6	3	0.174

**Appendix 1: Compilation of Buoyancy and Shear Parameters for 391 Tornado events from 1951–2011**  
**Table A5 (Continued) Compilation of results from 137 tornado proximity soundings for the 1990s**

Tornado Number	County of Occurrence	Date	Time (LST)	F-Rating	Latitude (°N)	Longitude	Width (Yards)	Length (Miles)	0-1 km ABVSHR (x10 <sup>-3</sup> s <sup>-1</sup> )	0-6 km ABVSHR (x10 <sup>-3</sup> s <sup>-1</sup> )	0-1 km Bulk Shear (x10 <sup>-3</sup> s <sup>-1</sup> )	0-6 km Bulk Shear (x10 <sup>-3</sup> s <sup>-1</sup> )	0-3 km CAPE (J/kg)	Total CAPE (J/kg)	CIN (J/kg)	0-1 km Total SRH (m/s) <sup>2</sup>	0-3 km Total SRH (m/s) <sup>2</sup>	EH1	BRN	VGP
torid #267	Fresno	2/14/1998	1441	F1	36.87	-120.48	3	30	7.5	4.8	8.8	4.8	270	453	0	98.9	281.7	0.1	2	0.155
torid #268	Contra Costa	2/19/1998	1230	F0	37.93	-121.7	0.2	30	3.9	3.4	6	2.8	62	62	0	4.1	19.9	0	1	0.039
torid #269	Orange	2/24/1998	0130	F0	33.67	-118	0.3	30	18.2	5	17.1	6.1	310	764	0	33.3	94.4	0.4	11	0.311
torid #270	Madera	3/24/1998	1346	F0	37.08	-120.35	2	30	2.2	4.2	2	6	445	1678	0	8.7	75.4	0.7	21	0.205
torid #271	Madera	3/28/1998	1635	F0	37.12	-120.25	0.3	30	11.2	3.4	4.2	1.4	118	684	0	5.5	13.7	0.1	346	0.157
torid #272	San Joaquin	3/28/1998	1720	F0	37.67	-121.33	0.1	30	8.3	2.9	4.9	1.5	238	1160	0	10.8	20.5	0.3	0	0.206
torid #273	Sacramento	4/24/1998	1330	F0	38.63	-121.38	0.1	30	2.8	2.2	1.2	1.9	49	49	0	11.1	46.4	0	5	0.028
torid #274	San Luis Obispo	5/5/1998	0440	F0	35.28	-120.67	0.3	30	7.1	2.8	6.9	2.6	195	525	-5	64.3	81	0.2	31	0.079
torid #275	Santa Clara	5/5/1998	1630	F1	37.38	-122.12	0.3	80	14.7	3.1	14.7	3.1		1732	0	70	111	0.6	3	0.174
torid #276	Santa Clara	5/5/1998	1643	F2	37.37	-122.03	0.6	100	14.7	3.1	14.7	3.1		1732	0	70	111	N/A	N/A	N/A
torid #277	Solano	5/12/1998	1530	F0	38.2	-122.02	0.2	30	4	2.2	3.6	1.1	125	333	0	11.5	3	0	0	0.074
torid #278	Ventura	5/13/1998	0905	F0	34.22	-119.08	0.1	30	3.9	2.2	3.1	1.6	236	836	0	8.3	50.6	0.2	60	0.1
torid #279	Riverside	5/13/1998	1445	F0	33.73	-117.12	0.2	40	13.3	5.1	7	4.7	624	1588	0	103.7	129.3	1.3	47	0.322
torid #280	Butte	5/16/1998	1325	F0	39.5	-121.75	0.1	30	11.8	4.3	10.1	6.1	333	531	0	88	113.8	0.3	11	0.14
torid #281	San Bernardino	8/25/1998	1120	F0	35.42	-115.33	1	30	5	2.5	8.7	1.7	38	1540	-9	35.6	33.9	0.4	1463	0.214
torid #282	Mendocino	12/5/1998	1557	F1	39.42	-123.82	1.7	50	4.2	4.8	7.2	4.8	39	24	-22	113.7	399.3	0.1	0	0.071
torid #283	Sonoma	12/5/1998	1820	F1	38.45	-122.7	1.5	150	4.9	4.8	8.8	5.1	76	76	-6	134.6	420.1	0.1	1	0.098
torid #284	Contra Costa	12/5/1998	1930	F0	37.93	-122.35	1.5	150	9.7	5.7	11.4	5.7	86	86	0	112.8	396.5	0.1	1	0.109
torid #285	Santa Cruz	12/5/1998	2030	F0	36.98	-122.02	1	100	7.8	5.4	8.3	2.7	40	40	-20	5	277.4	0	1	0.087
torid #286	Los Angeles	4/1/1999	1400	F0	34.25	-118.6	0.1	0	1.1	4.3	1.4	4.7	88	173	0	12	28.8	0	4	0.07
torid #287	Kern	4/3/1999	1630	F0	35.35	-118.97	0.1	10	13.4	7.6	16.4	8.8	145	154	0	26.1	3.6	0	1	0.114
torid #288	San Diego	7/12/1999	1745	F0	33.08	-116.48	0.1	30	8.3	3.4	6.2	1.1	108	2665	-1	28.8	11.9	1	335	0.352

**Appendix 1: Compilation of Buoyancy and Shear Parameters for 391 Tornado events from 1951–2011**  
**Table A6 Compilation of results from 102 tornado proximity soundings for the 2000s**

Tornado Number	County of Occurrence	Date	Time (LST)	F-Rating	Latitude (°N)	Longitude	Width (Yards)	Length (Miles)	0-1 km ABVSHR (x10 <sup>-3</sup> s <sup>-1</sup> )	0-6 km ABVSHR (x10 <sup>-3</sup> s <sup>-1</sup> )	0-1 km Bulk Shear (x10 <sup>-3</sup> s <sup>-1</sup> )	0-6 km Bulk Shear (x10 <sup>-3</sup> s <sup>-1</sup> )	0-3 km CAPE (J/kg)	Total CAPE (J/kg)	CIN (J/kg)	0-1 km Total SRH (m/s) <sup>2</sup>	0-3 km Total SRH (m/s) <sup>2</sup>	EH1	BRN	VGP
torid #289	Los Angeles	2/16/2000	1630	F0	34.08	-117.88	0.5	10	8.6	7.3	9.1	6.4	-17	0	-70	134.1	154.1	0	0	0.067
torid #290	Madera	2/27/2000	1337	F0	36.87	-120.2	1	50	8.6	5.5	12.8	5.9	24	23	-12	96.8	170.1	0	0	0.062
torid #291	Fresno	2/27/2000	1359	F0	36.7	-120.12	0.5	20	8.6	5.5	12.8	5.9	24	23	-12	96.8	170.1	0	0	0.062
torid #292	Fresno	2/27/2000	1410	F0	36.6	-119.87	0.5	20	8.6	5.5	12.8	5.9	24	22	-12	96.8	170.1	0	0	0.062
torid #293	Fresno	2/27/2000	1517	F0	36.65	-119.77	0.2	20	8.6	5.5	12.8	5.9	24	23	-12	96.8	170.1	0	0	0.062
torid #294	Glenn	7/5/2000	1715	F0	39.68	-122.3	0.2	0	13	3.8	12.6	3	-52	0	-73	84.4	61.4	0	2	0.037
torid #295	Los Angeles	8/28/2000	1345	F0	34.55	-117.98	0.1	0	25	6.2	18.1	1.8	94	1339	0	193.4	256.4	1.7	31	0.486
torid #296	Imperial	8/30/2000	1845	F0	33	-115.07	3	50	6.1	3.1	7	1.5	-14	1221	-20	22.2	105.7	0.8	53	0.205
torid #297	San Diego	11/10/2000	0930	F1	32.95	-117.02	0.4	30	4	3.1	4.9	4.1	304	690	0	35.6	60.4	0.3	20	0.122
torid #298	Orange	2/24/2001	1350	F0	33.78	-117.83	0.1	100	9.7	5.8	8.1	3.3	120	120	0	150.1	305.5	0.2	1	0.108
torid #299	Fresno	4/7/2001	1958	F0	36.82	-119.7	0.3	10	14.3	5.9	9.5	3.5	17	148	-24	113.2	112.3	0.1	24	0.112
torid #300	Mohave	4/21/2001	1135	F1	34.9	-114.62	3	50	12.5	7.8	5.4	4.1	19	28	0	1.5	19.6	0	1	0.056
torid #301	Mohave	4/21/2001	1135	F1	34.9	-114.62	1	50	12.5	7.8	5.4	4.1	19	28	0	1.5	19.6	0	1	0.056
torid #302	San Bernardino	7/7/2001	1245	F0	34.13	-116.32	1	0	9.3	4	10	1.2	-155	575	-156	17.9	22.3	0.2	0	0.19
torid #303	Santa Barbara	11/29/2001	1100	F0	34.95	-120.43	0.1	2	8.4	4.6	7.4	4.8	254	333	-3	30.1	53.8	0.1	5	0.14
torid #304	Santa Cruz	12/20/2001	1645	F1	36.97	-121.78	0.5	60	8.8	3.9	8.3	1.5	4	194	0	19.1	64.1	0	14	0.088
torid #305	Los Angeles	12/21/2001	0040	F0	34.02	-117.87	0.1	10	16.8	5.8	14.1	8.3	124	179	-13	164.5	245.8	0.3	1	0.123
torid #306	Madera	5/20/2002	1459	F1	36.93	-120.12	2.7	40	13.2	4.2	12.1	3	202	743	0	143.6	230.5	0.9	11	0.2
torid #307	Merced	12/16/2002	1240	F1	37.33	-120.52	1.3	45	23.4	5.3	20.9	7.4	266	624	0	265.1	292.7	1.1	6	0.247
torid #308	Merced	12/16/2002	1250	F0	37.35	-120.43	1	45	23.4	5.3	20.9	7.4	266	624	0	265.1	292.7	1.1	6	0.247
torid #309	San Luis Obispo	2/2/2004	1500	F0	35.1	-120.63	0.5	5	3.4	6.5	4.3	5.2	0	27	0	12.9	65.2	0	0	0.063
torid #310	Tulare	7/7/2004	1532	F0	36.63	-118.35	N/A	40	11	5.5	N/A	N/A	N/A	1368	N/A	N/A	146	0.3	276	0.199
torid #311	San Bernardino	8/14/2004	1118	F0	34.3	-116.55	1	200	3.5	4.1	0.9	1.6	-139	871	-140	6.4	6.8	0.3	276	0.199
torid #312	San Bernardino	8/14/2004	1140	F0	34.42	-117.57	1	800	3.5	4.1	0.9	1.6	-139	871	-140	6.4	6.8	1.3	13	0.32
torid #313	San Diego	10/17/2004	0608	F0	33.2	-117.38	0.2	25	11.4	5.9	9.9	3.8	334	1145	0	133.2	210.7	0.4	42	0.268



# Appendix 1: Compilation of Buoyancy and Shear Parameters for 391 Tornado events from 1951–2011

## Table A6 (Continued) Compilation of results from 102 tornado proximity soundings for the 2000s

Tornado Number	County of Occurrence	Date	Time (LST)	F-Rating	Latitude (°N)	Longitude	Width (Yards)	Length (Miles)	0-1 km ABVSHR (x10 <sup>-3</sup> s <sup>-1</sup> )	0-6 km ABVSHR (x10 <sup>-3</sup> s <sup>-1</sup> )	0-1 km Bulk Shear (x10 <sup>-3</sup> s <sup>-1</sup> )	0-6 km Bulk Shear (x10 <sup>-3</sup> s <sup>-1</sup> )	0-3 km CAPE (J/kg)	Total CAPE (J/kg)	CIN (J/kg)	0-1 km Total SRH (m/s) <sup>2</sup>	0-3 km Total SRH (m/s) <sup>2</sup>	EBI	BRN	VGP
torid #314	Tulare	10/20/2004	1305	F0	36.48	-119.32	0.5	15	9.5	3.4	10.5	3.6	412	1437	0	15.9	52.1	0.4	1	0.192
torid #315	Los Angeles	12/29/2004	2240	F0	33.78	-118.17	1	5	7.4	5.9	9.3	7.3	90	267	-2	96.2	234.9	0.2	5	0.143
torid #316	Los Angeles	12/29/2004	0015	F0	33.97	-118.3	0.5	5	7.9	3.5	5.4	4.8	152	392	-1	58.2	129.3	0.4	7	0.198
torid #317	Los Angeles	12/29/2004	0015	F0	33.95	-118.03	0.5	5	9.7	3.8	7.7	5.1	243	668	0	63.7	132.1	0.1	5	0.09
torid #318	Sonoma	12/29/2004	1210	F0	38.45	-122.7	0.2	3	12.1	4.2	8	4.2	152	180	-2	80.5	164.3	1.9	7	0.494
torid #319	Butte	1/8/2005	1645	F1	39.45	-121.57	0.1	0	14.1	8	13.4	8.9	37	41	-1	164.2	356.8	0.1	0	0.065
torid #320	Riverside	1/9/2005	1711	F0	33.72	-116.97	0.1	25	21.4	7.7	15.6	5.5	419	1092	0	252.3	352.9	0.3	3	0.251
torid #321	Ventura	1/10/2005	0645	F0	34.23	-119.17	0.1	1	14.9	6.7	14.3	5.4	146	279	-19	148.3	248.8	0.1	3	0.065
torid #322	Solano	1/11/2005	0650	F0	38.37	-121.98	0.1	0	11.4	3.3	12	2.7	61	77	-10	129.3	139.7	0.2	62	0.142
torid #323	Sonoma	1/27/2005	1930	F1	38.62	-123.12	0.5	25	7.8	2.7	7.6	2.9	186	243	-15	81	148	0.2	6	0.088
torid #324	Orange	2/19/2005	0742	F0	33.67	-118	0.2	20	11	4.2	11	1.1	154	584	-2	33.2	69.3	0.8	10	0.204
torid #325	San Diego	2/19/2005	0917	F0	33.35	-117.28	2.5	25	10.8	4	9.5	3.4	171	696	-3	142.4	173.7	0.8	10	0.204
torid #326	San Diego	2/19/2005	0930	F0	33.42	-117.15	2.2	15	10.8	4	9.5	3.4	171	696	-3	142.4	173.7	0.7	54	0.392
torid #327	Riverside	2/19/2005	0935	F1	33.48	-117.17	2.8	25	10.8	4	9.5	3.4	171	696	-3	142.4	173.7	0.8	10	0.204
torid #328	Yolo	2/21/2005	1330	F0	38.58	-121.53	0.1	0	26.4	8.7	13.3	1.9	161	456	0	243.6	293.6	0.7	54	0.392
torid #329	Sacramento	2/21/2005	1350	F0	38.57	-121.45	0.1	0	26.4	8.7	13.3	1.9	161	456	0	243.6	293.6	0.7	54	0.392
torid #330	Sacramento	2/21/2005	1354	F0	38.62	-121.47	0.3	0	26.4	8.7	13.3	1.9	161	456	0	243.6	293.6	0.1	101	0.07
torid #331	San Diego	2/23/2005	1050	F0	32.63	-117.08	0.1	10	4.5	2.2	4.3	2.3	118	474	-3	32.5	28.5	0	5	0.07
torid #332	Riverside	2/26/2005	1500	F0	33.7	-117.3	2	15	7	3.7	4.9	3.8	82	109	0	21.2	0.6	0.5	24	0.203
torid #333	San Bernardino	3/4/2005	1220	F0	34.1	-117.43	0.5	15	6.2	4.7	6.1	3.1	259	683	0	57.6	64	0.7	6	0.188
torid #334	Yolo	3/20/2005	1120	F0	38.88	-122.03	1.2	0	15.1	5	14.2	5	202	578	-6	170.3	209.9	0.3	3	0.131
torid #335	Stanislaus	3/20/2005	1320	F0	37.65	-121	0.1	0	14.1	4.2	12.8	4.8	111	298	0	157.6	196.4	0.2	0	0.143
torid #336	San Mateo	3/20/2005	1535	F1	37.65	-122.42	3	30	6.6	3.1	7	3.7	233	694	0	67.1	84.9	0.4	20	0.147
torid #337	Sutter	3/29/2005	1615	F0	39.13	-121.62	0.2	0	22.9	6.2	16.4	7.4	99	99	0	279.7	251.6	0.4	1	0.125
torid #338	San Joaquin	4/8/2005	1312	F0	37.82	-121.3	1.5	0	22.1	6.8	18	7.3	144	176	0	261.8	325.7	0.5	2	0.196

## Appendix 1: Compilation of Buoyancy and Shear Parameters for 391 Tornado events from 1951–2011

**Table A6 (Continued) Compilation of results from 102 tornado proximity soundings for the 2000s**

Tornado Number	County of Occurrence	Date	Time (LST)	F-Rating	Latitude (°N)	Longitude	Width (Yards)	Length (Miles)	0-1 km ABVSHR (x10-3 s-1)	0-6 km ABVSHR (x10-3 s-1)	0-1 km Bulk Shear (x10-3 s-1)	0-6 km Bulk Shear (x10-3 s-1)	0-3 km CAPE (J/kg)	Total CAPE (J/kg)	CIN (J/kg)	0-1 km Total SRH (m/s) <sup>2</sup>	0-3 km Total SRH (m/s) <sup>2</sup>	EHI	BRN	VGP
torid #339	Sacramento	4/8/2005	1455	F0	38.5	-121.3	0.1	0	27.4	8.4	23.8	8.2	144	278	-2	249	271.1	0.3	1	0.141
torid #340	Butte	4/8/2005	1505	F0	39.62	-121.8	0.1	0	18.8	8.1	17.1	7.7	93	155	-4	254.3	249.2	0.4	2	0.175
torid #341	Sacramento	4/8/2005	1522	F0	38.67	-121.47	0.1	0	22.3	7.6	19.4	7.6	145	279	-1	206.6	229.8	0.2	1	0.124
torid #342	Merced	4/8/2005	1720	F0	37.45	-120.72	1.2	50	22.2	7.6	18.2	7.4	85	138	-4	236.3	260	0.3	12	0.133
torid #343	Fresno	5/9/2005	1018	F0	36.63	-119.68	0	25	14.1	4.1	13.9	5.7	224	418	0	109.4	167	0.2	21	0.094
torid #344	Sutter	5/9/2005	1430	F0	39.1	-121.67	1	0	16.5	5.3	13.3	2.7	48	148	-8	174.8	169.4	0	0	0.047
torid #345	Glenn	6/6/2005	1430	F0	39.62	-122.2	0.1	6	22.4	6.6	13.1	7	10	10	-10	296.2	279.9	0.4	45	0.301
torid #346	Riverside	7/23/2005	1306	F0	33.73	-116.95	2	50	14.1	3.3	8.2	1.7	60	1527	-8	46.1	20.8	0.5	19	0.27
torid #347	Los Angeles	8/15/2005	1753	F0	34.72	-117.98	0.1	33	10.8	4.4	8	1.3	8	762	-5	48.9	201.7	0.3	2	0.21
torid #348	San Joaquin	12/26/2005	0245	F0	37.75	-121.43	0.3	0	15.1	7.3	17.8	6.8	10	236	-40	130.6	214.9	0.1	5	0.087
torid #349	Mariposa	1/14/2006	1425	F0	37.53	-120.28	0.1	25	11.3	4.4	10.6	4.5	153	269	0	58.7	38.1	0.2	1	0.116
torid #350	San Diego	3/10/2006	1638	F0	33.05	-117.3	0.2	15	9.8	4.1	9.6	5.9	91	156	-5	148.6	204.2	0.1	11	0.071
torid #351	San Diego	3/11/2006	1211	F0	33.1	-116.93	2	45	3.7	2.6	3.9	2.5	49	325	-16	44.3	63.6	0.2	29	0.204
torid #352	Merced	3/28/2006	1442	F0	37.33	-120.63	0.2	20	10.5	3.7	10	3.1	375	946	0	11.2	4.1	0.2	29	0.204
torid #353	Merced	3/28/2006	1448	F0	37.28	-120.47	0.2	30	10.5	3.7	10	3.1	375	946	0	11.2	4.1	0.2	29	0.204
torid #354	Merced	3/28/2006	1517	F0	37.32	-120.53	0.1	20	10.5	3.7	10	3.1	375	946	0	11.2	4.1	0.1	1	0.098
torid #355	Santa Barbara	3/29/2006	1255	F0	34.63	-120.45	0	4	4.3	4.5	6.4	5.8	141	141	-1	19.3	137.6	1.5	122	0.316
torid #356	Stanislaus	4/14/2006	1535	F1	37.65	-121	0.5	0	13.2	4.2	10.5	2	98	255	0	90.7	67	0.1	29	0.103
torid #357	Riverside	7/23/2006	1515	F0	33.73	-117.15	1	20	8.7	2.9	5.4	1.1	-52	2302	-56	11.2	96.4	0.1	0	0.153
torid #358	Sacramento	2/25/2007	1224	F0	38.39	-121.37	1	5	16.1	6.1	15.5	7.9	113	113	-8	84	196	0	0	0.124
torid #359	Santa Clara	4/14/2007	1605	F0	37	-121.6	0.2	30	12.2	3.8	7.9	0.4	227	418	0	40.3	61.8	0.2	1411	0.168
torid #360	Los Angeles	9/1/2007	1520	F0	34.65	-118.12	0.05	10	7.4	2.1	3.8	0.6	-153	1375	-161	14.3	24.6	0.2	1411	0.168
torid #361	Kern	9/1/2007	1530	F0	34.84	-118.21	13.05	75	7.4	2.1	3.8	0.6	-153	1375	-161	14.3	24.6	0.1	0	0.067
torid #362	Orange	9/22/2007	1000	F0	33.62	-117.93	0.1	15	7	6.1	9.9	7.5	60	60	-7	95.9	135.1	0.1	1	0.074
torid #363	San Diego	9/22/2007	1143	F0	33.02	-117.29	0.1	15	6	5.6	5.4	5.3	59	69	-5	39.3	122.6	0.8	5	0.27
torid #364	Ventura	1/24/2008	1915	F0	34.12	-119.12	0.1	5	8.6	6.3	9.9	5.9	250	640	0	124.5	195	0.8	16	0.266

# Appendix 1: Compilation of Buoyancy and Shear Parameters for 391 Tornado events from 1951–2011

## Table A6 (Continued) Compilation of results from 102 tornado proximity soundings for the 2000s

Tornado Number	County of Occurrence	Date	Time (LST)	F-Rating	Latitude (°N)	Longitude	Width (Yards)	Length (Miles)	0-1 km ABVSHR (x10-3 s-1)	0-6 km ABVSHR (x10-3 s-1)	0-1 km Bulk Shear (x10-3 s-1)	0-6 km Bulk Shear (x10-3 s-1)	0-3 km CAPE (J/kg)	Total CAPE (J/kg)	CIN (J/kg)	0-1 km Total SRH (m/s)^2	0-3 km Total SRH (m/s)^2	EBI	BRN	VGP
torid #365	Tulare	1/27/2008	1210	F0	36.33	-119.36	2.03	50	17.4	5.2	13.5	3	264	740	0	144.1	169.4	0.2	18	0.286
torid #366	Riverside	5/22/2008	1530	F0	33.84	-117.23	0.89	20	18.4	7.4	17.7	5.5	192	562	0	68.4	146.9	0.2	18	0.286
torid #367	Riverside	5/22/2008	1542	F2	33.88	-117.25	2.8	75	18.4	7.4	17.7	5.5	192	562	0	68.4	146.9	0.2	18	0.286
torid #368	Riverside	5/22/2008	1550	F0	33.87	-117.27	0.96	20	18.4	7.4	17.7	5.5	192	562	0	68.4	146.9	0.2	18	0.286
torid #369	Riverside	5/22/2008	1640	F0	33.8	-117.34	0.36	10	18.4	7.4	17.7	5.5	192	562	0	68.4	146.9	0.2	5	0.112
torid #370	San Bernardino	8/4/2008	1300	F1	34.35	-116.59	1.08	100	3.3	2.2	1.4	0.9	132	3441	0	3.8	20.1	0.4	1232	0.246
torid #371	Colusa	1/24/2009	1500	F0	39.36	-122.04	0.1	40	10	2.9	9	2.9	243	257	0	90.7	103.7	0.1	3	0.13
torid #372	Merced	2/9/2009	1132	F0	37.21	-120.6	0.1	20	12.8	6.2	10	7.8	118	203	-2	39.3	84.8	0.1	1	0.089
torid #373	Fresno	1/18/2010	1524	F0	36.73	-119.86	0.53	15	12.1	9.2	12.4	3.9	18	62	-1	127.1	135.4	1	1	0.207
torid #374	Santa Barbara	1/19/2010	1032	F0	34.42	-119.88	0.14	10	19.6	8.9	16.6	6	68	220	-14	409.2	696.1	0.9	15	0.252
torid #375	Los Angeles	1/19/2010	1255	F1	33.72	-118.13	4.62	25	14.5	6.4	13	5.7	230	613	0	201.3	317.9	1.1	4	0.24
torid #376	Ventura	1/21/2010	1225	F0	34.25	-119.2	1.51	67	15.4	4.1	11.6	3.2	296	810	0	157.7	210	0.9	13	0.262
torid #377	Riverside	1/21/2010	1510	F0	33.51	-114.75	14.26	100	10.3	4.9	18.4	5.9	512	1595	0	76.2	73.4	0.3	1	0.129
torid #378	Contra Costa	1/23/2010	1254	F1	37.91	-121.77	1.64	2	7.5	6.4	7.6	7	92	92	-5	95.1	139.5	0.1	1	0.095
torid #379	Kern	2/27/2010	1645	F0	35.3	-119.27	0.5	20	16.8	6.7	11.7	3.1	86	141	0	149.8	337.6	0.1	1	0.117
torid #380	Glenn	3/8/2010	1625	F0	39.73	-122.55	0.25	20	21.6	5.7	14.3	5.4	88	119	0	111.7	130.5	0.3	1	0.216
torid #381	El Dorado	11/23/2010	1100	F1	38.567	-120.97	0	0	14.2	5.8	13.6	4.3	85	85	0	149.8	182.7	0.1	1	0.085
torid #382	Sacramento	2/25/2011	1300	F0	38.55	-121.3	0	0	19.2	7.6	10.9	9.1	163	281	0	43.8	8.2	0.3	12	0.147
torid #383	Sonoma	3/18/2011	0700	F1	38.45	-122.7	0	0	6.6	5.1	7.1	5.3	38	20	-19	98.4	186.8	0.1	0	0.061
torid #384	Colusa	3/21/2011	1300	F0	39.267	-122.23	0	0	16.8	5.4	12.2	4.1	168	264	0	169.3	166.2	0.3	37	0.15
torid #385	Colusa	3/23/2011	1300	F0	39.15	-122.02	0	0	9.9	3.9	9.9	2.3	207	622	0	51.2	87.4	0.3	42	0.167
torid #386	Solano	4/7/2011	1400	F0	38.233	-122.12	0	0	7.5	3	6.3	1.5	228	736	0	46.8	60.1	0.8	19	0.214
torid #387	Glenn	5/25/2011	1400	F1	39.617	-122.15	0	0	15.8	10	15.3	8.7	187	191	0	20.1	174.5	0.2	1	0.176
torid #388	Glenn	5/25/2011	1400	F1	39.517	-122.2	0	0	15.8	10	15.3	8.7	187	191	0	20.1	174.5	0.2	1	0.176
torid #389	Butte	5/25/2011	1600	F2	39.6	-121.62	0	0	17.3	10.3	16.4	8.9	187	191	0	45.4	199.8	0.2	1	0.182
torid #390	Placer	6/1/2011	1500	F0	39.02	-121.07	0	0	13.5	3.5	10.6	4.8	386	887	0	126.4	159.4	0.4	19	0.151